Synthetic Constitution and Modulation of Microbial Metabolic Systems for Advanced BioChemical Generation

YUSUKE SASAKI

2020

博士（総合学術）

Synthetic Constitution and Modulation of Microbial Metabolic Systems for Advanced BioChemical Generation

バイオ化成物創製に向けた
微生物代謝システムの合成的構築と調整

佐々木　勇輔

京都大学大学院 総合生存学館

2020 年 3 月

This dissertation is dedicated to my late mother, Atsuko Sasaki,
who rested in peace on January 1st, 2020.

TABLE OF CONTENTS

ABSTRACT

Transitions of energy systems have been driven through energy crisis caused by national conflictions and wars (e.g., oil crisis; 1970s-1980s), geopolitical concerns for energy security, environmental issues related with petroleum use such as high global greenhouse gas (GHG) emissions, and natural and human-made disasters (e.g., Chernobyl disaster; 1986, Fukushima Daiichi nuclear disaster started by the Tohoku earthquake and tsunami; 2011). Renewable energy systems are one of the targeted alternatives to the historical petroleum-oriented structure. Biofuels, produced from a multitude of biomass, has the potential to be used as fuel for engines and flammable additives. The use of edible feedstock (e.g., sugarcane, corn etc.), which is called 1st generation feedstock, has been used as the primary source of biofuels. However, increased concerns for the food securities, 2nd and 3rd generation feedstock, cellulosic biomass, and algal biomass have been targeted as the next-generation sources.

Synthetic biology enables the rational metabolic pathway design and builds of genetic parts to create novel synthetic pathways. This technology offers new opportunities to explore microbial host engineering for use in a breadth of industrial, environmental, and medical fields. In the 1st chapter, we showed a novel strategy to convert hemicellulose into ethanol through co-factor optimization of xylose isomerase displayed *Saccharomyces cerevisiae*. In 2nd and 3rd chapter, we engineered *Corynebacterium glutamicum* for jet fuel candidate C5 alcohol production by harnessing a heterogenous mevalonate pathway.

Xylose isomerase (XylC) from *Clostridium cellulovorans* can simultaneously perform isomerization and fermentation of D-xylose, the main component of lignocellulosic biomass, and is an attractive candidate enzyme. In this study, we optimized a specified metal cation in a previously established *S.cerevisiae* strain displaying XylC. We investigated the effect of each

metal cation on the catalytic function of the XylC-displaying *S. cerevisiae*. Results showed that the divalent cobalt cations (Co^{2+}) notably enhanced the activity by 46-fold. Co^{2+} also contributed to D-xylose fermentation, which resulted in improving ethanol yields and xylose consumption rates by 6.0- and 2.7-fold, respectively. The utility of the extracellular xylose isomerization system was exhibited in the presence of mixed sugar. XylC-displaying yeast showed the faster D-xylose uptake than the yeast producing XI intracellularly. Furthermore, direct xylan saccharification and fermentation was performed by a unique yeast co-culture system. A xylan-degrading yeast strain was established by displaying two kinds of xylanases; endo-1,4-β-xylanase (Xyn11B) from *Saccharophagus degradans*, and β-xylosidase (XlnD) from *Aspergillus niger*. The yeast co-culture system enabled fine-tuning of the initial ratios of the displayed enzymes (Xyn11B:XlnD:XylC) by adjusting the inoculation ratios of Xylanases (Xyn11B and XlnD)-displaying yeast and XylC-displaying yeast. When the enzymes were inoculated at the ratio of 1:1:2 (1.39×10^{13}: 1.39×10^{13}: 2.78×10^{13} molecules), 6.0 g/L ethanol was produced from xylan.

Isopentenol (3-methyl-3-buten-1-ol), a biogasoline candidate, has an established heterologous gene pathway but is toxic to several microbial hosts. Reagents used in the pretreatment of plant biomass, such as ionic liquids, also inhibit the growth of many host strains. We explored the use of *C. glutamicum* as an alternative host to address these constraints. We found *C. glutamicum* ATCC 13032 to be tolerant of both the final product, isopentenol, as well to three classes of ionic liquids compared with the previous host (i.e., *Escherichia coli*). A heterologous mevalonate-based isopentenol pathway was engineered in *C. glutamicum*. Targeted proteomics for the heterologous pathway proteins indicated that the 3-hydroxy-3-methylglutaryl-coenzyme A reductase protein, HmgR, is a potential rate-limiting enzyme in this synthetic pathway. Isopentenol titers were improved from undetectable to 1.25 g/L by

combining three approaches: media optimization; substitution of an NADH-dependent HmgR homolog from *Silicibacter pomeroyi*; and development of a *C. glutamicum* Δ*poxB* Δ*ldhA* host chassis. Furthermore, we identified engineered strains of *C. glutamicum* that produce 5 g/L TMP and or co-produce both TMP and isopentenol. Ionic liquids also stimulate TMP production in the engineered strains. Using fed-batch cultivation, the strains stimulated by ionic liquids enabled to produce 2.2 g/L of TMP. We show that feedback from a specific heterologous gene pathway on host physiology leads to TMP's precursor accumulation (i.e., acetoin) and the production of TMP.

Chapter I Introduction

The transition of Energy and Motivation to Biofuels

Energy[1] is the capacity for doing work and may exist in various forms (e.g., potential, kinetic, thermal, electrical, chemical, and nuclear), which is essential to nearly all human activities and meeting the energy demand of all the nations is the challenge that the world faces today. "Industrial Revolution" happened in the latter half of the 18th century, brought the game-changing use of energy for industry, transportation, and communication that are lying the foundation of modern society.

Fossil fuels such as petroleum (e.g., crude oil and refined products generated from the processing of crude oil), coal, and natural gas have been the principal energy sources in the world[1]. However, the consumption of fossil fuels has raised concerns regarding environmental (e.g., global warming), political (e.g., energy security), and economic impacts (e.g., oil price). Seeking for sustainable and alternative energy sources has become an extensive area of research and been promoted by energy security, diversification of energy sources, energy footprints, and technological developments.

Petroleum fuel use has increased anthropogenic emissions of greenhouse gases (e.g., water vapor, carbon dioxide, nitrous oxide, methane, hydrofluorocarbons, perfluorocarbons, and sulfur hexafluoride), which may impact climatic inconsistency[2]. Renewable energy obtained from inexhaustible and infinite sources (i.e., sunlight, wind, geothermal, and biomass) is explored as future energy supply. Biomass is an organic non-fossil fuel-based material derived from a biological origin, which is generated from atmospheric CO_2, water, and sunlight

[1] The definition of Energy is described at https://sciencing.com/formula-energy-5215119.html

through biological photosynthesis. Hence, biomass has been pointed out to be one of the sustainable sources of renewable energy with net-zero carbon emission[3]. Biofuels (e.g., ethanol, biodiesel, biogas, and biobutanol) are advocated as eco-friendly and sustainable sources of energy, which are primarily used for transportation fuels by blending with petroleum fuels (e.g., gasoline and diesel fuel). The benefits of using these blending are that it can reduce the consumption of gasoline and diesel fuel produced from crude oil[4].

Global production of biofuels reaches 153 billion liters in the year 2018, which is a nearly 7% increase from the year 2017[1]. The United States and Brazil dominated the production of 69% of biofuels in the year 2018 followed by China (3.4%), Germany (2.9%), and Indonesia (2.7%)[1]. Bioethanol is the main product of biofuels with the production of 112 billion liters in 2018[1]. As a biomass source of commercial bioethanol production, edible feedstock such as, corn, sugar cane, and others crops, have been used and called as 1st generation feedstock; nevertheless, this feedstock would require farmland and crops for biofuels production, which could potentially affect food security, economic, and ethical problems primarily in developing countries. Therefore, lignocellulosic feedstocks and macroalgae are receiving considerable attention as 2nd and 3rd generation feedstock[5,6].

Lignocellulosic feedstocks (e.g., switchgrass) mainly consist of three polymers; cellulose (35-50%), hemicellulose (20-35%), and lignin (10-25%) with other auxiliary groups (e.g., acetyl and phenolic substituents)[5,7]. These polymers are cross-linked with each other in a hetero matrix to different degrees, where the architecture and quantify in the cell walls differ in line with species, tissues, growing stages, species, and source of the biomass[8,9]. In the cell walls, they organize in a three-dimensional structure, which results in forming the recalcitrance structure consist of the crystallinity of cellulose, hydrophobicity of lignin, and encapsulation of cellulose by the lignin-hemicellulose matrix[10].

Macroalgae is also marked as the next generation feedstock due to its advantages over terrestrial lignocellulosic biomass, low contents of recalcitrant compounds like lignin, no agricultural land use, and no fertilizer input such as pesticides and water[11]. Carbon neutrality is additional merit of macroalgae utilization because the uptake of CO_2 could offset the net CO_2 emission during biofuel production and combustion during photosynthesis[12]. The photosynthetic efficiency is reported by 6-8%, which is higher than terrestrial biomass (2%)[13].

Pretreatment of Biomass

'Pretreatment' is the process that transforms biomass consisting of polysaccharides into a form that is susceptible to the action of enzymatic hydrolysis to improve the efficiency of downstream steps (e.g., fermentation). Generally, pretreatment methods can be categorized into groups[14]; physical (e.g., comminution), chemical (e.g., acids and ionic liquids), biological (e.g., white-rot fungi), and combinatorial methods (e.g., steam pretreatment). Dilute acid pretreatment (DA) is one of the physicochemical pretreatments, where biomass is mixed with dilute acids such as sulfuric acid and hydrochloric acid and then heated with steam[15]. This method has achieved high reaction rates and improved biomass hydrolysis[16]. However, the pretreated hydrolysate includes inhibitors (e.g., weak acids, furan derivatives, and phenolic compounds) for the downstream microbial fermentation[17]. "Ionic liquids (ILs)" that are salts in liquid form at relatively low temperature (i.e., room temperature) is an emerging pretreatment method that can enhance enzymatic degradation[18]. ILs comprises of large organic cations (e.g., imidazolium cation) and (in)organic anions (e.g., chloride and acetate), where the combination of cation and anion determines the Physico-chemical characteristics (e.g., polarity and viscosity) of types of ionic liquids and has different effects on the pretreatment efficiency[18,19]. Compared with the conventional pretreatment such as the diluted acid method, a certain

hydrophilic ILs allows the rapid extraction with the relatively low loading lignocellulosic inhibitors[20,21]. A disadvantage is that certain ILs have intrinsic microbial toxicity, and thus, selection of IL-resistant microbial host and or engineering microbial hosts is required. This topic will be further discussed in Chapter III.

From Past to Present of Microbial Engineering

Microorganisms can be used for biocatalysts for the cost-effective production of fuels (e.g., ethanol, isobutanol, n-butanol, hydrocarbons, oils, and lipids), chemicals (e.g., succinic acids, 1,3-propanediol, 3-hydroxypropionic acid, 1,4-butanediol, acrylic acid, lactic acid, and isoprene), and pharmaceuticals (e.g., artemisinin and amorphadiene)[22]. Exploiting the metabolic diversity of bacteria, fungi, and microalgae enable the use of different starting substrates. The advent of plentiful genetic manipulation tools enable to engineer microorganisms to convert simple substrates (e.g., glucose, xylose, galactose, etc.) into several types of biofuels (e.g., alcohols, alkanes, fatty acid alkyl esters, and terpenes) with high titers, rate (or productivity), and yield[23]. Additionally, the replacement of conventional chemical synthesis with microbial-based production is reported to reduce environmental footprint regarding energy usage and emission[24]. The microbial-based production also takes advantages of producing molecules that are difficult to synthesize by other strategies (e.g., organic synthesis) due to chirality or the complexity of the targeted chemical structure[22]. Traditionally, microbial strains used for industrial applications have been identified through screening of naturally selected strains, developed through random mutagenesis and subsequent screening processes, directed evolution, and dominant selection schemes[25]. However, these traditional methods are slow, mostly uncontrolled, and unpredictable, which might result in unwanted alterations in the genome and the consequences of which leads to physiological changes in

cellular metabolism[26].

In the decade of the 1990s, the field of "Metabolic Engineering" was born with the following period of inquiry into the technological manifestations of genetical engineering with molecular biology (e.g., Polymerase Chain Reaction with Sanger sequencing, transformation techniques, and protein engineering), computational systems biology (e.g., in silico mathematical modeling, cell network analysis)[27]. "Synthetic Biology" is also an advocated study area intended for manipulating metabolic network for the synthesis of chemicals, the primary focus of which is fundamental biological research by the employment of synthesizing DNA fragments and controlling genetic circuits[22].

Metabolic Engineering is defined as "*the directed modulation of metabolic pathways using methods of recombinant technology for the purpose of overproducing fuels and chemical and pharmaceutical products"*[28]. It deals with the manipulation of native and or heterogeneous product synthesis pathways through optimizing physiological cellular processes for the desired compound production from a preferably cheap and simple substrate[29]. For instance, the success of metabolic engineering can be illustrated in amorphadiene[30], artemisinic acid[31], and opioid[32] production, where a biosynthesis pathway was transferred into a heterologous host with an enzyme characterization[27].

Synthetic Biology is defined as "*the design and construction of new biological components, such as enzymes, genetic circuits, and cells, or the redesign of existing biological systems*"[33,34]. This technology intents to design genetic building blocks (e.g., codon usage, ribosome binding sites, promoters, coding sequences, terminators, transcription factors, and transcription binding domains) and test the designed assemblies for the creation of artificial genetic circuits to obtain quantitative information of genetical landscapes[29]. Both these areas are dependent and require tools for genetic manipulation (e.g., mutagenesis, DNA assembly,

knockout of genes, integration of DNA blocks, and plasmids). Overall, metabolic engineering aims to apply all measured and or predicted information toward the optimization of the biological systems for the desired compound creation, where knowledge obtained from synthetic biology will be incorporated into the process.

Yeast cell surface engineering (also called "arming technology") is one of the engineering technologies to modify the external surface of yeast cells to display the desired protein for improving the catalytic ability of cells and easy separation of the product[35]. Extensive development of the technology has been implemented in *Saccharomyces cerevisiae*, which is known as an industrial relevant host with many strain engineering technologies and used for a variety of biochemical production. For instance, *S. cerevisiae* is capable of converting 93% of the input glucose into ethanol that is close to the theoretical yield (0.51 g ethanol/g of glucose)[36]. Chapter II describes the engineering *S. cerevisiae* with the yeast cell surface technology for simultaneous saccharification and fermentation of xylan.

Core Concept in Microbial Engineering

The rational functional expression of biosynthetic gene clusters in heterologous hosts is an ideal strategy for biochemical production. Due to strain-specific regulatory systems such as codon-usage (tRNA abundance), GC-bias, and extensive robustness of host cell metabolism (e.g., redundancy, regulation, and tight interaction of metabolism throughout the all cellular processes), the heterogeneous could be limited. "Design-Build-Test-Learn (DBTL)" cycle is marked as one of the central concepts for microbial engineering comprising of four structures: (1) Design of a biological circuit for the desired molecule biosynthesis; (2) Build the designed circuit by assembling DNA blocks and introduce into a production relevant microbial chassis, where tools are also developed from synthetic biology; (3) Test the function of the engineered

biological system to evaluate performance indices (i.e., titers, rates, and yield), growth, and physiology, where it is expedient to utilize high-throughput -omics approaches (e.g., genomics, transcriptomics, proteomics, and metabolomics) for global analysis; and (4) Learn of overall performance of the engineered systems to inform decision making for the next rounds[27].

Construction of Biological System

To harness rationally designed a pathway into microbial hosts, it is ideal to select amenable microbial hosts that executes the functional activation of the pathway with the tolerance for the harsh operating conditions such as tolerance to lignocellulosic inhibitors (e.g., furfural, 5-hydroxymethylfurfural, and acetate), pretreatment reagents (e.g., ionic liquids), and final products[37]. Generally, overexpression of the desired pathway modules is the start point of metabolic engineering followed by modulation of endogenous metabolism through knocking out competing pathways for precursors, product, and co-factors (e.g., electron carriers). For instance, metabolic engineering of the isoprenoid pathways has been implemented for diversified terpene-based compounds production (e.g., limonene[38] and farnesene[39]). The mevalonate (MVA) pathway, which exists in mammals, fungi, and plant cytosol, has been selected from *Saccharomyces cerevisiae* and harnessed into *E. coli* for biofuel production (e.g., 3-methyl-3-buten-1-ol (isopentenol) production in 2.23 g/L[40])[2]. Chapter III and IV show and discuss studies about the MVA pathway introduction and implementation in *Corynebacterium glutamicum* for biofuel production.

Improvement of Strain Performance

The predominant operational costs are coming from the fermentation process due to feedstock costs. The fermentation process is evaluated by three criteria (TRY); titer (final

product concentration), rate (production titer per unit of time), and yield (product concentration per unit of consumed raw biomass)[41]. Winnowing the best performer that meets the TRY demands is challenging because of the environmental gap between laboratory-scale cultures (e.g., shake flasks) and a commercial-scale bioreactor[42,43]. Chapter III and IV seek an optimal fermentation condition of an engineered *C. glutamicum* through testing and learning of extensive media optimization and metabolic engineering for scaled-up biofuel production under industrial relevant environments.

References

1. REN 21 Renewables Now. Renewables Global Status Report 2019. Galvanotechnik 105, (2019).
2. Liao, J. C., Mi, L., Pontrelli, S. & Luo, S. Fuelling the future: Microbial engineering for the production of sustainable biofuels. Nature Reviews Microbiology 14, 288–304 (2016).
3. Fargione, J., Hill, J., Tilman, D., Polasky, S. & Hawthorne, P. Land clearing and the biofuel carbon debt. Science, 319, 1235–1238 (2008).
4. Aydin, H. & Ilkiliç, C. Effect of ethanol blending with biodiesel on engine performance and exhaust emissions in a CI engine. Appl. Therm. Eng. 30, 1199–1204 (2010).
5. Isikgor, F. H. & Remzi Becer, C. Lignocellulosic biomass: a sustainable platform for the production of bio-based chemicals and polymers. Polym. Chem. 6, 4497 (2015).
6. Offei, F., Mensah, M., Thygesen, A. & Kemausuor, F. Seaweed bioethanol production: A process selection review on hydrolysis and fermentation. Fermentation 4, (2018).
7. Lynd, L. R., Weimer, P. J., van Zyl, W. H. & Pretorius, I. S. Microbial Cellulose Utilization: Fundamentals and Biotechnology. Microbiol. Mol. Biol. Rev. 66, 506–577 (2002).
8. Barakat, A., de Vries, H. & Rouau, X. Dry fractionation process as an important step in current and future lignocellulose biorefineries: A review. Bioresource Technology 134, 362–373 (2013).
9. Carere, C. R., Sparling, R., Cicek, N. & Levin, D. B. Third generation biofuels via direct cellulose fermentation. International Journal of Molecular Sciences 9, 1342–1360 (2008).
10. Scheller, H. V. & Ulvskov, P. Hemicelluloses. Annu. Rev. Plant Biol. 61, 263–289 (2010).
11. Wang, D., Kim, D. H. & Kim, K. H. Effective production of fermentable sugars from brown macroalgae biomass. Appl. Microbiol. Biotechnol. 100, 9439–9450 (2016).
12. Chirapart, A., Praiboon, J., Puangsombat, P., Pattanapon, C. & Nunraksa, N. Chemical composition and ethanol production potential of Thai seaweed species. J. Appl. Phycol. 26, 979–986 (2014).
13. Xu, X., Kim, J. Y., Oh, Y. R. & Park, J. M. Production of biodiesel from carbon sources of macroalgae, Laminaria japonica. Bioresour. Technol. 169, 455–461 (2014).

14. Agbor, V. B., Cicek, N., Sparling, R., Berlin, A. & Levin, D. B. Biomass pretreatment: Fundamentals toward application. Biotechnology Advances 29, 675–685 (2011).
15. Mosier, N. et al. Features of promising technologies for pretreatment of lignocellulosic biomass. Bioresour. Technol. 96, 673–686 (2005).
16. Sun, Y. & Cheng, J. Hydrolysis of lignocellulosic materials for ethanol production: A review. Bioresour. Technol. 83, 1–11 (2002).
17. Palmqvist, E. & Hahn-Hägerdal, B. Fermentation of lignocellulosic hydrolysates. II: Inhibitors and mechanisms of inhibition. Bioresour. Technol. 74, 25–33 (2000).
18. Stark, A. Ionic liquids in the biorefinery: A critical assessment of their potential. Energy Environ. Sci. 4, 19–32 (2011).
19. Brandt, A., Gräsvik, J., Hallett, J. P. & Welton, T. Deconstruction of lignocellulosic biomass with ionic liquids. Green Chemistry 15, 550–583 (2013).
20. Alvira, P., Tomás-Pejó, E., Ballesteros, M. & Negro, M. J. Pretreatment technologies for an efficient bioethanol production process based on enzymatic hydrolysis: A review. Bioresour. Technol. 101, 4851–4861 (2010).
21. Li, C. et al. Comparison of dilute acid and ionic liquid pretreatment of switchgrass: Biomass recalcitrance, delignification and enzymatic saccharification. Bioresour. Technol. 101, 4900–4906 (2010).
22. Tyo, K. E., Alper, H. S. & Stephanopoulos, G. N. Expanding the metabolic engineering toolbox: more options to engineer cells. Trends in Biotechnology 25, 132–137 (2007).
23. Zhang, F., Rodriguez, S. & Keasling, J. D. Metabolic engineering of microbial pathways for advanced biofuels production. Current Opinion in Biotechnology 22, 775–783 (2011).
24. Saling, P. Eco-Efficiency Analysis of biotechnological processes. Applied Microbiology and Biotechnology 68, 1–8 (2005).
25. Derkx, P. M. et al. The art of strain improvement of industrial lactic acid bacteria without the use of recombinant DNA technology. 31,
26. Park, J. H. & Lee, S. Y. Towards systems metabolic engineering of microorganisms for amino acid production. Current Opinion in Biotechnology 19, 454–460 (2008).
27. Nielsen, J. & Keasling, J. D. Engineering Cellular Metabolism. Cell 164, 1185–1197 (2016).
28. Metabolic Engineering: Principles and Methodologies - George Stephanopoulos, Aristos

A. Aristidou, Jens Nielsen - Google Books. Available at: https://books.google.co.jp/books?hl=en&lr=&id=9mGzkso4NVQC&oi=fnd&pg=PP1&ots=sl3a2zWYwg&sig=RbcMupmoTULCSPnNARoIBXXlrAk&redir_esc=y#v=onepage&q&f=false. (Accessed: 12th December 2019)

29. García-Granados, R., Lerma-Escalera, J. A. & Morones-Ramírez, J. R. Metabolic Engineering and Synthetic Biology: Synergies, Future, and Challenges. Front. Bioeng. Biotechnol. 7, (2019).
30. Westfall, P. J. et al. Production of amorphadiene in yeast, and its conversion to dihydroartemisinic acid, precursor to the antimalarial agent artemisinin. Proc. Natl. Acad. Sci. U. S. A. 109, (2012).
31. Paddon, C. J. et al. High-level semi-synthetic production of the potent antimalarial artemisinin. Nature 496, 528–532 (2013).
32. Luo, X. et al. Complete biosynthesis of cannabinoids and their unnatural analogues in yeast. Nature 567, 123–126 (2019).
33. Ingram, L. O. et al. Metabolic engineering for production of biorenewable fuels and chemicals: Contributions of synthetic biology. Journal of Biomedicine and Biotechnology 2010, (2010).
34. Keasling, J. D. Synthetic biology for synthetic chemistry. ACS Chemical Biology 3, 64–76 (2008).
35. Kuroda, K. & Ueda, M. Arming technology in yeast-novel strategy for whole-cell biocatalyst and protein engineering. Biomolecules 3, 632–650 (2013).
36. Majidian, P., Tabatabaei, M., Zeinolabedini, M., Naghshbandi, M. P. & Chisti, Y. Metabolic engineering of microorganisms for biofuel production. Renewable and Sustainable Energy Reviews 82, 3863–3885 (2018).
37. Ruegg, T. L. et al. An auto-inducible mechanism for ionic liquid resistance in microbial biofuel production. Nat. Commun. 5, 1–7 (2014).
38. Frederix, M. et al. Development of an E. coli strain for one-pot biofuel production from ionic liquid pretreated cellulose and switchgrass. Green Chem. (2016). doi:10.1039/C6GC00642F
39. Meadows, A. L. et al. Rewriting yeast central carbon metabolism for industrial isoprenoid production. Nature 537, 694–697 (2016).

40. George, K. W. et al. Metabolic engineering for the high-yield production of isoprenoid-based C5 alcohols in E. coli. Sci. Rep. 5, 11128 (2015).
41. Nielsen, J. & Keasling, J. D. Leading Edge Review Engineering Cellular Metabolism. Cell 164, 1185–1197 (2016).
42. Wehrs, M. et al. Engineering Robust Production Microbes for Large-Scale Cultivation. Trends in Microbiology 27, 524–537 (2019).
43. Humphrey, A. Shake Flask to Fermentor: What Have We Learned? Biotechnol. Prog. 14, 3–7 (1998).

Chapter II Enhanced Direct Ethanol Production by Cofactor Optimization of Cell Surface-Displayed Xylose

Production and use of liquid biofuels have been promoted to address issues that the current world faces[1]. Bioethanol is one of the sustainable and renewable energies, the majority of which is generated from edible sources in Brazil and the USA[2]. However, increasing concerns with food security such as competition with food supply and limited farm area, utilization of non-edible biomass has gradually promoted. The non-edible biomass (i.e., lignocellulosic biomass[3] and macroalgae[4]) has several advantages over the edible biomass; non-competition with food supply, high abundance, and large-scale availability.

Cellulose and hemicellulose are major components of the non-edible biomass[5]. Cellulose is the most abundant organic polymer, while hemicellulose is the second abundant polymer consisting of 30-40% lignocellulose[6]. Xylan is composed of β-1,4-linked xylopyranoside units and accounts for over 90% of the hemicellulose[7]. Bioconversion of xylan into bioethanol will promote the non-edible biomass use.

In the previous study[8], a direct ethanol production from birchwood xylan was performed through an engineered *S. cerevisiae*[9]. The engineered yeast allows direct decomposition of xylan into D-xylose by co-displaying two xylanases,[10] an endo-1,4-β-xylanase (EC 3.2.1.8) and β-xylosidase (EC 3.2.1.37), on the cell surface[11,12]. To metabolize the produced monomer, D-xylose, two oxidoreductase enzymes have predominantly studied[13], NAD(P)H-dependent D-xylose reductase (XR; EC 1.1.1.307), and xylitol dehydrogenase (XDH; EC 1.1.1.9). However, these enzymes are known to cause intracellular redox imbalance, which results in decreasing ethanol yields due to the accumulation of sub-products such as xylitol and glycerol[14-16].

Xylose isomerase (XI; EC 5.3.1.5), broadly produced in bacteria, is known to catalyze the reversible isomerization of D-xylose into D-xylulose.[17] The use of XI instead of the XR/XDH improves the ethanol theoretical yields from 0.46 g ethanol/g xylose to 0.51 g ethanol/g xylose[18]. In the previous study, an *S. cerevisiae* strain displaying xylose isomerase (XylC) from *Clostridium cellulovorans* has been developed and demonstrated the simultaneous isomerization and fermentation (SIF)[19] of D-xylose[20]. Isomerization of the extracellular D-xylose into D-xylulose could improve D-xylose import because D-xylulose is readily assimilated by yeast cells[21,22]. However, ethanol yields of the previous study[20] remained low, which could be due to the limited activity of XylC. Metal cations such as Mg^{2+}, Mn^{2+}, or Co^{2+} are reported to improve the catalytic activity and stability of XIs[23,24]. Therefore, I aimed to optimize the metal cation against XylC

Recently, Motone et al.[25] reported a yeast co-culture system, which realized ethanol fermentation from laminarin by optimizing inoculation ratios of Gly5M- and BG-displaying yeast strains. The co-culture system enables to adjust the initial ratio of yeast strains. In this study, I applied the yeast co-culture system for simultaneous saccharification and fermentation of xylan. For the saccharification purpose of xylan, a xylan-degrading *S. cerevisiae* strain that co-displays Xyn11B (an endo-1,4-β-xylanase from *Saccharophagus degradans* 2-40[26]) and XlnD (a β-xylosidase from *Aspergillus niger*[27]) was designed and built in this study.

Materials and Methods

Strains, media, and culture conditions

Escherichia coli strain DH5α [*F*$^-$, Φ80d*lac*ZΔM15 (*lac*ZYA-*arg*F) U169, *deo*R, *rec*A1, *end*A1, *hsd*R17 (r_K^-, m_K^+), *phoA*, supE44, λ$^-$, *gyr*A96, *rel*A1] (Toyobo, Osaka, Japan) was used as a host for recombinant DNA manipulation. Bacteria were grown in Luria-Bertani medium [1% (*w/v*) tryptone, 0.5% (*w/v*) yeast extract, and 0.5% (*w/v*) sodium chloride] containing 100 μg/mL ampicillin.

S. cerevisiae strain BY4741/*Δsed1* (*MAT***a**, *his3Δ1*, *leu2Δ0*, *met15Δ0*, *ura3Δ0*, *YDR077w::kanMX4*), which was obtained from EUROSCARF (Frankfurt, Germany), was used as a host for cell-surface display of proteins. Yeast cells were aerobically cultured in yeast extract peptone dextrose medium [1% (*w/v*) yeast extract, 2% (*w/v*) glucose, and 2% (*w/v*) peptone] for transformation. For activity assays of xylanases and xylose isomerase, yeast cells were cultivated in synthetic dextrose (SDC) medium [0.67% (*w/v*) yeast nitrogen base without amino acids, 2% (*w/v*) glucose, 2% (*w/v*) casamino acids, 0.002% (*w/v*) L-histidine, 0.003% (*w/v*) L-leucine, and 0.003% (*w/v*) L-methionine] buffered with 50 mM 2-morpholino-ethanesulfonic acid (MES) at pH 6.0. For ethanol fermentation from D-xylose, yeast cells were cultivated in SXC medium [0.67% (*w/v*) yeast nitrogen base without amino acids, 50 mM D-xylose, 2% (*w/v*) casamino acids, appropriate amino acids, 100 mM MES (pH 6.7), and 0-10 mM cobalt(II) chloride (Sigma Aldrich, MO, USA)]. For uptake assay of mixed sugar, yeast cells were cultivated in SDXC medium [0.67% (*w/v*) yeast nitrogen base without amino acids, 3% (*w/v*) glucose, 2% (*w/v*) xylose, 2% (*w/v*) casamino acids, appropriate amino acids, 100 mM MES (pH 6.7), and 3 mM cobalt(II) chloride]. For ethanol fermentation from xylan, yeast cells were cultivated in SXNC medium [0.67% (*w/v*) yeast nitrogen base without amino acids, 10% (*w/v*) birchwood xylan

(Sigma Aldrich, MO, USA), 2% (*w/v*) casamino acids, appropriate amino acids, 100 mM MES (pH 6.7), and 3 mM cobalt(II) chloride].

Construction of plasmids

All primers used for the plasmid construction are listed in **Table 1**. The gene encoding endo-1,4-β-xylanase, *Xyn11B* (*Sde_3061*), was amplified from the genomic DNA of *S. degradans* 2-40 (ATCC 43961) by polymerase chain reaction (PCR) using KOD-Plus-Neo DNA polymerase (Toyobo, Osaka, Japan), where the primer pair, Infusion-Xyn11B-F and Infusion-Xyn11B-R was used. The gene encoding xylosidase gene, *XlnD* from *Aspergillus niger* (ATCC9142), was codon-optimized and chemically synthesized (GENEWIZ, NJ, USA) for expression in *S. cerevisiae*, and amplified by PCR using the primer pair, Infusion-XlnD-F and Infusion-XlnD-R. The gene encoding xylose isomerase, *XylC* (*Clocel_0590*), was amplified from the genomic DNA of *C. cellulovorans* (ATCC 43961) by PCR using the primer pairs, Infusion-XylC-F and Infusion-XylC-R, or Infusion-XylCI-F and Infusion-XylCI-R. Amplified DNA fragments were cloned into appropriate vectors using the In-Fusion HD cloning kit (Takara Bio, Shiga, Japan).

Amplified DNA fragment encoding *Xyn11B* was inserted into the *Bgl* II-*Xho* I fragment of pULD1[28] for display on the yeast cell surface. Amplified DNA fragments encoding *XylC* was inserted into the *Bgl* II-*Xho* I fragment of pULD1 and the *EcoR* I-*Xho* I fragment of pULI1[29] for intracellular production. The resultant plasmids were named pULD1-Xyn11B, pULD1-XylC, and pULI1-XylC-I, respectively. The amplified DNA fragment of *XlnD* was cloned into the *Bgl* II-*Xho* I fragment of pULDP for display on the yeast cell surface, and the resultant plasmid was named pULDP-XlnD. The pULDP was constructed as follows: (i) The *PGK1* promoter region was amplified from pGK426 (NBRP; BYP7373) by PCR using the primer pair, pGK426-PGK1-PF and pGK426-PGK1-PR. The *PGK1* terminal region was amplified by PCR using the primer

pair, pGK426-PGK1-TF and pGK426-PGK1-TR. (ii) The region, encoding multiple cloning site, its epitope region of $(His)_6$-tag, and α-agglutinin, was amplified from pULD1 by PCR using the primer pair, pULD1-PCR-MF and pULD1-PCR-MR. (iii) The region, encoding *ori*, *Amp*^{r}, *URA3*, *2μm*, and *leu2-d*, was amplified by PCR using the primer pair, pULD1-PCR-F and pULD1-PCR-R. (iv) These amplified DNA fragments were fused together, and the resultant plasmid was named pULDP. The *URA3* sequence of the pULDP-XlnD was replaced with *HIS3* as follows. First, the pULDP-XlnD except for the *URA3* region was amplified by PCR using the primer pair, pULD1-URA3-F and pULD1-URA3-R. Next, the *HIS3* gene was amplified from pRS423[30] by PCR using the primer pair, pRS423-HIS3-F and pRS423-HIS3-R. Finally, these amplified DNA fragments were fused together, and the resultant plasmid was named pHLD1-XlnD.

Table 1. Primers used in this study

Primers	Feature or sequence (5'-3')
Infusion -Xyn11B-F	CTTTGCTCGTTTCTGCCAAGTCAATCAATGTATGCGGCAGACG
Infusion -Xyn11B-R	CTTGTAATCAGATCCACCTTGTGAGTTACAGGTATTTTGCGAAAC
Infusion -XlnD-F	TTGCTCGTTTCTGCCGCACACAGTATGTCAAGACCAG
Infusion -XlnD-R	AGACCAAGATCCACCTTCTTTACCAGGCCATTTC
Infusion -XylC-F	GCTAAAGAGTACTTCCCACAGATTCAGAAG
Infusion -XylC-R	TTGATACATTGCGATAATAGCTTCGTACAATTCCTG
Infusion -XylCI-F	AAACACACATAAACAAGAGAATATTTTGCAAATGTACCG
Infusion -XylCI-R	GTCATCCTTGTAATCGTCGTTGAAGATGTATTGGTTAAC
pGK426-PGK1-PF	GATTACGCCAAGCTTAAGATGCCGATTTGGGCGCGAATC
pGK426-PGK1-PR	GTTTTATATTTGTTGTAAAAAGTAGATAATTACTTCCTTGATGATC
pGK426-PGK1-TF	ATTGAATTGAATTGAAATCGATAGATCAATTTTTTTCTTTTCTCTTTC
pGK426-PGK1-TR	CTACATCGCGGTACCAACGCAGAATTTTCGAGTTATTAAACTTAAAATACGCTG
pULD1-PCR-MF	CAACAAATATAAAACGAATTCATGCAACTGTTCAATTTGCCATTGAAAG
pULD1-PCR-MR	TCAATTCAATTCAATTTAGAATAGCAGGTACGACAAAAGCAGAAAAATG
pULD1-PCR-F	GGTACCGCGATGTAGTAAAACTAGCTAG
pULD1-PCR-R	AAGCTTGGCGTAATCATGGTCATAGCTG
pULD1-URA3-F	TATACATGCATTTACTTATAATACAGTTTT
pULD1-URA3-R	CGTCTTCAAGAATTAGCTTTTCAA
pRS423-HIS3-F	CAATAGCATATCTTTGTTAACGAAGCATCTGTGCTTC
pRS423-HIS3-R	CGAAAAGTGCCACCTGACGTCTAAGAAACCATTATTATCATG

Yeast transformation

The constructed plasmids were introduced into yeast cells based on the lithium acetate method[31] by EZ-Yeast transformation kit (BIO 101, CA, USA). Transformed yeast cells were isolated on a selective SD medium plate at 30 ºC for 2-3 days. The transformant harboring pULD1, pULD1-s, pULI1, pULD1-Xyn11B, pHLD1-XlnD, pULD1-Xyn11B and pHLD1-XlnD, pULD1-XylC, pULI1-XylC, was named, BYs-Emp, BYs-Emps, BYs-Emp-I, BYs-Xyn11B, BYs-XlnD, BYs-Xyn11B_XlnD, BYs-XylC, and BYs-XylC-I, respectively (**Table 2**).

Table 2. Constructed yeast strains and plasmids in this study

Yeast strains and Plasmids	Features	Sources or reference
Yeast strains		
BY4741/*Δsed1*	*MAT***a**, *his3Δ1*, *leu2Δ0*, *met15Δ0*, *ura3Δ0*, *YDR077w::kanMX4*	EUROSCARF
BYs-Emp	Control strain harboring empty pULD1 and/or pHLD1	Kuroda et al. (2009)
BYs-Emps	Control strain harboring empty pULD1-s	Kuroda et al. (2009)
BYs-Emp-I	Control strain harboring empty pULI1	This study
BYs-Xyn11B	Display of Xyn11B (pULD1-Xyn11B)	This study
BYs-XlnD	Display of XlnD (pHLD1-XlnD)	This study
BYs-Xyn11B_XlnD	Co-display of Xyn11B (pULD1-Xyn11B) and XlnD (pHLD1-XlnD)	This study
BYs-XylC	Display of XylC (pULD1-XylC)	This study
BYs-XylC-I	Intracellular production of XylC (pULI-XylC)	
Plasmids		
pULD1	*URA3, GADPH* promoter and terminator, 3'half α-aggulutinin, FLAG tag	Kuroda et al. (2009)
pULD1-s	*URA3, GADPH* promoter and terminator, 3'half α-aggulutinin, Strep tag	Kuroda et al. (2009)
pULI1	*URA3, GADPH* promoter and terminator, FLAG tag	Miura et al. (2013)
pULDP	*URA3 PGK1* promoter and terminator	This study
pHLD1	*HIS3, PGK1* promoter and terminator	This study
pULD1-Xyn11B	*URA3*, display of *S. degradans* Xyn11B	This study
pHLD1-XlnD	*HIS3*, display of *A. niger* XlnD	This study
pULD1-XylC	*URA3*, display of *C. cellulovorans* XylC	This study
pULI1-XylC	*URA3*, intracellular production of *C. cellulovorans* XylC	

Immunofluorescence microscopy

Displayed proteins were immunofluorescently labeled as previously described[32]. Yeast cells were labeled with two primary antibodies at a dilution rate of 1:300 under gentle shaking for 1.5 h at room temperature. Mouse immunoglobulin G (IgG) against the FLAG peptide tag (Sigma Aldrich, MO, USA) was used for Xyn11B and XylC labeling and rabbit IgG against $(His)_6$

(QIAGEN, Hilden, Germany) was used for XlnD labeling. After washing with phosphate-buffered saline (PBS; pH 7.4), yeast cells were incubated with secondary antibodies at a dilution rate of 1:300 under gentle shaking for 1.5 h at room temperature. Goat anti-mouse IgG conjugated with Alexa Fluor 488 (Invitrogen, CA, USA), and goat anti-rabbit IgG conjugated with Alexa Fluor 405, were used as the secondary antibody. After washing with PBS (pH 7.4), yeast cells were observed by Inverted microscope IX71 (Olympus, Tokyo, Japan) equipped with a U-MNIBA2 mirror unit, a BP470-490 excitation filter, a DM505 dichronic mirror, and a BA510-550 emission filter (Olympus, Tokyo, Japan). Live images were obtained by Digital change-coupled device camera (Hamamatsu Photonics, Shiga, Japan) and Aqua Cosmos 2.0 software (Hamamatsu Photonics, Shiga, Japan).

Activity assay of the xylose isomerase-displaying yeast

After pre-cultivation, yeast cells were aerobically cultivated in SDC medium at 30 ºC for 48 h, 1 mL of yeast culture with OD_{600} of 20 was centrifuged at 13,000 *g* for 1 min. After washing twice with PBS (pH 7.4), yeast cells were re-suspended in 1 mL of the solution including 50 mM D-xylose, 50 mM MES (pH 6.5), and 10 mM metal cations from first transition series (Mn^{2+}, Fe^{2+}, Fe^{3+}, Co^{2+}, Co^{3+}, Ni^{2+}, Cu^{2+}, and Mg^{2+}). After incubation at 60 °C for 1.5 h, the mixture was centrifuged at 13,000 *g* at 4 ºC for 5 min, and purified with Ultrafree-MC 0.45-μm centrifugal filter device (Millipore, Darmstadt, Germany). Compounds were analyzed by High-performance liquid chromatography (HPLC) instrument (Shimadzu, Kyoto, Japan) equipped with a sugar-D column (Nacalai Tesque, Kyoto, Japan), and detected by Coulochem III electrochemical detector (EC) (Thermo Fisher Scientific, MA, USA). The system was operated at 40 °C with 80% (*v/v*) acetonitrile (flow rate, 0.5 mL/min) and 0.4 M KOH (flow rate, 0.3 mL/min) as the mobile phase.

Examinations of the optimal Co^{2+} concentration (0-20 mM) against XylC-displaying yeast were also performed as the same procedure.

Quantitative determination of sugars and ethanol

Concentrations of D-xylose and ethanol were measured by HPLC system equipped with an Aminex HPX-87H column (Bio-Rad, CA, USA) and a RID-10A refractive index detector (Shimadzu, Kyoto, Japan). The system was operated at 60 °C with 5 mM H_2SO_4 (flow rate, 0.75 mL/min) as the mobile phase.

Ethanol fermentation from D-xylose

After pre-cultivation, yeast cells were aerobically cultivated in SDC medium at 30 ºC for 48 h, and 1 mL of yeast culture with OD_{600} of 20 was centrifuged at 13,000 *g* for 1 min. After washing twice with PBS (pH 7.4), yeast cells were re-suspended in 1.0 mL of the SXC medium containing 0-10 mM cobalt(II) chloride and incubated at 30 °C under gentle shaking. All fermentations were performed in closed tubes at 30 ºC on a rotator.

Uptake assay of mixed sugars

After pre-cultivation, yeast cells were aerobically cultivated in SDC medium at 30 ºC for 48 h, and 1 mL of yeast culture with OD_{600} of 3 was centrifuged at 13,000 *g* for 1 min. After washing twice with PBS (pH 7.4), yeast cells were re-suspended in 1.0 mL of the SDXC medium and incubated at 30 °C under gentle shaking. All fermentations were performed in closed tubes at 30 ºC on a rotator.

Xylan hydrolysis by xylanases-co-displaying yeast

After pre-cultivation, yeast cells were aerobically cultivated in SD medium at 30 ºC for 48 h, and 1 mL of yeast culture with OD_{600} of 10 was centrifuged at 13,000 *g* for 1 min. After washing twice with PBS (pH 7.4), yeast cells were re-suspended in 1.0 mL of a PBS solution (pH 7.4) containing 1% (*w/v*) xylan and/or 3 mM cobalt(II) chloride and incubated under gentle shaking at 30 ºC for 3 h. After harvesting yeast cells by centrifugation at 13,000 *g* for 1 min, supernatants were mixed with a 3,5-dinitrosalicylic acid (DNS) solution (NaOH, 16 g/L; potassium sodium tartrate, 300 g/L; DNS, 5 g/L)[33] at a 1:2 ratio, and incubated at 100 ºC for 5 min. Each 200 μL of the solution was transferred into a 96-well transparent flat bottom microplate, and absorbance at 530 nm was measured using D-xylose as the standard.

Xylan fermentation

After pre-cultivation, each yeast cell was aerobically cultivated in SD medium at 30 ºC for 48 h, 1 mL of yeast culture with OD_{600} of 50 was centrifuged at 13,000 *g* for 1 min. After washing twice with PBS (pH 7.4), each yeast cell was inoculated into SXNC medium at different ratios, including 10% (*w/v*) xylan, and/or 3 mM cobalt(II) chloride, where total inoculated amount of yeast cells were fixed as OD_{600} of 100. Ethanol fermentation was performed at 30 ºC in a closed tube on the rotator.

Results and Discussion

Determination of the optimal metal cation for XylC

Our previous study determined optimal parameters such as pH and temperature of XylC (xylose isomerase from *C. cellulovorans*)-displaying yeast strain as pH 6.5 and 60 °C, respectively[20]. The feature (e.g., thermal stability, optimal temperature, and pH) of displayed enzymes has identical characteristic with secreted enzymes[34]. Although C-terminal of XylC is connected with α-agglutinin, the active site of XylC is distantly positioned from the terminal and thus the anchoring would not affect its activity. To improve the catalytic activity of XylC, metal cations known to associate with XI activity were screened. After the display of XylC was confirmed (**Figure 1**), the engineered yeast cells were incubated with D-xylose and eight types of metal cations. Results showed that divalent cobalt cation (Co^{2+}) significantly improved the catalytic activity by 46-fold (**Figure 2**). Co^{3+} and Mn^{2+} also enhanced the activity by 28-and 10-fold, respectively. Metal cations; Fe^{2+}, Fe^{3+}, Ni^{2+}, and Cu^{2+} did not support the catalytic activity (data not shown). The optimal concentration of Co^{2+} were determined as 6-10 mM (**Figure 3**).

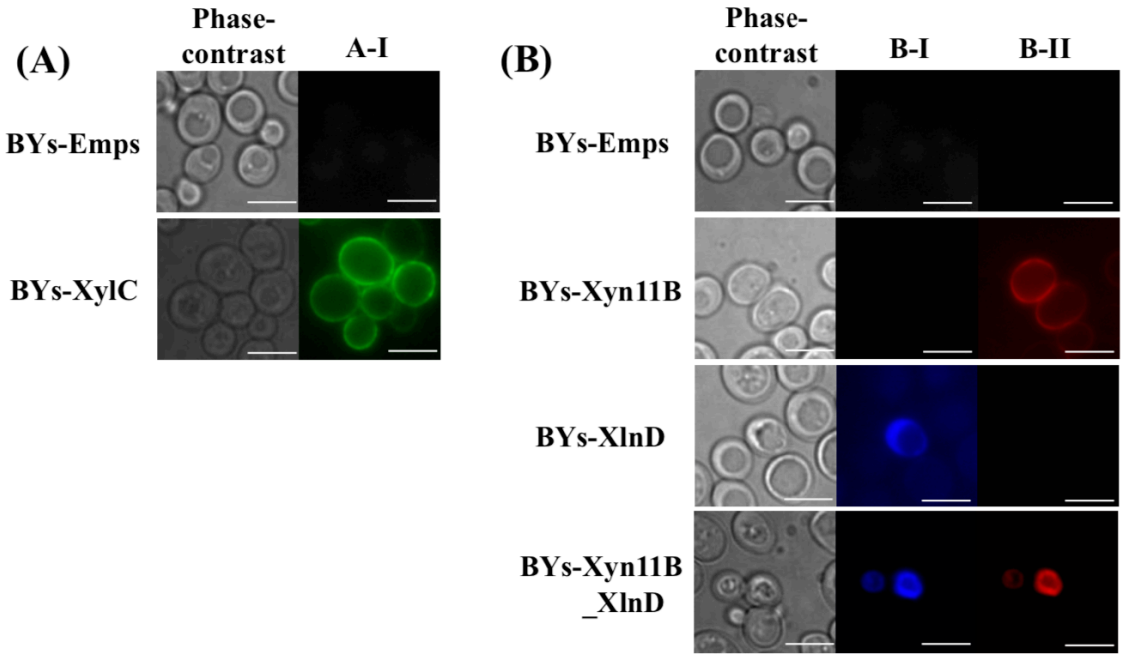

Figure 1. Fluorescence observation of the displaying cells after immunofluorescence labeling (A) xylose isomerase (XylC), and (B) endo-1,4-β-xylanase (Xyn11B) and β-xylosidase (XlnD). Yeast cells were labeled with rabbit anti-(His)6 antibody and goat anti-mouse IgG conjugated with Alexa Fluor 405 (column I). Yeast cells were labeled with mouse anti-FLAG antibody and goat anti-mouse IgG conjugated with Alexa Fluor 488 (column A-I) or Alexa Fluor 546 (column B-II). Yeast expressing pULD1-s harboring Strep-tag was used as a negative control. The scale bar is 5 μm.

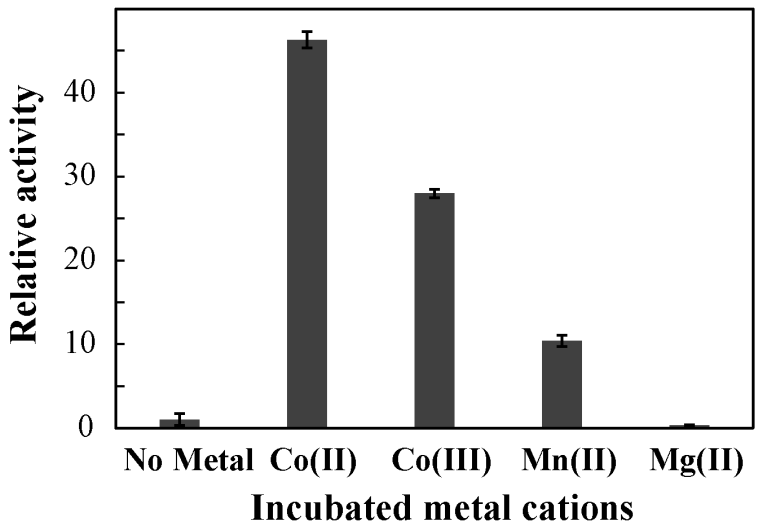

Figure 2. Effect of individual metal cations on the enzymatic activity of displayed XylC.

XylC-displaying yeast (OD_{600} of 20) was inoculated into a solution containing 50 mM D-xylose and 10 mM individual metal cations. Effects of individual cofactors were evaluated by measuring the amounts of produced D-xylulose, and evaluation of the relative activities was performed using a strain incubated with no cation as the reference. Results are shown as means of the triplicate experiments, and error bars represent the standard errors.

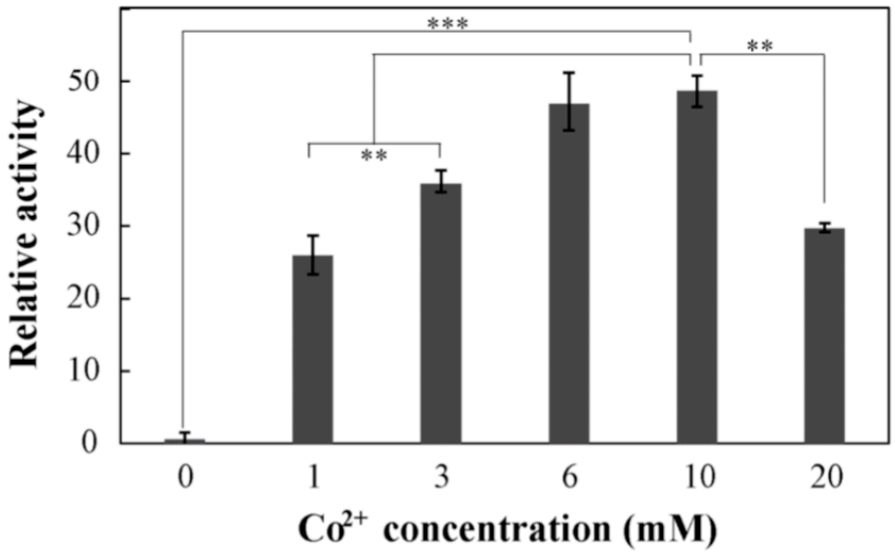

Figure 3. Examination of optimal Co^{2+} concentration on XylC-displaying yeast strain
XylC-displaying yeast strain (OD_{600} of 20) was incubated with 0-20 mM cobalt(II) chloride. The asterisks indicate data points, in which a significant difference between the 10 mM Co^{2+} incubated yeast strain and other 0, 1, 3, and 20 mM Co^{2+} incubated yeast strains was observed (Tukey's test : ***$p < 0.001$, **$p < 0.01$, *$p < 0.05$). Data shown are the average (n=3) ± standard errors.

Effect of Co^{2+} on ethanol production from D-xylose in XylC-displaying yeast

I hypothesized that Co^{2+} supplementation into fermentation media would improve ethanol yields from D-xylose. Firstly, the effects of different Co^{2+} concentrations were determined. The result showed that 3 mM Co^{2+} was the most effective for the ethanol fermentation (**Figure 4**), where ethanol-specific production rate and D-xylose consumption rate were 38 ± 7.1 mg ethanol·g-cell^{-1}·h^{-1} and 150 ± 3.6 mg xylose·g-cell^{-1}·h^{-1}, respectively (**Figure 5**). These results were markedly higher than the control (incubated without Co^{2+}); 6.3 ± 0.79 mg ethanol·g-cell^{-1}·h^{-1} and 56 ± 2.7 mg xylose·g-cell^{-1}·h^{-1} that are 6.0- and 2.7-fold, respectively (**Table 3**).

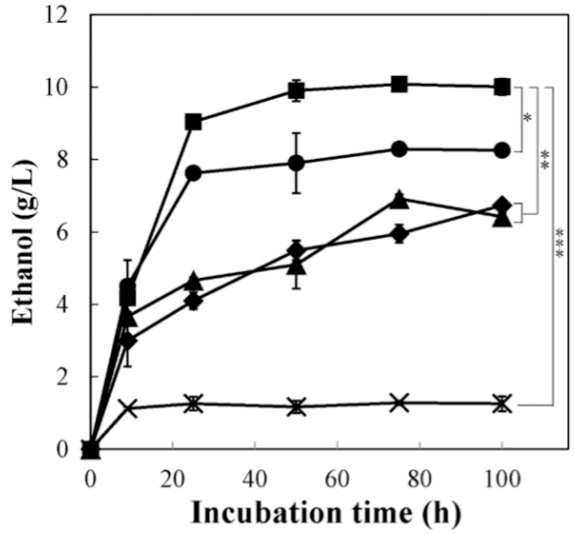

Figure 4. Examination of optimal Co^{2+} in ethanol fermentation from D-xylose

Ethanol production profiles were illustrated as BYs-XylC incubated with different Co^{2+} concentrations: 0 mM (×), 0.25 mM (▲), 3 mM (■), 6 mM (●), and 10 mM (◆). Data shown are the average (n=3) ± standard errors and analyzed by one-way ANOVA. Multiple comparisons were corrected by Bonferroni test: ***$p < 0.001$, **$p < 0.01$, *$p < 0.05$

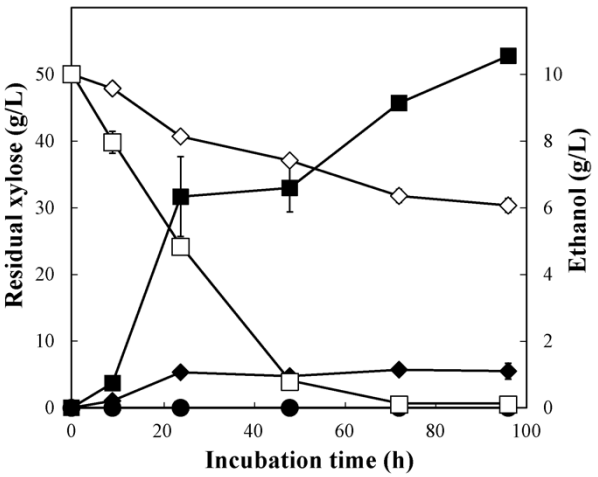

Figure 5. Ethanol production from D-xylose by XylC-displaying yeast strain.

XylC-displaying yeast (OD_{600} of 20) was inoculated into SXC medium, containing 5% (*w/v*) D-xylose as a sole carbon source buffered at pH 6.7 with 100 mM MES, and supplemented with 3 mM cobalt(II) chloride. Ethanol production profiles were illustrated as BYs-Emp (●), BYs-XylC without Co^{2+} (◆), and BYs-XylC with Co^{2+} (■). D-Xylose consumption profiles were illustrated as BYs-XylC without Co^{2+} (◇), and BYs-XylC with Co^{2+} (□). Results are shown as means of triplicate experiments, and error bars represent the standard errors.

Table 3. Effect of Co^{2+} on D-xylose consumption and ethanol production rates using the XylC-displaying yeast strain

Strain	Specific xylose consumption rate (mg/g-cell/h)	Specific ethanol productivity (mg/g-cell/h)	Ethanol yield (mg/g-xylose)
BYs-XylC with no cation	56 ± 2.7	6.3 ± 0.79	130 ± 14
BYs-XylC with Co^{2+}	150 ± 3.6	38 ± 7.1	250 ± 46
Fold change*	2.7 ± 0.20	6.0 ± 2.1	1.9 ± 0.57

* Fold change was calculated by BYs-XylC-Co (II) cation/ BYs-XylC-no cation.

Effects of the extracellular isomerization on D-xylose uptake

Transporting D-xylose into yeast cells has been a great challenge in previous studies because *S. cerevisiae* lacks a dedicated transport system for pentose sugars[35]. To improve the D-xylose uptake, researchers have introduced heterologous D-xylose transporters[36,37]. Extracellular D-xylose isomerization could be an alternative approach for tackling the issue because it relies on the natural mechanism that yeast can import and utilize D-xylulose.

To proof the advantage of the extracellular D-xylose isomerization, D-xylose uptake properties were analyzed between BYs-XylC and BYs-XylC-I that intracellularly produces XylC in the presence of mixed sugars. Each yeast strain was incubated in the media including both D-xylose and D-glucose at a 2:3 ratio, which was determined based on the general lignocellulosic composition ratio. In the early phase, BYs-XylC showed faster D-xylose uptake than other strains (**Figure 6**). After 55 hours, BYs-XylC showed the highest D-xylose consumption. All yeast strains completely consumed the supplied D-glucose within 10 hours (**Figure 6**). An analysis of the BYs-XylC fermentation media showed that there remained a negligible quantity of D-xylulose in the supernatant (**Figure 7**). The produced D-xylulose was supposed to be immediately incorporated into yeast cells. Therefore, the extracellular D-xylose isomerization would improve the D-xylose uptake.

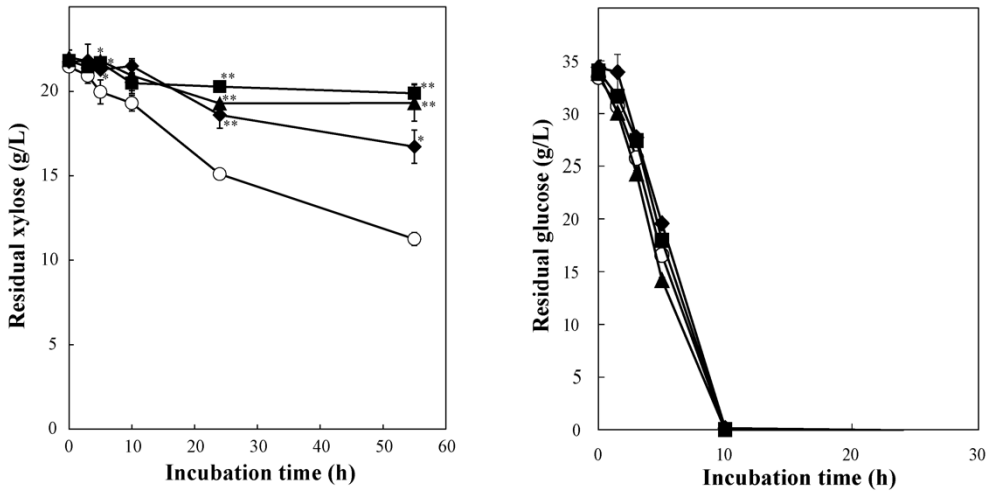

Figure 6. Sugar uptake property of XylC-displaying yeast in the mixture sugars

Both XylC-displaying yeast and XylC-intracellularly-producing yeast (OD_{600} of 20) were inoculated into fermentation media containing 3% (*w/v*) glucose, 2% (*w/v*) xylose, and 3 mM cobalt(II) chloride buffered at pH 6.7 with 100 mM MES. Residual concentrations of xylose (A) and glucose (B) in the culture supernatant were illustrated as BYs-Emp (■), BYs-Emp-I (▲), BYs-XylC-I (◆), and BYs-XylC (○). Data shown are the average (n=3) ± standard errors and analyzed by one-way analysis of variance (ANOVA) followed by Tukey's test to correct multiple comparisons (**$p < 0.01$, *$p < 0.05$).

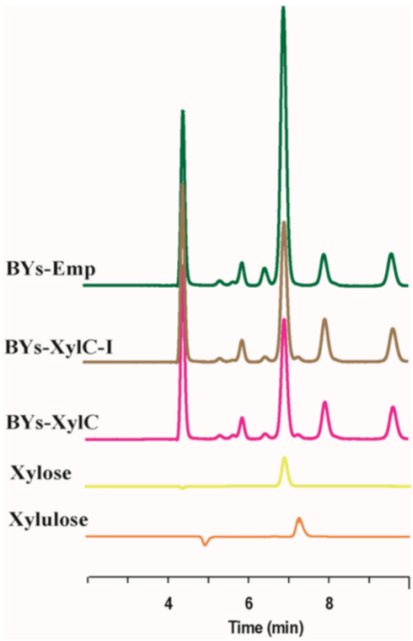

Figure 7. HPLC analysis of xylulose and products from xylose

Yeast displaying XylC (BYs- XylC), yeast producing XylC intracellularly (BYs-XylC-I), and control yeast (BYs-XylC-I) are shown.

Co-display of endo-1,4-β-xylanase and β-xylosidase on the yeast cell surface for direct conversion of xylan into D-xylose

To achieve direct decomposition of xylan into D-xylose, a yeast strain co-displaying Xyn11B (endo-1,4-β-xylanase from *S. degradans* 2-40) and XlnD (β-xylosidase from *Aspergillus niger*) was designed and developed (named as BYs-Xyn11B_XlnD). The co-display of these xylanases was confirmed by immunofluorescence labeling (**Figure 1**).

HPLC analysis showed that BYs-Xyn11B_XlnD enabled to degrade xylan into D-xylose as the leading products (**Figure 7**). The DNS assay result showed that BYs-Xyn11B_XlnD released more substantial amounts of reducing sugars (344 mg/L) than the single enzyme-displaying strains, BYs-Xyn11B (250 mg/L) and BYs-XlnD (58 mg/L) (**Table 4**).

Table 4. Hydrolysis of xylan by xylanases-displaying yeast strains

Strain	Amounts of reducing sugars (mg/L)
BYs-Emp	45 ± 3.0
BYs-XlnD	58 ± 0.0
BYs-Xyn11B	250 ± 16.0
BYs-Xyn11B_XlnD	344 ± 1.0

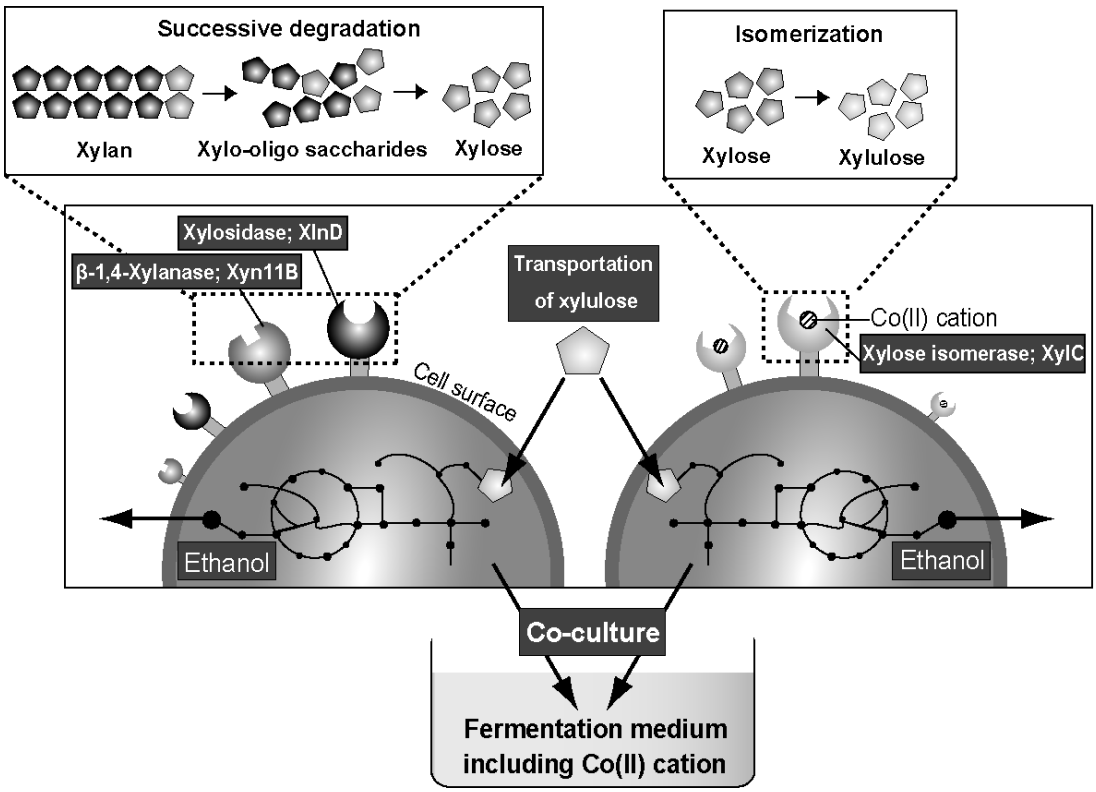

Figure 8. Diagram of the co-culture system designed for xylan saccharification and fermentation.

Yeast co-culture platform, including both xylanases-displaying yeast strain and xylose isomerase-displaying yeast strain, is illustrated. Xylan is degraded into D-xylose by Xyn11B- and XlnD-co-displaying yeast strain. The produced D-xylose is converted into D-xylulose by XylC-displaying yeast strain, and the D-xylulose is metabolized for ethanol fermentation by both yeast strains.

Direct ethanol fermentation from xylan using the yeast co-culture system

To achieve direct ethanol fermentation from xylan, the yeast co-culture system consisting of each yeast strain; xylan-degrading yeast and xylose-isomerizing yeast was built (**Figure 8**). An optimal inoculation ratio was determined by inoculating each yeast strain in 5 ratios under 3 mM Co^{2+} supplementation. When both yeast strains were inoculated at the equal ratio, the maximum ethanol titer (6 g/L) was achieved after 200 hours fermentation (**Figure 9**). The Co^{2+} effect against xylanases were confirmed to be insignificant (**Figure 10**).

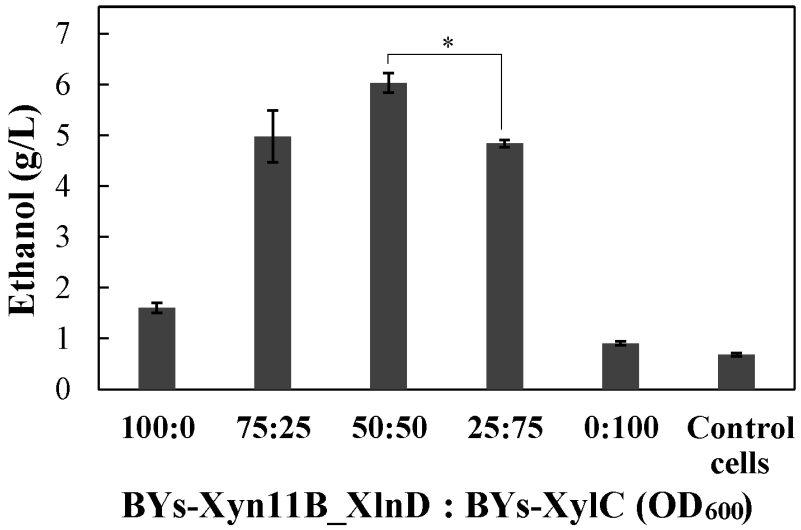

Figure 9. Comparison of different inoculation ratios uses for xylan fermentation.
Each yeast strain was inoculated into the fermentation medium, containing 10% (*w/v*) xylan as a sole carbon source buffered at pH 6.7 with 100 mM MES, and supplemented with 3 mM cobalt(II) chloride. All initial OD_{600} values were adjusted to 100, and five ratios (100:0, 75:25, 50:50, 25:75, and 0:100) between BYs-Xyn11B_XlnD and BYs-XylC were examined. Results are presented as means of triplicate experiments, and error bars represent the standard errors. Three different ratios (75:25, 50:50, and 25:75) were analyzed by Tukey's test (**$p < 0.01$, *$p < 0.05$).

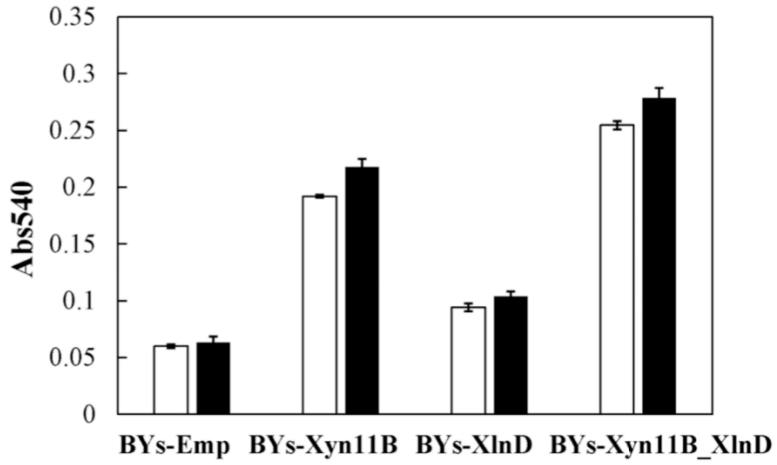

Figure 10. Effects of Co^{2+} on the catalytic activity of xylanases

Catalytic activity of each strain was determined by measuring the degraded amounts of reducing sugars using the DNS assay. White bars show no Co^{2+} addition, whereas black bars represent 3 mM Co^{2+} addition.

To investigate the usability of the yeast co-culture system, I calculated the optimal ratio of each displayed enzyme and corresponding effects on ethanol productivity. A relationship between the number of displayed enzymes (**Table 5**) and ethanol productivity was evaluated after incubation for 200 h (**Figure 9**). For simplification, I defined that displayed enzymes are evenly distributed on the yeast cell surface, and the number of enzymes and yeast cells were fixed in the calculation. The following variables were used: n_{en} (around 10^4 molecules), the number of displayed enzymes on the yeast cell surface[38]; n_{yc} (5.55×10^7 cells; OD_{600} of 1), the number of yeast cells used in fermentation[39]; and n_{ten}, the total number of displayed enzymes in fermentation. The inoculated Xyn11B:XlnD:XylC ratio of 1:1:2 (1.39×10^{13}: 1.39×10^{13} : 2.78×10^{13} molecules) represented the maximum ethanol yield as shown in Figure 5. The ethanol yield was 1.2- and 1.25-fold higher than others, 1:1:6 (0.69×10^{13}: 0.69×10^{13}: 4.16×10^{13} molecules) and 3:3:2 (2.08×10^{13}: 2.08×10^{13}: 1.39×10^{13} molecules), respectively. The result points to the importance of designing an appropriate inoculation ratio of each specified yeast strain for efficient ethanol fermentation from xylan, which could expand the utility of yeast co-culture system.

Table 5. Effects of the inoculated number of enzymes in the co-culture system

OD_{600} of the strains		Co-displayed xylanases ($\times10^{13}$ molecules)		Displayed xylose isomerase ($\times10^{13}$ molecules)	Ethanol (g/L)
BYs-Xyn11B_XlnD	BYs-XylC	Xyn11B	XlnD	XylC	
100	0	2.78	2.78	—	1.6 ± 0.096
75	25	2.08	2.08	1.39	5.0 ± 0.51
50	50	1.39	1.39	2.78	6.0 ± 0.19
25	75	0.69	0.69	4.16	4.8 ± 0.071
0	100	—	—	5.55	0.91 ± 0.038
0	0	—	—	—	0.68 ± 0.037

In case of OD_{600} of the strains (0:0), BYs-Emp was inoculated as the control.

In the optimal fermentation condition, 6.0 g/L ethanol production was achieved (**Figure 11**), where the inoculation ratio of xylan-degrading yeast (OD_{600} of 50) and xylose-isomerizing yeast (OD_{600} of 50) was Xyn11B:XlnD:XylC ratio of 1:1:2 (1.39×10^{13}: 1.39×10^{13} : 2.78×10^{13} molecules). The yield was superior to those of single cultured strains, xylan-degrading yeast and xylose-isomerizing yeast. The supernatant composition analysis of BYs-Xyn11B_XlnD indicated that initial releases of oligosaccharides and the subsequent productions of D-xylose from xylan. After incubation for 200 hours, 6.1 g/L ethanol was produced by BYs-Xyn11B_XlnD, while low levels of D-xylose were detected from the co-cultured medium (data not shown). This result indicates that the produced D-xylose was immediately isomerized and then consumed by yeast cells.

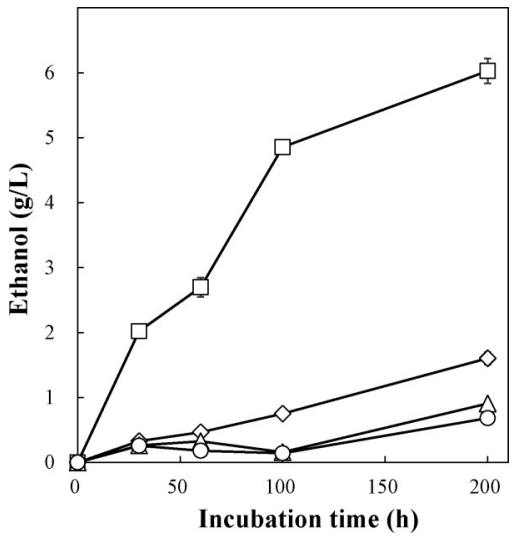

Figure 11. Direct production of ethanol from birchwood xylan using a yeast co-culture system.

Ethanol production was examined at different inoculation ratios between Xyn11B- and XlnD-co-displaying yeast strain and XylC-displaying yeast strain. Each yeast strain was inoculated into SXC medium, containing 10% (*w/v*) xylan as a sole carbon source buffered at pH 6.7 with 100 mM MES, and supplemented with 3 mM cobalt(II) chloride. All initial OD_{600} values were adjusted to 100. Ethanol fermentation was performed at following inoculation ratios between BYs-Xyn11B_XlnD and BYs-XylC: 100:0 (◇), 50:50 (□), 0:100 (△), while BYs-Emp was inoculated as the control (○). Results are shown as means of triplicate experiments, and error bars represent the standard errors.

The previous study reported the co-display of an endo-xylanase (Xyn II) and a xylosidase (XylA) on the cell surface of *S. cerevisiae* that possesses *XR*, *XDH*, and *XK* genes[40]. In contrast, I applied the yeast co-culture system because excess enzyme productions on the single yeast cell surface could decrease the number of displayed enzymes[41]. Furthermore, the yeast co-culture system would be useful since the introduced number of each yeast strain can be readily optimized depending on biomass compositions.

Summary

In this chapter, Co^{2+} was identified as a critical cofactor to enhance the catalytic activity of XylC displayed yeast. Supplementation of Co^{2+} into fermentation media contributed to the improved catalytic activities of XylC and ethanol fermentation from D-xylose. The advantage of extracellular D-xylose isomerization was demonstrated as a D-xylose utilization. By optimizing the inoculated enzyme ratio to 1:1:2 (1.39×10^{13}: 1.39×10^{13}: 2.78×10^{13} molecules), 6 g/L ethanol production from xylan was achieved.

References

1 Himmel, M. E. et al. Biomass recalcitrance: engineering plants and enzymes for biofuels production. Science 315, 804-807, doi:10.1126/science.1137016 (2007).

2 Sanchez, O. J. & Cardona, C. A. Trends in biotechnological production of fuel ethanol from different feedstocks. Bioresource technology 99, 5270-5295, doi:10.1016/j.biortech.2007.11.013 (2008).

3 Service, R. F. Cellulosic ethanol. Biofuel researchers prepare to reap a new harvest. Science 315, 1488-1491, doi:10.1126/science.315.5818.1488 (2007).

4 Ross, A. B., Jones, J. M., Kubacki, M. L. & Bridgeman, T. Classification of macroalgae as fuel and its thermochemical behaviour. Bioresource technology 99, 6494-6504, doi:10.1016/j.biortech.2007.11.036 (2008).

5 Carroll, A. & Somerville, C. Cellulosic Biofuels. Annu Rev Plant Biol 60, 165-182, doi:10.1146/annurev.arplant.043008.092125 (2009).

6 Cano, A. & Palet, C. Xylooligosaccharide recovery from agricultural biomass waste treatment with enzymatic polymeric membranes and characterization of products with MALDI-TOF-MS. J Membrane Sci 291, 96-105, doi:10.1016/j.memsci.2006.12.048 (2007).

7 Saha, B. C. Hemicellulose bioconversion. Journal of industrial microbiology & biotechnology 30, 279-291, doi:10.1007/s10295-003-0049-x (2003).

8 Katahira S, Fujita Y, Mizuike A, Fukuda H, Kondo A. Construction of a xylan-fermenting yeast strain through codisplay of xylanolytic enzymes on the surface of xylose-utilizing Saccharomyces cerevisiae cells. Appl Environ Microbiol 70, 5407– 5414 (2004).

9 Kondo, A. & Ueda, M. Yeast cell-surface display-applications of molecular display. Applied microbiology and biotechnology 64, 28-40, doi:10.1007/s00253-003-1492-3 (2004).

10 Kulkarni, N., Shendye, A. & Rao, M. Molecular and biotechnological aspects of xylanases. FEMS microbiology reviews 23, 411-456 (1999).

11 Lynd, L. R., Weimer, P. J., van Zyl, W. H. & Pretorius, I. S. Microbial cellulose utilization: fundamentals and biotechnology. Microbiology and molecular biology reviews : MMBR 66, 506-577, table of contents (2002).

12 Kuroda, K. & Ueda, M. Arming Technology in Yeast-Novel Strategy for Whole-cell Biocatalyst and Protein Engineering. Biomolecules 3, doi:10.3390/biom3030632 (2013).

13 Eliasson, A., Christensson, C., Wahlbom, C. F. & Hahn-Hagerdal, B. Anaerobic xylose fermentation by recombinant Saccharomyces cerevisiae carrying XYL1, XYL2, and XKS1 in mineral medium chemostat cultures. Applied and environmental microbiology 66, 3381-3386, doi:Doi 10.1128/Aem.66.8.3381-3386.2000 (2000).

14 Van Vleet, J. H. & Jeffries, T. W. Yeast metabolic engineering for hemicellulosic ethanol production. Current opinion in biotechnology 20, 300-306, doi:10.1016/j.copbio.2009.06.001 (2009).

15 Matsushika, A., Inoue, H., Kodaki, T. & Sawayama, S. Ethanol production from xylose in engineered Saccharomyces cerevisiae strains: current state and perspectives. Applied microbiology and biotechnology 84, 37-53, doi:10.1007/s00253-009-2101-x (2009).

16 Kim, D. M. et al. Reduction of PDC1 expression in S. cerevisiae with xylose isomerase on xylose medium. Bioprocess and biosystems engineering 35, 183-189, doi:10.1007/s00449-011-0638-4 (2012).

17 Bhosale, S. H., Rao, M. B. & Deshpande, V. V. Molecular and industrial aspects of glucose isomerase. Microbiological reviews 60, 280-300 (1996).

18 Lee, S. M., Jellison, T. & Alper, H. S. Directed evolution of xylose isomerase for improved xylose catabolism and fermentation in the yeast Saccharomyces cerevisiae. Applied and environmental microbiology 78, 5708-5716, doi:10.1128/AEM.01419-12 (2012).

19 Lastick, S. M., Tucker, M. Y., Beyette, J. R., Noll, G. R. & Grohmann, K. Simultaneous Fermentation and Isomerization of Xylose. Applied microbiology and biotechnology 30, 574-579 (1989).

20 Ota, M. et al. Display of Clostridium cellulovorans xylose isomerase on the cell surface of Saccharomyces cerevisiae and its direct application to xylose fermentation. Biotechnology progress 29, 346-351, doi:10.1002/btpr.1700 (2013).

21 Chiang, L. C., Gong, C. S., Chen, L. F. & Tsao, G. T. D-Xylulose Fermentation to Ethanol by Saccharomyces-Cerevisiae. Applied and environmental microbiology 42, 284-289 (1981).

22 Chu, B. C. H. & Lee, H. Genetic improvement of Saccharomyces cerevisiae for xylose fermentation. Biotechnology advances 25, 425-441, doi:10.1016/j.biotechadv.2007.04.001 (2007).

23 Hartley, B. S., Hanlon, N., Jackson, R. J. & Rangarajan, M. Glucose isomerase: insights into protein engineering for increased thermostability. Biochimica et biophysica acta 1543, 294-335 (2000).

24 Callens, M. et al. Metal ion binding to D-xylose isomerase from Streptomyces violaceoruber. The Biochemical journal 250, 285-290 (1988).

25 Motone, K., Takagi, T., Sasaki, Y., Kuroda, K. & Ueda, M. Direct ethanol fermentation of the algal storage polysaccharide laminarin with an optimized combination of engineered yeasts. Journal of biotechnology 231, 129-135, doi:10.1016/j.jbiotec.2016.06.002 (2016).

26 Weiner, R. M. et al. Complete genome sequence of the complex carbohydrate-degrading marine bacterium, Saccharophagus degradans strain 2-40 T. PLoS genetics 4, e1000087, doi:10.1371/journal.pgen.1000087 (2008).

27 La Grange, D. C., Pretorius, I. S., Claeyssens, M. & van Zyl, W. H. Degradation of xylan to D-xylose by recombinant Saccharomyces cerevisiae coexpressing the Aspergillus niger beta-xylosidase (xlnD) and the Trichoderma reesei xylanase II (xyn2) genes. Applied and environmental microbiology 67, 5512-5519, doi:Doi 10.1128/Aem.67.12.5512-5519.2001 (2001).

28 Kuroda, K. et al. Enhancement of display efficiency in yeast display system by vector engineering and gene disruption. Applied microbiology and biotechnology 82, 713-719, doi:10.1007/s00253-008-1808-4 (2009).

29 Miura, N. et al. Spatial reorganization of Saccharomyces cerevisiae enolase to alter carbon metabolism under hypoxia. Eukaryotic cell 12, 1106-1119, doi:10.1128/EC.00093-13 (2013).

30 Mumberg, D., Muller, R. & Funk, M. Yeast vectors for the controlled expression of heterologous proteins in different genetic backgrounds. Gene 156, 119-122 (1995).

31 Ito, H., Fukuda, Y., Murata, K. & Kimura, A. Transformation of intact yeast cells treated with alkali cations. Journal of bacteriology 153, 163-168 (1983).

32 Nakanishi, A., Kuroda, K. & Ueda, M. Direct fermentation of newspaper after laccase-treatment using yeast codisplaying endoglucanase, cellobiohydrolase, and beta-glucosidase. Renew Energ 44, 199-205, doi:10.1016/j.renene.2012.01.078 (2012).

33 Sharon, A., Bailey, B. A., McMurtry, J. P., Taylor, R. & Anderson, J. D. Characteristics of ethylene biosynthesis-inducing xylanase movement in tobacco leaves. Plant physiology 100, 2059-2065 (1992).

34 Ueda, M. et al. Molecular breeding of polysaccharide-utilizing yeast cells by cell surface engineering. Annals of the New York Academy of Sciences 864, 528-537 (1998).

35 Hamacher, T., Becker, J., Gardonyi, M., Hahn-Hagerdal, B. & Boles, E. Characterization of the xylose-transporting properties of yeast hexose transporters and their influence on xylose utilization. Microbiology 148, 2783-2788, doi:10.1099/00221287-148-9-2783 (2002).

36 Hector, R. E., Dien, B. S., Cotta, M. A. & Mertens, J. A. Growth and fermentation of D-xylose by Saccharomyces cerevisiae expressing a novel D-xylose isomerase originating from the bacterium Prevotella ruminicola TC2-24. Biotechnology for biofuels 6, 84, doi:10.1186/1754-6834-6-84 (2013).

37 Katahira, S. et al. Improvement of ethanol productivity during xylose and glucose co-fermentation by xylose-assimilating S. cerevisiae via expression of glucose transporter Sut1. Enzyme Microb Tech 43, 115-119, doi:10.1016/j.enzmictec.2008.03.001 (2008).

38 Shibasaki, S. et al. Quantitative evaluation of the enhanced green fluorescent protein displayed on the cell surface of Saccharomyces cerevisiae by fluorometric and confocal laser scanning microscopic analyses. Applied microbiology and biotechnology 55, 471-475 (2001).

39 Bae, J., Kuroda, K. & Ueda, M. Proximity Effect among Cellulose-Degrading Enzymes Displayed on the Saccharomyces cerevisiae. Applied and environmental microbiology 81, 59-66, doi:10.1128/Aem.02864-14 (2015).

40 Katahira, S., Fujita, Y., Mizuike, A., Fukuda, H. & Kondo, A. Construction of a xylan-fermenting yeast strain through codisplay of xylanolytic enzymes on the surface of xylose-utilizing Saccharomyces cerevisiae cells. Applied and environmental microbiology 70, 5407-5414, doi:10.1128/AEM.70.9.5407-5414.2004 (2004).

41 Sakamoto, T., Hasunuma, T., Hori, Y., Yamada, R. & Kondo, A. Direct ethanol production from hemicellulosic materials of rice straw by use of an engineered yeast strain codisplaying three types of hemicellulolytic enzymes on the surface of xylose-utilizing Saccharomyces cerevisiae cells. Journal of biotechnology 158, 203-210, doi:10.1016/j.jbiotec.2011.06.025 (2012).

Chapter III Engineering *Corynebacterium glutamicum* to produce the biogasoline isopentenol from plant biomass

Microbial hosts used for the rapid discovery and development of metabolic pathways as well as process costs can have drawbacks that limit their biotechnological applications beyond the laboratory scale. These disadvantages include inhibition from components of the growth media and toxicity from metabolic intermediates or final products[1]. Solutions to several industrially relevant parameters and host sensitivities have been described, especially in model microbes such as *Escherichia coli* or *Saccharomyces cerevisiae*[2,3], and are increasingly considered important for scale-up in an industrial process. However, if genetic tractability does not limit the choice of the host organism, it is reasonable that any microbe could be utilized as a host for the expression of a heterologous gene pathway. Rather than develop solutions for individual aspects of an industrially relevant process, I viewed the choice of a microbial host as a means to bypass product and process reagent toxicities that would be encountered in the industrial process.

Corynebacterium glutamicum is a biotechnologically relevant host that presents several ideal characteristics for scale-up, such as a rapid phenotypic adjustment in response to environmental changes (e.g., oxygen levels and substrate availability), which are major causes of performance losses in industrial scale bioreactors[4,5]. Of particular relevance for renewable biofuel production is its capacity of simultaneously utilizing glucose and xylose, two major components of plant biomass hydrolysates[6,7], as well as *p*-coumaric and ferulic acids as carbon sources[8,9]. These factors have contributed to the development of *C. glutamicum* as a production host for many bioproducts[10-12]. As a broad category, terpene based compounds represent a rich source of biofuels and product targets[13]. Production of terpene compounds has been explored in *C.*

glutamicum but reported titers currently range from 0.2 mg/L to 23 mg/L for terpenes such as pinene and β-Carotene, respectively[14]. Isopentenol (also known as 3-methyl-3-buten-1-ol) is a prominent example of a terpene compound that is desirable as both biogasoline as well as a platform chemical and has been developed in other microbial systems (e.g., *E. coli*)[15], but not in *C. glutamicum*.

Growth inhibitory effects of residual pretreatment reagents, used to release metabolizable carbon sources from plant biomass, is another factor to be considered in the use of renewable carbon sources. Ionic liquids (ILs) represent one such class of pretreatment reagents[16-18] and have advantages over conventional pretreatments such as favorable sugar solubilization rates, less degradation of monosaccharides, and compatibility with downstream enzymatic processing[19]. Ionic liquids derived from 1-ethyl-3-methylimidazolium ($[C_2C_1im]^+$) are known to be toxic against several eukaryotes[20] and gram-negative bacteria[16]. New classes of ILs, such as cholinium ($[Ch]^+$) derived ILs[21] and protic ILs (such as ethanolamine acetate [ETA][OAc] and diethanolamine acetate [DEOA][OAc]) are emerging as equally effective but less toxic reagents for this application[22]. In contrast to other microbial hosts[23,24], the physiological response of *C. glutamicum* has not been explored in detail to any of these ILs that remain as residual components in the biomass hydrolysate.

In this chapter, I explore the tolerance of *C. glutamicum* ATCC 13032 as a microbial platform for the heterologous mevalonate-based production pathway of isopentenol (**Figure 1**). I characterized the innate tolerance of *C. glutamicum* to isopentenol, which is known to be toxic to other microbes[25], as well as three classes of ILs. Using proteomics, I identify a critical protein in the heterologous mevalonate pathway for isopentenol production. Furthermore, engineering the host strain background achieved isopentenol production in minimal defined media and IL extracted plant biomass hydrolysates in titers of 1.25 g/L and 1.1 g/L, respectively. These results

highlight the potential of *C. glutamicum* as a sustainable production chassis to produce terpene-based biofuels and bioproducts.

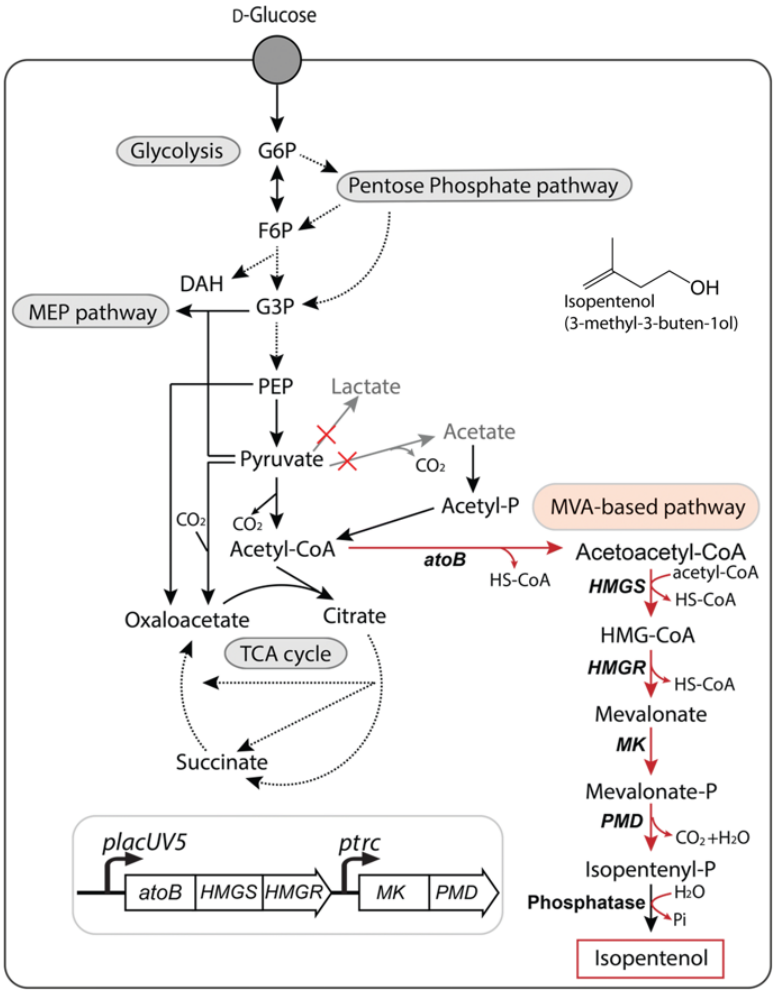

Figure 1. Global map of central metabolic pathways in *C. glutamicum* ATCC 13032 and the heterologous mevalonate-based pathway for isopentenol production. The mevalonate-based isopentenol biosynthesis pathway was described by Kang et al [31]. Broken lines show intermediate pathways omitted in glycolysis and the tricarboxylic acid cycle. The disrupted pathways in this work are shown in grey and indicated with a red "X". Relevant reactions are represented by the genes encoding their corresponding enzymes. Reactions involved in isopentenol biosynthesis are displayed with red arrows. Abbreviations: *atoB*, acetyl-CoA acetyltransferase; *HMGS*, hydroxymethylglutaryl-CoA synthase; *HMGR*, 3-hydroxy-3-methylglutaryl-CoA reductase; *MK*, mevalonate kinase; *PMD*, phosphomevalonate decarboxylase; MEP, methylerythritol-4-phosphate; MVA, mevalonate; G6P, glucose-6-phosphate; F6P, fluctose-6-phosphate; DAH, dihydroxyacetone phosphate; G3P, glyceraldehyde-3-phosphate; PEP, phosphoenolpyruvic acid; HMG-CoA, 3-hydroxy-3-methyl-glutaryl-coenzyme A; HS-CoA, coenzyme A; Pi, inorganic phosphate.

Materials and Methods

Chemicals and Reagents

All chemicals and reagents were purchased from Sigma-Aldrich (St. Louis, MO) or as otherwise indicated, and were of molecular biology grade or higher. When cells were cultivated in a microtiter dish format, plates were sealed with a gas-permeable film (Sigma-Aldrich, St. Louis, MO).

Strain and Plasmid Construction

All strains and plasmids used in this study are listed in Table 1 and 2, and their sequences are available at http://public-registry.jbei.org. Oligo-nucleotide primers were synthesized by Integrated DNA Technologies, Inc. (San Diego, CA). Q5 High-Fidelity DNA Polymerase (New England Biolabs, Ipswich, MA) was used for a polymerase chain reaction. Isothermal DNA assembly[26] was utilized to assemble plasmids using 40 nucleotide overhangs (NEBuilder HiFi DNA Assembly Master Mix, New England Biolabs, Ipswich, MA). Plasmids were constructed using chemically competent *E. coli* DH10β (New England Biolabs). Where indicated, the heterologous isopentenol production pathway was modified to incorporate the *hmgr* homolog from *Silicibacter pomeroyi* (NCBI: WP_011241944.1) to replace the existing gene from *S. cerevisiae* and the sequence was confirmed by Sanger sequencing. Integrated gene cassettes and gene deletions were confirmed by colony PCR to verify the complete excision at the targeted open reading frame using and inspected by agarose gel electrophoresis.

Table 1. Strains used in this study

Strain	Description	Selection	Reference
JBEI-7936	*Corynebacterium glutamicum* ATCC 13032 / NHRI 1.1.2, biotin auxotroph	Nx^R	Gift from Jay Keasling
JBEI-19571	JBEI-7936 harboring p/JBEI-19559	Kan^R	This study
JBEI-19652	JBEI-7936 harboring p/JBEI-19628	Kan^R	This study
JBEI-19658	JBEI-7936 harboring p/JBEI-19634	Kan^R	This study
JBEI-19563	JBEI-7936 Δ*poxB*	Suc^R, Kan^S	This study
JBEI-19566	JBEI-7936 Δ*poxB* Δ*ldhA*	Suc^R, Kan^S	This study
JBEI-19572	JBEI-19566 harboring p/JBEI-19559	Kan^R	This study
JBEI-19646	JBEI-19566 harboring p/JBEI-19625	Kan^R	This study
JBEI-19655	JBEI-7936 *cg1122:*P_{lacI}*-lacI-*P_{lacUV5}*–lacZα-T7 gene1:cg1121* "(DE3)"	Suc^R, Kan^S	This study
JBEI-19654	JBEI-19655 harboring p/JBEI-19632	Kan^R	This study
JBEI-18084	*C. glutamicum* Δ*cgIIM* Δ*cgIIR* Δ*cgIIIR* (methylation deficient strain)	Nx^R	This study
JBEI-19703	JBEI-18084 Δ*idsA*	Suc^R, Kan^S	This study
JBEI-19702	JBEI-19703 p/JBEI-19559	Kan^R	This study
JBEI-19657	*C. glutamicum* Δ*cgIIM* Δ*cgIIR* Δ*cgIIIR* Δ*idsA::*P_{LacUV5}*-atoB-ScHMGS-ScHMGR-*P_{trc}*-MK-ScPMD*	Suc^R, Kan^S	This study
JBEI-19656	JBEI-19657 harboring p/JBEI-19626 ("HMGR augmented")	Kan^R	This study
E. coli DH1	$F^- \lambda^-$ *endA1 recA1 relA1 gyrA96 thi-1 glnV44 hsdR17(*$r_K^- m_K^-$*)*		Meselson and Yuan, 1968
E. coli DH10β	F^- *endA1 deoR*$^+$ *recA1 galE15 galK16 nupG rpsL* Δ*(lac)X74* φ80*lacZΔM 15 araD139* Δ*(ara,leu)7697 mcrA* Δ*(mrr-hsdRMS-mcrBC)* Str^R λ^-		Invitrogen

Table 2. Plasmids used in this study

Plasmid	Description	Selection	Reference
JBEI-2600	pEC-XK99E, *E. coli-C. glutamicum* shuttle expression vectors based on the medium-copy number plasmid including *pGA1*, Kan^R, *ori*V, P_{trc}	Kan^R	Kirchner et al., 2003
pK18mobsacB	*sacB* counter-selection plasmid, *ori*V origin of replication	Kan^R	Schafer et al., 1994
JBEI-19558	pK18mobsacB-Δ*idsA*	Suc^s, Kan^R	This study
JBEI-19556	pK18mobsacB-Δ*poxB*	Suc^s, Kan^R	This study
JBEI-19557	pK18mobsacB-Δ*ldhA*	Suc^s, Kan^R	This study
JBEI-9321	pA5c-MevT(O)-T21-MKco-PMDsc "IPP-bypass pathway"	Cm^R	Kang et al., 2016
JBEI-19559	pEC-XK99E-AK-IP-bypass	Kan^R	This study
JBEI-19628	pTE221 pEC-XK99E-AK-IP-bypass-*S. aureus mvaK1, mvaS* (substitution)	Kan^R	This study
JBEI-19634	pTE222 pEC-XK99E-AK-IP-bypass-*C. kroppenstedtii mvaK1, mvaA* (substitution)	Kan^R	This study
JBEI-19625	pTE202 pEC-XK99E-AK-IP-bypass-*S. pomeroyi HMGR* (substitution)	Kan^R	This study
JBEI-19632	pTE155 pEC-XK99E-AK-IP-bypass, T7 promoter	Kan^R	This study
JBEI-19626	pLacUV5-*HMGR*	Kan^R	This study

Sorghum Biomass Pretreatment and Regeneration

Whole commercial-grade sorghum plants derived from *Sorghum bicolor* were grown, harvested, and milled in the 2017 harvest cycle by Chromatin Inc (New Deal, Texas). This biomass was pretreated with [Ch][Lys] and afterward, enzymatically saccharified for a total time of 72 hours

as described elsewhere[27]. To make CGXII amended with hydrolysate, CGXII was prepared using stock solutions of the individual components as described below. The hydrolysate was defrosted from storage at -80 ˚C, filter sterilized through a 0.45-micron filter, and added in place of water in CGXII media. Crystalline D-glucose was added to CGXII media with hydrolysate to increase the concentration up to 3.5% or 4% (w/v) as indicated.

Preparation of Electrocompetent C. glutamicum Cells

C. glutamicum was made electrocompetent as previously described[28]. In brief, cells were grown in NCM medium supplemented with 3% (v/v) glycine and electroporated with a Micro Pulser Electroporator (Bio-Rad Laboratories, Inc., Hercules, CA) at 10 μF, 600 Ω, and 1800 V. After electroporation cells were immediately mixed with 400 μL of BHIS broth and heat-shocked for 6 minutes at 46 ˚C. After a two-hour outgrowth at 30 ˚C, cells were plated on the appropriate selective media.

Growth Media Composition

Isopentenol production was analyzed in several different common growth medias. Lysogeny-Broth (LB): 10 g/L tryptone, 5 g/L yeast extract, and 5 g/L NaCl. Tryptone and yeast extract were purchased from BD Biosciences (Franklin Lakes, NJ). M9 minimal medium (Sambrook and Russell, 2001): 2 g/L $(NH_4)_2PO_4$, 2 g/L KH_2PO_4, 1 g/L K_2HPO_4, 1 g/L NH_4Cl, 0.5 g/L NaCl, 0.06 g/L $MgSO_4$, 1.1 g/L $CaCl_2$, 20 mg/L thiamine, and 0.2 mg/L biotin. CGXII minimal medium [29,30]: 20 g/L $(NH_4)_2SO_4$, 5 g/L urea, 1 g/L KH_2PO_4, 1 g/L K_2HPO_4, 0.25 g/L $MgSO_4$-$7H_2O$, 10 mg/L $CaCl_2$, 10 mg/L $FeSO_4$-$7H_2O$, 10 mg/L $MnSO_4$-H_2O, 1 mg/L $ZnSO_4$-$7H_2O$, 0.2 mg/L $CuSO_4$-$5H_2O$, 0.02 mg/L $NiCl_2$-$6H_2O$, 0.2 mg/L biotin, 30 mg/L 3,4-dihydroxybenzoic acid, and 21 g/L

3-morpholinopropanesulfonic acid (MOPS); pH 7.0). D-glucose was used as a carbon source at the % (w/v) concentration as indicated.

Toxicity Assays

To assess the impact of ILs on the growth of *C. glutamicum,* cells were first adapted to growth in CGXII media with 4% (w/v) D-glucose (described below). Then, cells were back diluted into fresh CGXII media at a starting OD_{600} of 0.1 supplemented with the following ILs: 1-ethyl-3-methylimidazolium acetate ([C_2C_1im][OAc], also referred to as [EMIM][OAc]), 1-ethyl-3-methylimidazolium chloride ([C_2C_1im][Cl] also referred to as [EMIM][Cl]), cholinium acetate ([Ch][OAc]), cholinium chloride ([Ch][Cl]), cholinium lysinate ([Ch][Lys]), ethanol amine acetate [ETA][OAc], and diethanol amine acetate [DEOA][OAc] at the concentrations indicated. These cultures (100 µL volume per well) were grown at 30 ˚C in 96 well microtiter plates on a Synergy 4 plate reader (BioTek Instruments, Winooski VT) and shaken on the "high" setting. Optical density was tracked at a wavelength of 600 nm.

For the isopentenol toxicity assay, single colonies of *C. glutamicum* and *E. coli* were inoculated in 5 mL LB and grown overnight at 30 ˚C with shaking at 200 rpm. Each strain was serially diluted, inoculated on LB agar plates containing 2% (w/v) isopentenol. Photomicrographs were taken after 2 days of incubation at 30 ˚C.

Isopentenol Consumption or Evaporation

Isopentenol evaporation was quantified in a 5 mL culture tube format and 24-well deep well plate format as described before[15]. To measure isopentenol consumption by *C. glutamicum*, wild-type *C. glutamicum* precultures were prepared in LB and back-diluted to an initial OD_{600} of 0.1 into

fresh LB spiked with a serial dilution of the commercial standard isopentenol. The remaining isopentenol was quantified as described in the following section.

Cultivation of C. glutamicum for Isopentenol Production

All cells taken from -80 ˚C glycerol stocks were plated on LB agar plates containing the appropriate antibiotic. A single colony was inoculated and grown overnight in 5 mL LB at 30 ˚C for *C. glutamicum* on a rotary shaker at 200 rpm. Where necessary, kanamycin was added to growth media at a final concentration of 50 μg/mL. Unless otherwise noted, all seed cultures were first inoculated for growth in culture tubes. If cells were grown in a 24-well deep well format, 2 mL of culture media was used per well. Deep well plates were incubated Infors Multitron Incubator with a 3 mm Orbital Shaking Platform shaken at 999 rpm (Bottmingen, Switzerland). When grown in a 5 mL culture tube format, 5 mL of culture media was used per cultivation. Cultures were shaken at 200 rpm on a platform shaker.

When grown in rich media, the heterologous isopentenol production pathway was induced when the OD_{600} reached ~0.8 with 500 μM IPTG without adaptation. When minimal media was used, cells from a seed culture were sub-cultured twice to adapt cells to grow in the media. In brief, pre-cultured cells in LB were diluted 1:10 into minimal media and grown overnight at 30 ˚C with shaking at 200 rpm using deep well plates. The adapted cultures were then diluted 1:10 into fresh minimal media and grown overnight at 30 ˚C with the same cultivation format. After a second back dilution to allow for complete adaptation to growth in minimal media, cultures were then used for growth assays and production in minimal media. The D-glucose concentration was held constant throughout all passaging steps required for adaptation. Where hydrolysate was used as the carbon source, CGXII media was prepared, substituting the volume used for dH_2O with the hydrolysate. Crystalline D-glucose was added to this solution to increase

the starting D-glucose concentration. The isopentenol production pathway was induced at the same OD_{600} as with rich media, and with the same concentration of IPTG.

To assess isopentenol production under IL stress condition, the adapted cultures of *C. glutamicum* were first back-diluted to OD_{600} of 0.1 into CGXII minimal medium, including 4% (w/v) D-glucose and the ILs at the concentrations described above. The production pathway was then induced as before when cultures reached an OD_{600} of ~0.8.

Analytical Methods for Isopentenol Quantification

To quantify isopentenol, 300 μL of cell culture was added to 300 μL of ethyl acetate containing n-butanol (10 mg/L) as an internal standard and processed as described previously[31]. Briefly, sample mixtures were shaken at maximum speed for 15 minutes using an MT-400 microtube mixer (TOMY Seiko, Tokyo, Japan) and then centrifuged at 14,000*g* for 3 minutes to separate the organic phase from the aqueous phase. 60 μL of the organic layer was transferred into an Agilent glass insert placed inside of a GC vial and 1 μL was analyzed by Agilent GCMS equipped with a DB-5 column (Agilent Technologies, Santa Clara, CA) or Thermo GC-FID equipped with a DB-WAX column (Agilent Technologies) for quantification of isopentenol. Analytical grade standards were used to calculate analyte concentrations and confirm identification of peaks. Sugars and organic acids were quantified exactly as described before[32].

Reported isopentenol titers from experiments conducted in the 24-well deep well plate were corrected for evaporation at the 48 hour timepoint by accounting for the amount of product lost from the 24 hour timepoint. The reported isopentenol titers for the 48 hour timepoint are the sum of the amount detected by GC analysis plus the estimated isopentenol lost from the 24 hour timepoint. Product loss from evaporation was estimated using a fitted logarithmic curve from the evaporation rates determined in Additional File 1D with different isopentenol starting

concentrations after 24 hours incubation. The formula used was y = -0.129ln(x) + 1.5375 and r^2=0.9833.

Proteomics

A targeted SRM (Selected Reaction Monitoring) method was developed to quantify relative levels of pathway proteins in samples under the various tested conditions in a 5 mL cultivation format. At the timepoints indicated, 1 mL of each sample was pelleted by centrifugation at 14,000*g* and flash frozen with liquid nitrogen at -80 ˚C until ready for processing. Cells were lysed in 100 mM $NaHCO_3$ using 0.1 mm glass beads using a Biospec Beadbeater (Biospec Products, Bartlesville, OK) with 60 second bursts at maximum power and repeated three times. Cell lysates were cooled on ice between each round. The clarified supernatant was harvested by centrifugation at 14,000*g* and the soluble protein concentration was determined with the BCA method (ThermoFisher Scientific / Pierce Biotechnology, Waltham, MA). The SRM targeted proteomic assays and analyses were performed as described previously[33], on an Agilent 6460 QQQ mass spectrometer system coupled with an Agilent 1290 UHPLC system (Agilent Technologies, Santa Clara, CA). Equal amount (20 μg) of peptides in each sample were loaded and separated on an Ascentis Express Peptide C18 column [2.7-mm particle size, 160-Å pore size, 5-cm length × 2.1-mm inside diameter (ID), coupled to a 5-mm × 2.1-mm ID guard column with the same particle and pore size, operating at 60 °C; Sigma-Aldrich] operating at a flow rate of 0.4 mL/min via the following gradient: initial conditions were 98% solvent A (0.1% formic acid), 2% solvent B (99.9% acetonitrile, 0.1% formic acid). Solvent B was increased to 35% over 6.5 minutes, then increased to 80% over 1.5 minutes, and held for 1.5 minutes at a flow rate of 0.6 mL/min, followed by a ramp back down to 2% of B over 0.5 minute where it was held for 1 minute to re-equilibrate the column to original conditions. The data were acquired using Agilent MassHunter version B.08.02.

Acquired SRM data were analyzed by Skyline software version 3.70 (MacCoss Lab Software). The SRM methods and data are available at Panoramaweb[34] (https://goo.gl/GgQGns). Peptide abundances of the same protein were summed together to assign the protein abundance of a given protein. The average protein value is shown from samples in biological triplicate to assess different timepoints and growth conditions.

Determination of sugars, organic acids and monomeric aromatics in the hydrolysate.

Sugars and organic acids were quantified by HPLC using an Agilent Technologies 1200 series instrument equipped with an Aminex HPX-87H column (BioRad Laboratories, USA) and a refractive index detector. 4 mM sulfuric acid was used as mobile phase with a flow rate of 0.6 mL/min and a column temperature of 60°C. To quantify monomeric aromatics, the same instrument equipped with an Eclipse Plus Phenyl-hexyl column (250 mm length, 4.6 mm diameter, 5 µm particle size; Agilent Technologies, USA) kept at 50 ºC, and a diode array detector were used. The mobile phase was composed of 10 mM ammonium acetate in water (solvent A) and 10 mM ammonium acetate in acetonitrile 90% (solvent B), prepared from a stock solution of 100 mM ammonium acetate and 0.7% formic acid in water. The following mobile phase gradient profile was used: 30% B (0 min; 0.5 mL/min), 80% B (12 min; 0.5 mL/min), 100% B (12.1 min; 0.5 mL/min), 100% B (12.6 min; 1 mL/min), 30% B (12.8 min; 1 mL/min), 30% B (15.6 min; 1 mL/min). Prior to analysis, samples were filtered using 0.45 µm centrifuge filters and 5 µL sample injection volumes were used in all cases. The resulting peak areas were compared to calibration curves made with authentic standards.

Results

C. glutamicum is tolerant to three classes of ILs and exogenous isopentenol

I examined three broad IL classes: 1-ethyl-3-methyl imidazolium ($[C_2C_1im]^+$) derived; cholinium ($[Ch]^+$) derived; and protic: ethanolamine acetate [ETA][OAc] and diethanolamine acetate [DEOA][OAc]) in different cation/anion configurations, for toxicity against *C. glutamicum*. The specific growth rate of *C. glutamicum* in the absence of any IL was 0.28 doublings per hour. *C. glutamicum* grown in the presence of exogenous $[C_2C_1im][OAc]$ or $[C_2C_1im][Cl]$ indicated that this organism was tolerant to ~250 mM $[C_2C_1im]^+$ (**Figure 2A**). Its growth rate decreased four-fold and is a three to six-fold increase in tolerance of $[C_2C_1im]^+$ compared to wild-type *E. coli* (**Figure 3A**). Of the cholinium based ILs, both [Ch][Lys] and [Ch][OAc] decreased growth rate by two to four-fold at 50 mM or higher. [Ch][Lys] was inhibitory at 250 mM, while [Ch][OAc] decreased growth rate but was not inhibitory at concentrations of 150 mM and above (**Figure 2B**). [Ch][Cl] was nontoxic to *C. glutamicum*, and no growth defect was observed, even when supplemented to 600 mM (**Figure 2B**). In contrast, *E. coli* was highly sensitive to [Ch][Lys], as it was inviable when [Ch][Lys] was added to the growth media at 40 mM (**Figure 3B**). Ethanolamine- and diethanolamine-based ILs did not show a dosage dependent inhibition on *C. glutamicum* growth (**Figure 2C**), suggesting that at tested concentrations these two representative protic ILs have no deleterious impact on *C. glutamicum* growth. As the concentration of ILs is below 100 mM in many commonly used hydrolysate preparations[35,36], these results indicated that wild-type *C. glutamicum* was innately tolerant to most forms of the trace ILs remaining in extracted hydrolysates from biomass. No further optimization was required to grow *C. glutamicum* in the presence of additional ILs from these three classes.

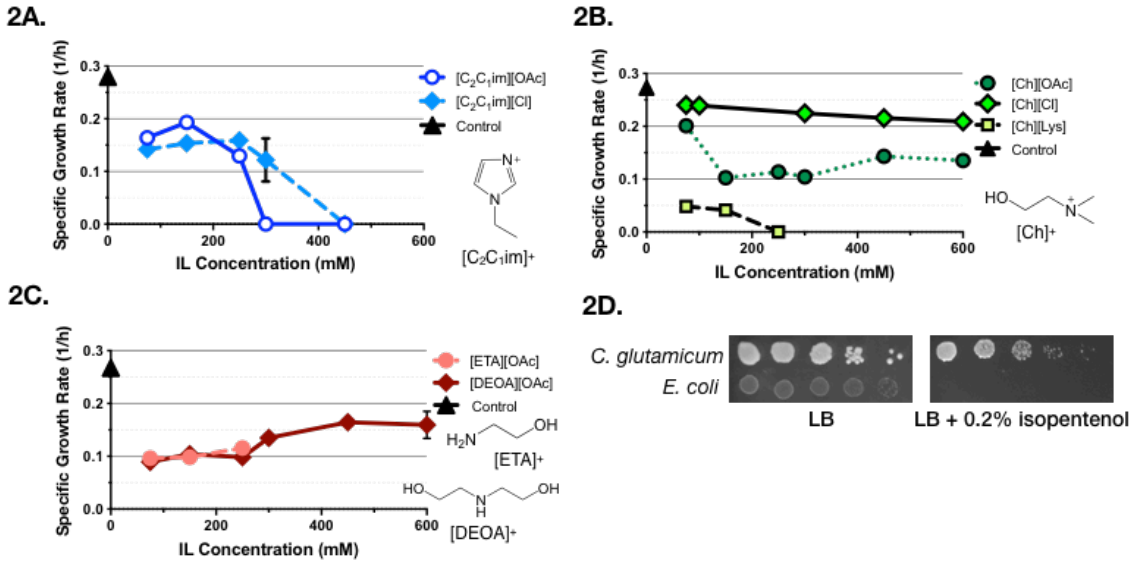

Figure 2. Assessment of *C. glutamicum* Resistance to Three Classes of ILs and Exogenous Isopentenol. (A-C) Growth assay for assessment of *C. glutamicum* resistance to ILs: *C. glutamicum* was cultured in CGXII minimal medium containing 4% D-glucose and the type and concentration of IL as indicated. Strains were cultivated in a 96 well microtiter plate. The growth rate in either control media or supplemented with exogenous IL as indicated (1/h) was calculated and plotted as a function of IL concentration. Data is the average of three independent biological replicates, and error bars indicate standard error. **(D)** Spot assay for assessment of *C. glutamicum* and *E. coli* resistance to isopentenol. Cells were serially diluted 10 fold onto solid LB agar media with or without 0.2% (w/v) isopentenol as indicated and incubated at 30 ˚C. Photomicrographs were taken after plates were incubated for 2 days.

To examine the tolerance of *C. glutamicum* to isopentenol and compare it against that in *E. coli* (known to show toxicity to exogenous isopentenol at a concentration of 0.2% (w/v)[25], I monitored and counted formation of colony forming units (CFUs) on agar plates. I confirmed that *E. coli* is inviable in the presence of 0.2% (w/v) isopentenol (**Figure 2D**). In contrast, *C. glutamicum* is unperturbed at this concentration of isopentenol, as I observe a similar number of CFUs, albeit smaller and slower growing (**Figure 2D**, compare the growth of LB plate to LB plus 0.2% (w/v) isopentenol plate). Wild-type *C. glutamicum* does not consume exogenous isopentenol in liquid cultures as detected by GC-FID after 24 or 48 hours (**Additional File 1C**), where the decrease in isopentenol concentration was comparable to isopentenol evaporation in a

side-by-side comparison (**Additional File 1C**). Isopentenol evaporation was dependent on the cultivation format and was more pronounced in a 24-well deep well plate format **(Additional File 1D)**. These results indicated that *C. glutamicum* has a higher tolerance of exogenous isopentenol compared to *E. coli,* and *C. glutamicum* does not consume this final product as a carbon source. Together, these results suggested that selecting *C. glutamicum* as the microbial chassis is justified due to its inherent tolerance for a suite of relevant biofuel-related molecules.

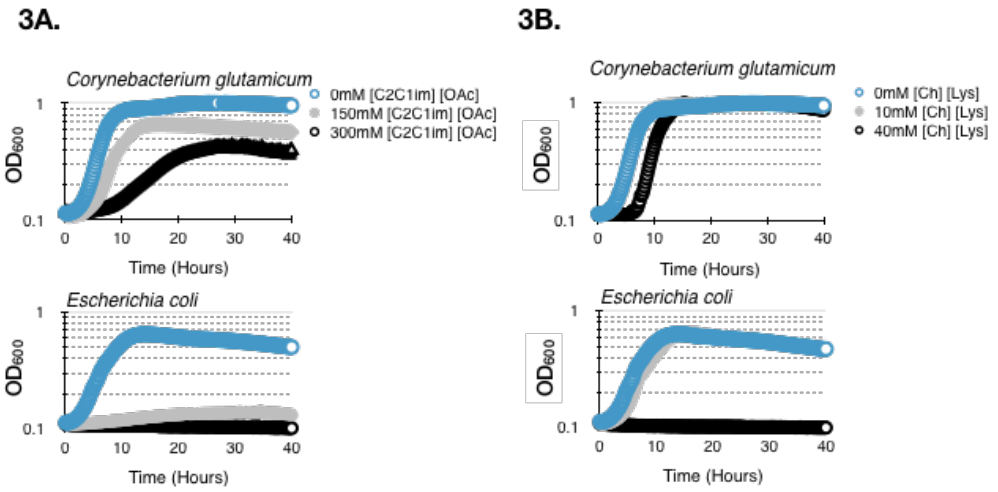

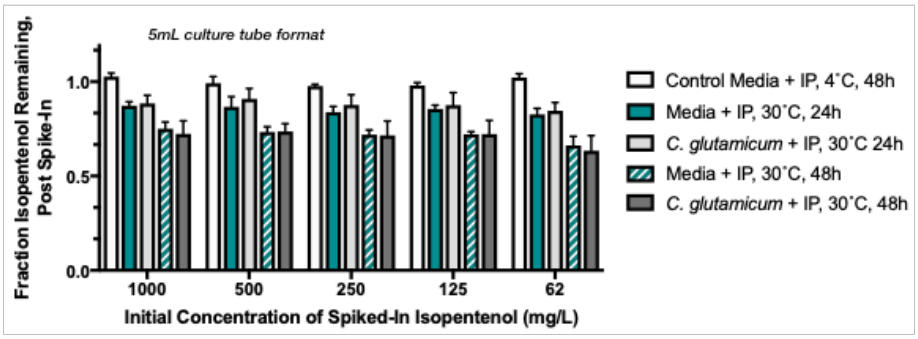

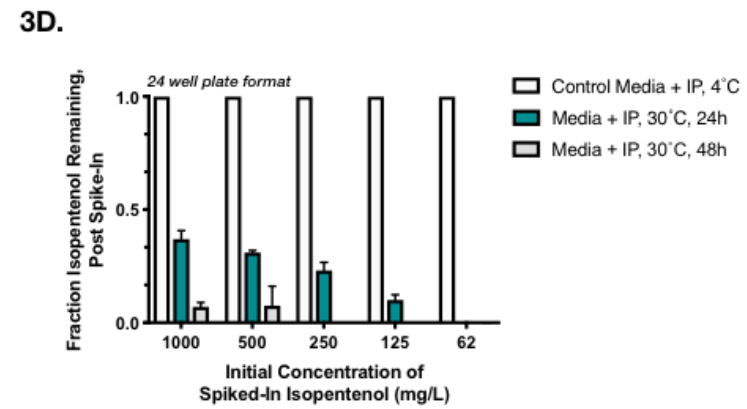

Figure 3. Evaluation of Production Condition and *C. glutamicum* Properties as the Isopentenol Production Chassis. (A-B) Growth assay of *E. coli* and *C. glutamicum* to ILs; 0-300 mM [C_2C_1im][OAc] and 0-40 mM [Ch][Lys] in LB in 96 well microtiter plates. **(C)** Analysis of isopentenol evaporation or consumption by *C. glutamicum* in a 5 mL cultivation format. **(D)** The same evaporation assay as in (C), but in a 24 well format.

Media, carbon and nitrogen levels dramatically impact isopentenol titers in C. glutamicum

Next, I expressed a heterologous mevalonate-based isopentenol biosynthesis pathway[31] in *C. glutamicum* (**Figure 1**). Acetyl-coA is converted to mevalonate-phosphate by four enzymatic reactions, which in turn is decarboxylated to isopentenyl monophosphate (a promiscuous activity from *PMD*). Isopentenyl monophosphate is then spontaneously dephosphorylated by an endogenous phosphatase to yield isopentenol **(Figure 1)**. To identify the cultivation conditions for optimal production of isopentenol in *C. glutamicum,* I tested M9 and CGXII media, a *C. glutamicum* specific minimal media as well as LB (Lysogeny Broth), and conditions were determined based on previous studies for non-native metabolite production [37]. I detected robust isopentenol production in CGXII media, at ~250 mg/L after 24 hours and ~380 mg/L after 48 hours (**Figure 4A**). However, no isopentenol was detected when the strain was grown in either M9 media or LB irrespective of the additional D-glucose supplementation from 1% to 4% (w/v) (**Figure 4A and 4B**). The D-glucose concentration was an apparent difference between the CGXII medium and the other media. These observations demonstrated that the starting D-glucose concentration alone is insufficient to induce isopentenol production in *C. glutamicum* and growth in M9 or LB inhibits the production of isopentenol. This result is in contrast to *E. coli*, where production of isopentenol (and terpenes in general) is typically robust under nutrient-rich conditions, but limited under minimal media conditions[13,15].

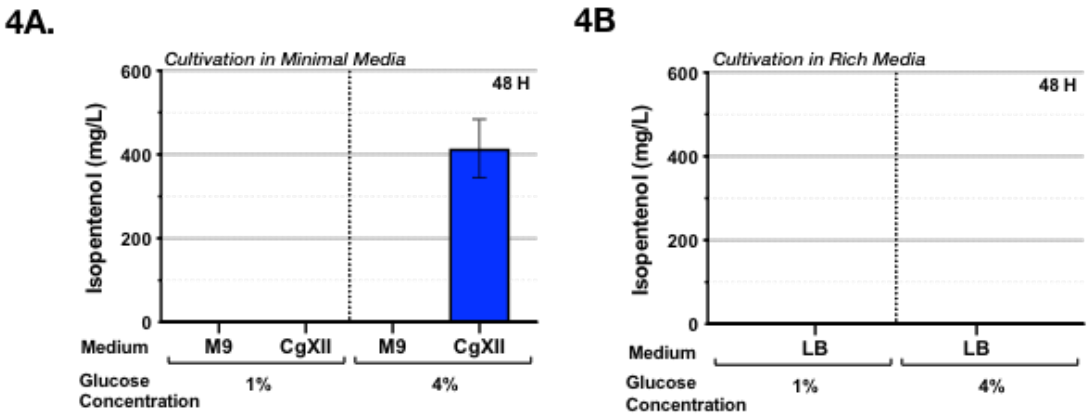

Figure 4. Isopentenol Production in *C. glutamicum* Strains Cultivated in Rich vs. Minimal Media. (A) Isopentenol production in minimal media: *C. glutamicum* was prepared for isopentenol production in two minimal media; M9 and CGXII supplemented with either 1% or 4% D-glucose as the carbon source in 5 mL tubes.
(B) Isopentenol production in rich media: *C. glutamicum* was prepared for isopentenol production in LB media supplemented with either 1% or 4% D-glucose as the carbon source in a 5 mL culture tube. Data shown are production 48 hours after induction and is the average of biological triplicates; error bars represent standard error.

To examine the role of initial D-glucose concentration for production in CGXII media, I supplemented the medium with a range of starting D-glucose concentrations [0.25% to 10% (w/v)] and repeated the isopentenol production (**Figure 5A**). No isopentenol was detectable in the strains grown with less than 2% of initial D-glucose (**Figure 5A**). Above 4% of D-glucose, I detected close to ~450 mg/L of isopentenol titers after 48 hours of induction (**Figure 5A**). The isopentenol titers were comparable up to 8% of D-glucose but dropped three-fold down to 100 mg/L at 10% of D-glucose (**Figure 5A**). In the presence of 10% D-glucose, *C. glutamicum* strains first accumulated both lactate and acetate at the 24 hour timepoint, and continued to accumulate additional acetate at the 48 hour timepoint (**Figure 5B and 5C**). The measured D-glucose concentration using HPLC indicated that it was completely consumed after 24 hours in the strains grown with less than 4% D-glucose, but partially remained when they were grown with 4% or higher initial D-glucose concentration, even after 48 hours (**Figure 6A**). The isopentenol

production strains also produced 1 g/L of succinate, which did not change appreciably over the range of initial D-glucose (**Figure 6B**). While there were differences in OD_{600} values among these strains cultured in different initial D-glucose concentrations, there was no correlation between culture density with isopentenol titer, as r^2=0.00053 **(Figure 6C)**. These results confirm that the starting D-glucose concentration can impact batch-mode production of isopentenol using *C. glutamicum*. A two-fold change in the initial D-glucose concentration can have a 30-fold impact on isopentenol titer.

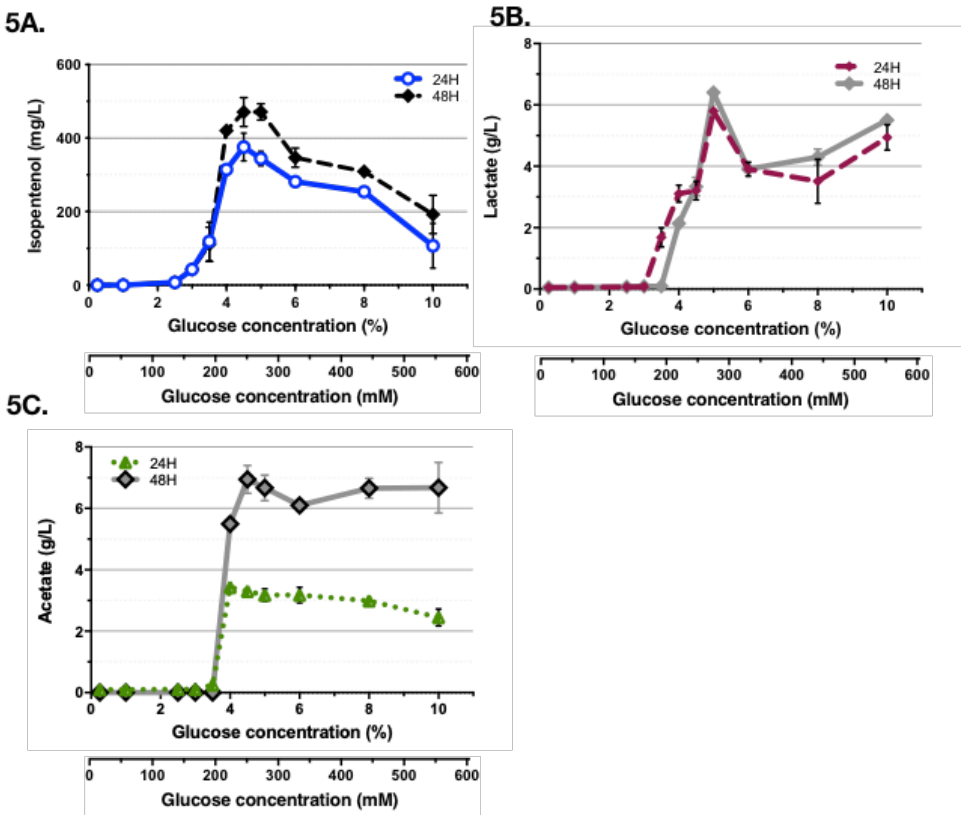

Figure 5. Analysis of Different D-Glucose Concentrations for Isopentenol Production in *C. glutamicum*. (A) Impact of different starting D-glucose concentrations on isopentenol production titer. *C. glutamicum* was cultivated for isopentenol production in CGXII medium amended with D-glucose concentration from 0.25% to 10% (w/v) (13.9 mM to 550 mM) in 24-well deep well plates. For clarity, both the mM and % (w/v) D-glucose concentrations are indicated on the x axis. **(B-C)** Analysis of generated lactate **(B)** and acetate **(C)** titer during the isopentenol production at the 24 hour and 48 hour timepoints. For all experiments, data was generated from three independent biological replicates for each condition, and error bars indicate standard error.

Next, I examined if the initial nitrogen concentration also influenced isopentenol titer. The nitrogen concentration in CGXII media was varied (the ratio of ammonium sulfate and urea were kept the same) and the D-glucose concentration was held constant at the standard 4% D-glucose (222 mM). There was a decrease in isopentenol titer as I varied the initial nitrogen concentration in either direction from the standard of 151 mM ammonium sulfate with 83.3 mM urea [30] **(Figure 6D).** Historically, the carbon:nitrogen ratio (C:N ratio) is known to impact the detectable levels of metabolites in log phase cultures[38]. The C:N ratio in the published CGXII media is 2.8 (6 x 222 mM D-glucose / 2 x 151 mM ammonium sulfate plus 2 x 83.3 mM urea). I combined the data for isopentenol production when I varied either nitrogen or D-glucose and re-plotted isopentenol production as a function of the C:N ratio **(Figure 6E)**. The optimal C:N ratio in CGXII media was between 2.8 and 4.3. The C:N ratio in M9 media is considerably higher at 17.8 (6 x 55.5 mM D-glucose / 18.7 mM ammonium chloride), as the nitrogen concentration is 25-fold lower. This ratio may contribute to the differences in measured isopentenol production, since no production in M9 media was observed **(Figure 6A)**. These results illustrated that in terms of the C:N ratio, observed isopentenol titer was limited to a defined concentration range in which strains could produce detectable isopentenol titers.

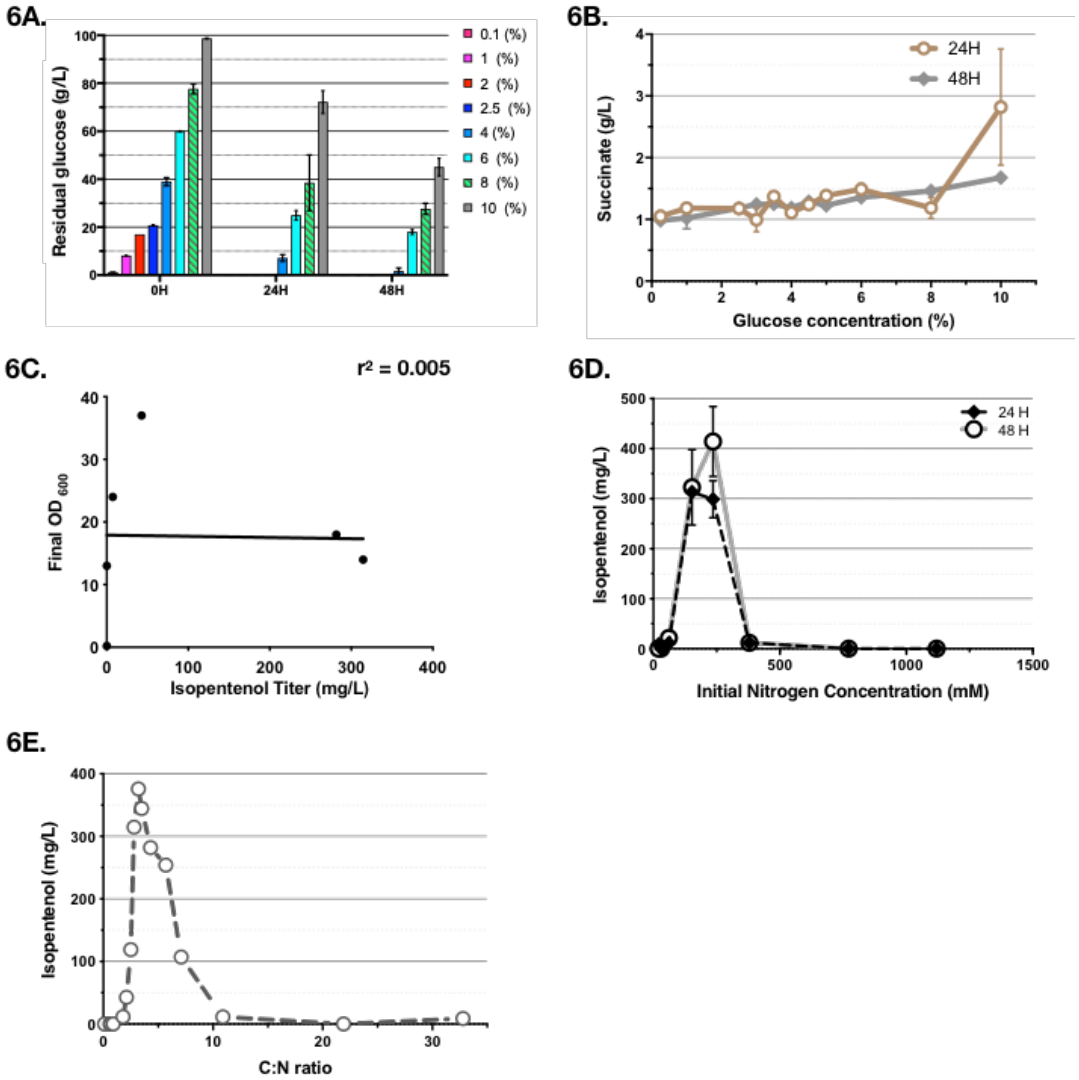

Figure 6. Impact of Initial Glucose and Nitrogen Concentrations On Isopentenol Production in *C. glutamicum*. **(A)** Analysis of residual D-glucose in CGXII media with a range of starting D-glucose concentrations as indicated in 24-well deep well plates. **(B)** Analysis of the generated succinate titer during isopentenol production in Figure 3A. **(C)** Correlation of OD_{600} of samples grown at different D-glucose concentrations with isopentenol titer at the 24 hour timepoint. Correlation was determined using linear regression for the Pearson correlation coefficient (PCC) for the two variables, and r^2=0.00053, and is indicated with a solid black line. **(D)** Impact of different nitrogen concentrations on isopentenol production: *C. glutamicum* was cultivated for isopentenol production in CGXII media, where the nitrogen concentration was varied from 20.3 mM to 1120 mM at the fixed D-glucose concentration of 220 mM. **(E)** Visualization of carbon:nitrogen (C:N) ratio: The C:N ratio ranged from 0.1 to 32.8. For simplicity, the potential contribution of carbon from 3,4-dihydroxybenzoic acid was excluded from this calculation. When cultivated with 5.5 mM D-glucose in CGXII media, *C. glutamicum* showed poor growth. No other gross differences in biomass were noted at other conditions.

Blocking Organic Acid Formation Yields Limited Improvements to Isopentenol Titer

Acetate and lactate formation increased under the cultivation conditions I used for isopentenol production (**Figure 5A-C**). To test if isopentenol titer could be improved by blocking formation of these organic acids, I targeted the genes encoding pyruvate oxidase (*poxB*) or lactate dehydrogenase (*ldhA*) for deletion. I generated the single mutant strains Δ*poxB* and Δ*ldhA,* as well as a double mutant strain Δ*poxB* Δ*ldhA* to redirect flux away from either or both acetate or lactate. Resulting strains were then transformed with the isopentenol production plasmid. The wild-type *C. glutamicum* produced ~225 mg/L at 24 hour timepoint, which was slightly lower to previous production runs with this strain but within the error range, likely due to batch to batch variation in media preparation **(Figure 7)**. The Δ*poxB* mutant did not significantly improve isopentenol titer (**Figure 7**), even though accumulation of acetate was reduced from 5 g/L down to ~35 mg/L. The Δ*ldhA* strain did not produce more than trace isopentenol **(Figure 7)**. The Δ*poxB* Δ*ldhA* strain continued to show marked improvement over wild-type strain at the 48 hour timepoint, producing ~500 mg/L isopentenol in the Δ*poxB* Δ*ldhA* strain **(Figure 7)**. The rational gene deletions in *C. glutamicum* lowered accumulation of side-products, but improvements to isopentenol titer were limited to at most a two-fold increase.

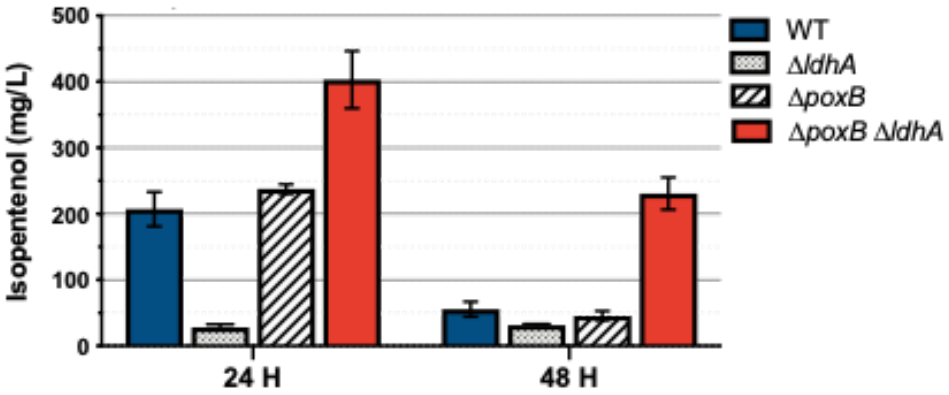

Figure 7. Rational Engineering of *C. glutamicum* Host Chassis and Isopentenol Production Pathway. **(A)** Analysis of *C. glutamicum* strains Δ*poxB*, Δ*ldhA,* and double mutant Δ*poxB* Δ*ldhA* strains on isopentenol production: Strains of the indicated genotype (WT, Δ*poxB*, Δ*ldhA,* and Δ*poxB* Δ*ldhA*) were cultivated in 24-well deep well plates. Isopentenol titer was measured as described in Additional File 4A and B. Data was generated from three independent biological replicates for each genotype, and error bars indicate standard error.

Expression of the Isopentenol Pathway Protein HmgR Strongly Correlates With Isopentenol Titer

To examine if isopentenol titers correlate with pathway protein expression, I used selected reaction monitoring (SRM) based proteomics[39-41] to assess relative protein levels across these conditions. Samples were grown in LB, M9, or CGXII media and collected at 24 and 48 hour timepoints for proteomic analysis and GC analysis. I observed a similar dependence on the initial D-glucose concentration in CGXII media and a failure to produce isopentenol in M9 or LB irrespective of cultivation format (**Figure 8A**). Crude lysates were prepared for peptide analysis to quantify the five proteins constituting the isopentenol pathway.

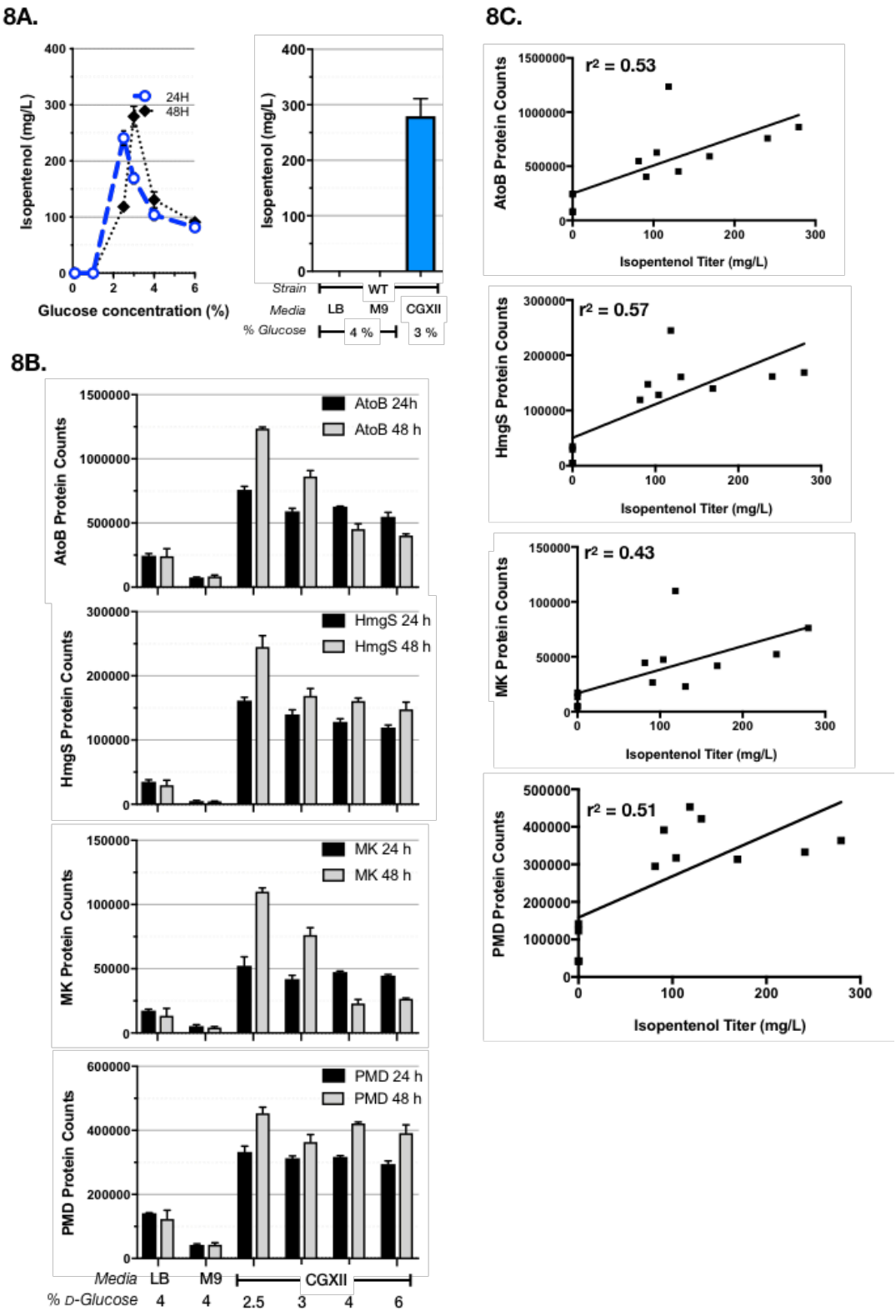

Figure 8. Analysis of Pathway Protein Abundance vs. Isopentenol Titer in Three Kinds of Media.

(A) *Left*. Analysis of isopentenol titer measured in wild-type *C. glutamicum*. Production of isopentenol from *C. glutamicum* in CGXII media with D-glucose concentrations as indicated. *Right*. The same strain was cultivated for isopentenol production in LB with 4% D-glucose, or M9 media with 4% D-glucose. The production of isopentenol from CGXII media with 3% D-glucose is replotted from the left-hand graph for ease of comparison. The relevant media and % D-glucose are indicated below the graph. Data was generated from three independent biological replicates for each condition and the error bars indicate standard error. **(B)** Proteomic analysis of AtoB, HmgS, MK, and PMD protein abundances: Each protein abundance is shown at the 24 hour and 48 hour timepoint in wild-type *C. glutamicum* cultivated with 4% starting D-glucose in LB and M9 media, and 2.5-6% starting D-glucose in CGXII media. **(C)** Correlation between isopentenol titer and each protein abundance at the 24 hour timepoint. Correlation was determined using linear regression for the Pearson correlation coefficient (PCC) for the two variables. Cultivations for proteomics samples were performed as described in Materials and Methods.

The targeted protein analysis indicated the highest protein abundance in the optimal condition (CGXII with 3% D-glucose), whereas in LB, all proteins in the isopentenol production pathway were reduced in their abundance ranging from two-fold (PMD) to 10-fold (HmgR) lower (**Figure 9A** and **Figure 8B**). Pathway proteins from *C. glutamicum* grown in M9 media were reduced even further, as protein enrichment was decreased from seven-fold (PMD) to twenty-seven-fold (HmgS) (**Figure 9B** and **Figure 8B**). This analysis suggests that the failure to produce isopentenol in either LB or M9 media was due to the decreased abundance of the isopentenol pathway proteins.

Proteomics data also revealed potential bottlenecks in the isopentenol production pathway. Across the range of cultivation parameters and timepoints tested in wild-type *C. glutamicum*, I observed that HmgR protein levels and its isopentenol production titer were strongly correlated ($r^2 = 0.93$) **(Figure 9B)**. The other four pathway proteins (AtoB, HmgS, MK, and PMD) were weakly correlated with the isopentenol titer **(Figure 8C)**.

To test if higher expression levels of *HMGR* could improve isopentenol production, I built a set of strains in which the isopentenol production pathway was chromosomally integrated at the *idsA* locus. The Δ*idsA* strains form white colonies instead of the wild-type yellow color[42]

facilitating screening for heterologous pathway integration. The control Δ*idsA* strain harboring a plasmid-borne isopentenol production pathway produces ~20 mg/L isopentenol (**Figure 9C**). The Δ*idsA* strain with a chromosomally integrated isopentenol pathway was able to produce isopentenol, but less than the control strain with the plasmid-borne isopentenol pathway, at titers of ~12 mg/L (**Figure 9C**). However, when HmgR expression was augmented in the chromosomally integrated production strain with an additional, plasmid-borne copy of *HMGR* under a *trc* promoter, the isopentenol titer improved 4x over the original strain and produced 60 mg/L isopentenol. While the cause of lower isopentenol production in the Δ*idsA* strains remain unclear, these results provide evidence consistent with the hypothesis where HmgR is a rate limiting step in isopentenol production and provided a target for further pathway optimization.

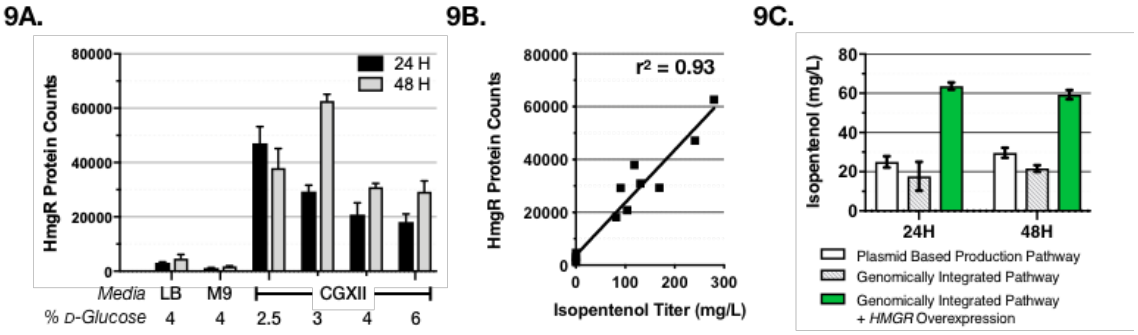

Figure 9. Analysis of HmgR Protein Abundance vs. Isopentenol Titer. All strains were prepared for isopentenol production in CGXII medium at the % (w/v) D-glucose concentration indicated below the graph. **(A)** Proteomic analysis of HmgR protein abundance: Absolute abundance for HmgR at the timepoints indicated are plotted as a function of cultivation condition. **(B)** Correlation analysis between isopentenol titer and HmgR protein abundance. Correlation was determined using a linear regression for the Pearson correlation coefficient (PCC) for the two variables. **(C)** Role of increased *HMGR* expression on isopentenol titer. All strains were cultivated for isopentenol production in CGXII medium amended with 4% D-glucose concentration in 24-well deep well plates. White bars: *C. glutamicum* Δ*idsA* harboring the plasmid-borne isopentenol production pathway. Grey hatched bars: Δ*idsA* with a chromosomally integrated isopentenol production pathway at the *idsA* locus. Green bars: Δ*idsA* with the same chromosomally encoded isopentenol production pathway as well as a plasmid-borne *HMGR* overexpression cassette. For all experiments, data was generated from three independent biological replicates for each condition, and error bars indicate standard error.

Production of Isopentenol in C. glutamicum using IL Pretreated Sorghum

To test this process with industrially relevant carbon sources, I demonstrated that *C. glutamicum* could produce isopentenol from plant biomass hydrolysate. I pretreated sorghum biomass using the IL [Ch][Lys] to generate a hydrolysate that contained 29.2 g/L D-glucose, 16.4 g/L D-xylose, and 5.1 g/L acetic acid **(Figure 10A and B)**. This hydrolysate also contained 0.01 mM 4-hydroxybenzoic acid and 1.36 mM benzoic acid. When the production strains were grown in the hydrolysate-amended CGXII media, no significant growth defect was observed compared to the growth in pure D-glucose supplemented CGXII media. Substituting hydrolysate for all added water in CGXII media results in a starting concentration of D-glucose at 1.7% (w/v). Based on the results in **Figures 5A and 9A**, I also prepared two other production conditions, where I supplemented pure D-glucose such that the concentration was increased to 3.5% or 4.0% (w/v). In the original hydrolysate-amended condition (with 1.7% D-glucose), I detected trace isopentenol production of ~15 mg/L (**Figure 11A**). When the D-glucose concentration was increased to 3.5% or 4.0%, the titer increased to ~200 mg/L (**Figure 11A**). Any potential contaminants from IL treated sorghum biomass also did not completely inhibit isopentenol production at these concentrations. These results demonstrate that *C. glutamicum* has the capacity to function as a microbial chassis for terpenes-based chemical production from renewable starting materials.

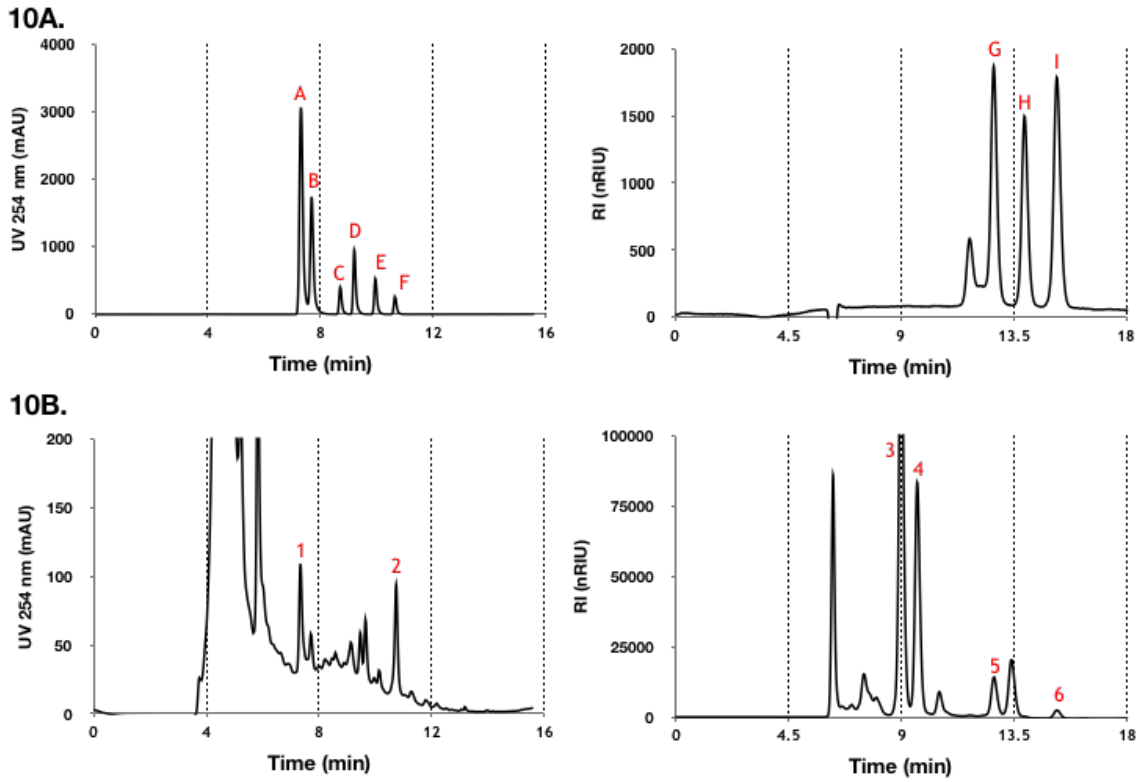

Figure 10. Determination of sugars and aromatics in hydrolysate by HPLC. (A) *Left Panel.* Standards for aromatics (0.5 g/L of each compound): A = 4-hydroxybenzoic acid; B = vanillic acid; C = *p*-coumaric acid; D = ferulic acid; E = vanillin; F = benzoic acid. *Right Panel***.** Organic acids standards (1 g/L of each compound): G = lactic acid; H = formic acid; I = acetic acid. **(B)** Representative traces for aromatics and organic acids from [Ch][Lys] pretreated hydrolysate. *Left Panel.* Aromatics. Peaks are numbered as follows as identified in hydrolysate: 1 = 4-hydroxybenzoic acid; 2 = benzoic acid. *Right Panel.* Sugars and organic acids identified in hydrolysate: 3 = D-glucose; 4 = D-xylose; 5 = lactic acid; 6 = acetic acid. Concentrations of the sugars and aromatics from the [Ch][Lys] pretreated sorghum biomass are as follows. D-Glucose: 29.2 g/L; D-xylose: 16.4 g/L; acetic acid: 5.1 g/L; lactic acid: 6.69 g/L; 4-hydroxybenzoic acid: 0.0018 g/L; benzoic acid: 0.167 g/L. The analytes for vanillic acid, *p*-coumaric acid, ferulic acid, and vanillin were detected but below the linear range for quantification (<1mg/L).

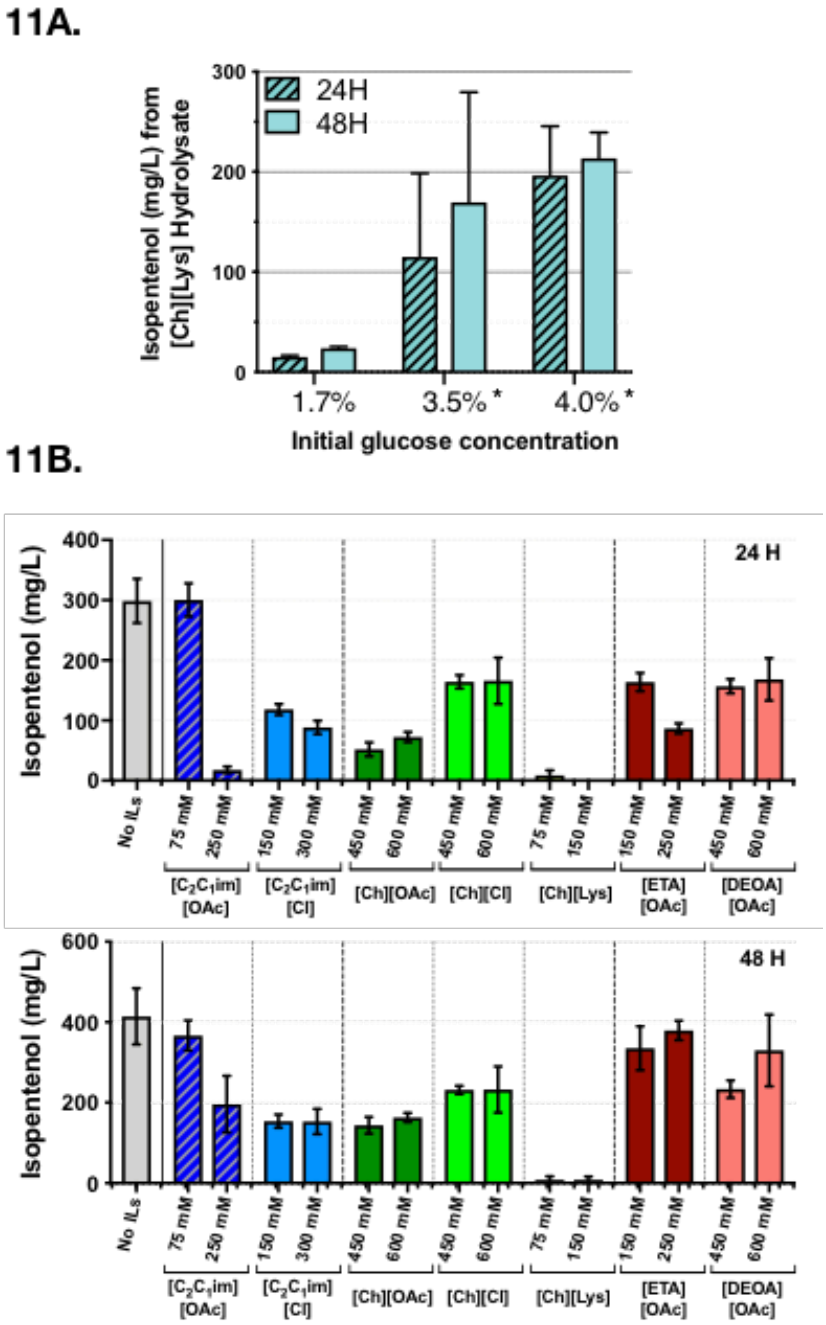

Figure 11. Isopentenol Production from [Ch][Lys] Pretreated Sorghum Hydrolysates as the Carbon Source. **(A)** *C. glutamicum* was prepared for isopentenol production in CGXII media with hydrolysate in 5 mL culture tubes. Additional D-glucose was supplemented as indicated (*). Isopentenol production values are the average of three independent biological replicates, and the error bars represent standard error. **(B)** Isopentenol production in the presence of ILs: CGXII minimal media including 4% starting D-glucose was used with or without IL. The IL concentrations tested are as listed on the x axis. Samples were cultivated in 24-well deep well plates. Data shown are after 24 hours and 48 hours of induction; the isopentenol production values are the average of biological triplicates, and the error bars represent standard error.

Ionic Liquids Do Not Block Isopentenol Production

C. glutamicum isopentenol production strains were tested for isopentenol production with tolerated levels of ILs **(**refer to **Figure 2A-C)** higher than the 0.03% (w/v) remaining ILs after the ethanol/water washing regime[43]. Specifically, IL concentrations ranged from 75 mM to 600 mM, depending on where a growth defect was observed **(Figure 2A-C)**. After 24 hours post induction, all strains except for [Ch][Lys] reached similar high OD_{600nm} measurements; the [Ch][Lys] treated strains grew very poorly and did not reach saturation. Isopentenol production was measured both 24 and 48 hours post induction.

For [C_2C_1im][OAc], 75 mM had no impact on isopentenol production (**Figure 11B, dark blue bars**). 250 mM [C_2C_1im][OAc] delayed isopentenol production, as no final product was recovered at 24 hours, but the isopentenol titer was partially recovered at 48 hour timepoint. Samples grown in the presence of [C_2C_1im][Cl] produced half as much isopentenol as the untreated control (**Figure 11B, light blue bars**). As [Ch][Lys] was inhibitory to *C. glutamicum* growth (**Figure 2B**), the strain failed to produce isopentenol in its presence (**Figure 11B, lime green bars**). [Ch][OAc] and [Ch][Cl] had stronger effects on final product titer, decreasing isopentenol titer approximately 2-3x compared to the control, with [Ch][OAc] having a larger impact on final product titer than [Ch][Lys] (**Figure 11B, green bars**). The reduction of isopentenol titer of these strains largely correlated with the severity of the growth defect, with the exception of [Ch][Cl], which exhibited no impact on doubling time but had a measurable impact on isopentenol production (refer to **Figure 2B**).

In contrast to the cholinium and imidazolium based ILs, one of the protic ILs had modest effects on the production of isopentenol. Exogenous [DEOA][OAc] had a modest inhibition on isopentenol production (**Figure 11B, salmon pink bars**), which is reasonably similar to [Ch][Cl]. However, strains grown in the presence of exogenous ethanolamine ([EOA][OAc]) had a

similarly reduced titer at the 24 hour timepoint, but the isopentenol titer was similar to production in the control strain when sampled at the 48 hour timepoint (**Figure 11B, dark red bars**). Taken together, these results indicate that *C. glutamicum* is competent to maintain the isopentenol titers in the presence of ILs and across several commonly used IL formats.

Both strain background engineering and pathway engineering improve isopentenol titers

Additional *HMGR* expression improves isopentenol production (**Figure 9C**). HmgR from *S. cerevisiae* is a class I HmG-CoA reductase, and preferentially uses NADPH as the cofactor rather than NADH[44,45]. The use of a class II HmG-CoA reductase from *Silicibacter pomeroyi* which relies on NADH as a cofactor instead of NADPH has been reported previously[46]. I cloned the *S. pomeroyi hmgr* homolog into the isopentenol production plasmid and assessed isopentenol production in the Δ*poxB* Δ*ldhA* background. With the original isopentenol production pathway, *C. glutamicum* produces ~125 mg/L isopentenol with similar titers at both 24 hour and 48 hour timepoints (see **Figure 12A**). In contrast, Δ*poxB* Δ*ldhA* strains showed a delay in initial isopentenol production, with lower production after 24 hours (~100 mg/L) but an improvement over wild type to ~500 mg/L after 48 hours (refer to **Figure 12A**).

While titers were comparable at the 24 hour timepoint with either the *S. cerevisiae HMGR* or *S. pomeroyi hmgr* genes by the 48 hour timepoint, the *S. pomeroyi* variant strains produced close to 1,120 mg/L of isopentenol (**Figure 12A**). At the 72 hour timepoint, I detected an increase to 1,250 mg/L of isopentenol relative to ~750 mg/L from the unmodified heterologous pathway. This improvement in isopentenol production using the pathway variant suggests that the NADH dependent allele of HmgR was advantageous for isopentenol production in *C. glutamicum*.

Finally, to complete our process characterization, I assayed isopentenol production from [Ch][Lys] pretreated hydrolysate with the optimized *C. glutamicum* Δ*poxB* Δ*ldhA* strain harboring the NADH dependent *S. pomeroyi hmgr*, in the 5 mL cultivation format. The starting D-glucose concentration was supplemented to 4% as determined to be in the range for optimal final product titer. At the 48 hour timepoint, the isopentenol production titer reached ~1,100 mg/L, equivalent to the observed titer from when pure D-glucose was used as the carbon source (**Figure 12B**). Our % theoretical yield of isopentenol[47] from glucose was 9.7 %, and % theoretical yield from sorghum hydrolysate was 8.6 %. These results demonstrate the completion of our microbial bioprocess for isopentenol production in the industrially relevant organism *C. glutamicum.*

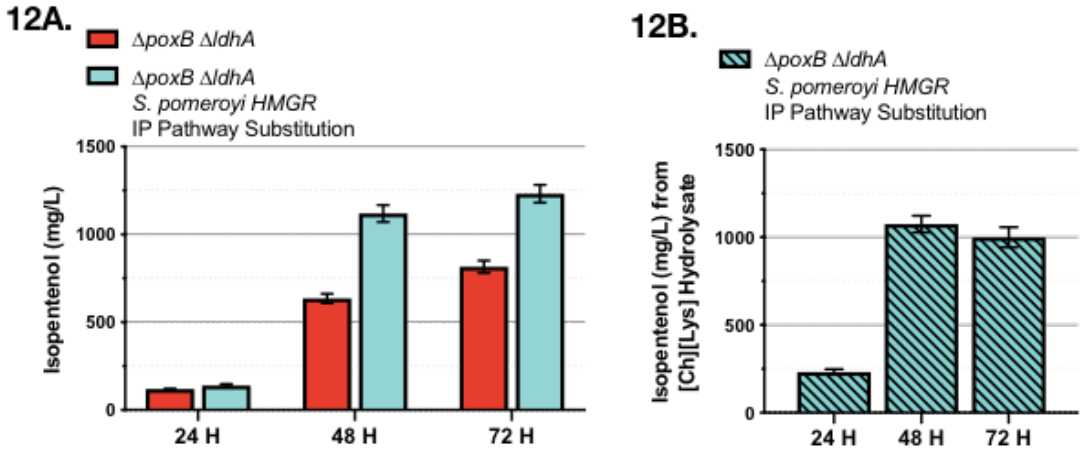

Figure 12. An Engineered *C. glutamicum* Host Chassis With Modified Isopentenol Production Pathway Produces Isopentenol Using IL-Pretreated Sorghum Biomass. **(A)** Analysis of the engineered isopentenol production pathway using a *hmgr* homolog from *S. pomeroyi* in a 5 mL cultivation format: Isopentenol production was performed in a Δ*poxB* Δ*ldhA* strain harboring either the original isopentenol production pathway or a variant where the *S. cerevisiae HMGR* was replaced with a *hmgr homolog* from *S. pomeroyi*. One additional timepoint at 72 hours post induction was harvested. **(B)** Isopentenol production using IL-pretreated sorghum hydrolysate: CGXII minimal media was prepared as described previously in Figure 5A. *C. glutamicum* Δ*poxB* Δ*ldhA* was adapted to growth in CGXII minimal media containing hydrolysate and assessed for isopentenol production at the timepoints indicated. All isopentenol values are the average of biological triplicates, and the error bars represent standard error.

Discussion

Different microbial hosts have innate physiological differences that make them more or less suitable for a final bioconversion process. However, it is unclear *a priori* what parameters dictate final product titer of a given heterologous gene pathway. Here I have evaluated the advantages of an industrially relevant microorganism, *C. glutamicum,* to express a non-native mevalonate pathway consisting of five-genes with the goal of producing isopentenol from IL pretreated plant biomass. Our highest isopentenol titers with sugars derived from plant biomass are comparable to titers published in *E. coli* which was cultivated in rich media with pure sugars[31,48]. I also observed that *C. glutamicum* was natively resistant to a wide range of toxic compounds associated with the pretreatment process (i.e., ILs) and final product (i.e., isopentenol).

Carbon and nitrogen metabolism are closely linked through energy-driven processes such as the generation of ATP. Thus, the carbon to nitrogen ratio (C:N) is a critical parameter and its effect on growth and production has been reported in variety of microbial hosts[49,50]. This study demonstrates a relationship between initial D-glucose concentrations in CGXII media and isopentenol production, which corresponds to a C:N ratio of 2.8-4.3 where I observed isopentenol production. A link between starting D-glucose concentration and its impact on gene expression (in the context of a heterologous gene pathway) has not been described before. This compositional profile indicates that common peptone-based media such as LB (or alternatively, defined M9 media) were not optimal for our purposes. Our observations are supported by evidence in *E. coli,* where cells exhibit differential transcriptional RNA levels and enzyme activities under nitrogen as well as carbon limitation[51]. However, it is still unclear how the initial cell physiology during exponential phase can impact on the physiology after D-glucose exhaustion, where much of our

batch-mode production occurs. A previous study also examined the impact of C:N ratio on the production of a native molecule[52], but testing a range of C:N values is not yet common practice when characterizing new products. The absolute starting D-glucose concentration (or C:N ratio) may be a general determinant of final product titer and could be beneficial for optimizing other heterologous gene pathways in *C. glutamicum*, such as for the production of the anthocyanin food colorant, cyanidin 3-*O*-glucoside[53].

Strain background engineering also played an important role in improving isopentenol titer. Having observed the undesirable formation of acetate and lactic acid in our isopentenol production experiments, I generated new strains to redirect metabolic flux away from these two organic acids. The single gene deletion strains Δ*ldhA* and Δ*poxB* did not accumulate their appropriate side products, but also did not appreciably increase isopentenol titer. On the other hand, the isopentenol titer was increased in the double mutant (Δ*ldhA* Δ*poxB*), which was a synergistic improvement over either of the single mutants. Genome-scale metabolic flux modeling and analysis[54] of these strains could reveal unappreciated nuances in host physiology which could inform future metabolic engineering work.

Finally, guided by proteomic analysis, pathway engineering resulted in the highest improvements in product titers to the grams per liter level. A strong correlation between the abundance of HmgR and isopentenol titer suggested HmgR as a potential rate-limiting step in this pathway. While increasing HmgR protein levels improved isopentenol production four-fold, the greatest absolute improvement of isopentenol titer was obtained by utilizing a class II NADH-dependent variant of HmgR from *S. pomeroyi*[46]. I suggest that additional mutagenesis of *HMGR* could lead to broadly applicable improvements for other molecules derived from the mevalonate pathway.

Summary

This chapter describes the successful deployment of a heterologous mevalonate pathway in the gram-positive industrial microorganism, *C. glutamicum,* for isopentenol production. A detailed technoeconomic analysis[55] is needed to fully understand the complex variables necessary to realize isopentenol production at an industrial scale. Currently, ILs are valuable and recycled after generating hydrolysates by extensive washing, and thus their concentration in hydrolysate is low[43,56]. However, removal of ILs is not cost-effective in large-scale industrial applications. As they become less expensive, or used in consolidated one-pot processes[57,58], host strains that can tolerate higher IL concentrations have the potential for an outsized impact on process cost in the future. A higher D-glucose concentration in the hydrolysate could simplify the cultivation process I utilized for producing isopentenol with sorghum biomass. The system developed in this study sets the stage for characterization of this platform under simulated industrial bioreactor conditions, such as the scale down approach for 1,5-diaminopentane[5]. Overall, this study highlights the intrinsic capability of *C. glutamicum* as a valuable industrial host through characterizing phenotypic responses to the emerging ionic liquids agents and implementing genetic engineering and process optimization for terpene production.

References

1 Mukhopadhyay, A. Tolerance engineering in bacteria for the production of advanced biofuels and chemicals. Trends Microbiol 23, 498-508, doi:10.1016/j.tim.2015.04.008 (2015).

2 Deparis, Q., Claes, A., Foulquié-Moreno, M. R. & Thevelein, J. M. Engineering tolerance to industrially relevant stress factors in yeast cell factories. FEMS yeast research 17 (2017).

3 Jullesson, D., David, F., Pfleger, B. & Nielsen, J. Impact of synthetic biology and metabolic engineering on industrial production of fine chemicals. Biotechnology advances 33, 1395-1402 (2015).

4 Käß, F. et al. Rapid assessment of oxygen transfer impact for Corynebacterium glutamicum. Bioprocess and Biosystems Engineering 37, 2567-2577, doi:10.1007/s00449-014-1234-1 (2014).

5 Limberg, M. H. et al. Metabolic profile of 1, 5-diaminopentane producing Corynebacterium glutamicum under scale-down conditions: blueprint for robustness to bioreactor inhomogeneities. Biotechnology and bioengineering 114, 560-575 (2017).

6 Kawaguchi, H., Vertes, A. A., Okino, S., Inui, M. & Yukawa, H. Engineering of a xylose metabolic pathway in Corynebacterium glutamicum. Appl Environ Microbiol 72, 3418-3428, doi:10.1128/AEM.72.5.3418-3428.2006 (2006).

7 Dutta, T. et al. Characterization of Lignin Streams during Bionic Liquid-Based Pretreatment from Grass, Hardwood, and Softwood. ACS Sustainable Chemistry & Engineering 6, 3079-3090 (2018).

8 Rodriguez, A. et al. Base-Catalyzed Depolymerization of Solid Lignin-Rich Streams Enables Microbial Conversion. ACS Sustainable Chemistry & Engineering 5, 8171-8180, doi:10.1021/acssuschemeng.7b01818 (2017).

9 Kallscheuer, N. et al. Identification of the phd gene cluster responsible for phenylpropanoid utilization in Corynebacterium glutamicum. Applied Microbiology and Biotechnology 100, 1871-1881, doi:10.1007/s00253-015-7165-1 (2016).

10 Zhao, N., Qian, L., Luo, G. & Zheng, S. Synthetic biology approaches to access renewable carbon source utilization in Corynebacterium glutamicum. Applied microbiology and biotechnology, 1-13 (2018).

11 Hermann, T. Industrial production of amino acids by coryneform bacteria. Journal of biotechnology 104, 155-172 (2003).

12 Becker, J. & Wittmann, C. Bio-based production of chemicals, materials and fuels–Corynebacterium glutamicum as versatile cell factory. Current opinion in biotechnology 23, 631-640 (2012).

13 Peralta-Yahya, P. P. et al. Identification and microbial production of a terpene-based advanced biofuel. Nat Commun 2, 483, doi:10.1038/ncomms1494 (2011).

14 Heider, S. A. E. & Wendisch, V. F. Engineering microbial cell factories: metabolic engineering of Corynebacterium glutamicum with a focus on non-natural products. Biotechnology Journal 10, 1170-1184, doi:10.1002/biot.201400590 (2015).

15 George, K. W. et al. Metabolic engineering for the high-yield production of isoprenoid-based C(5) alcohols in E. coli. Sci Rep 5, 11128, doi:10.1038/srep11128 (2015).

16 Ghanem, O. B. et al. Effect of imidazolium-based ionic liquids on bacterial growth inhibition investigated via experimental and QSAR modelling studies. J Hazard Mater 297, 198-206, doi:10.1016/j.jhazmat.2015.04.082 (2015).

17 Li, C. et al. Comparison of dilute acid and ionic liquid pretreatment of switchgrass: Biomass recalcitrance, delignification and enzymatic saccharification. Bioresource Technology 101, 4900-4906, doi:https://doi.org/10.1016/j.biortech.2009.10.066 (2010).

18 George, A. et al. Design of low-cost ionic liquids for lignocellulosic biomass pretreatment. Green Chemistry 17, 1728-1734 (2015).

19 Li, C. et al. Comparison of dilute acid and ionic liquid pretreatment of switchgrass: Biomass recalcitrance, delignification and enzymatic saccharification. Bioresour Technol 101, 4900-4906, doi:10.1016/j.biortech.2009.10.066 (2010).

20 Dickinson, Q. et al. Mechanism of imidazolium ionic liquids toxicity in Saccharomyces cerevisiae and rational engineering of a tolerant, xylose-fermenting strain. Microb Cell Fact 15, 17, doi:10.1186/s12934-016-0417-7 (2016).

21 Liu, Q.-P., Hou, X.-D., Li, N. & Zong, M.-H. Ionic liquids from renewable biomaterials: synthesis, characterization and application in the pretreatment of biomass. Green Chemistry 14, 304-307, doi:10.1039/C2GC16128A (2012).

22 Tang, S., Baker, G. A. & Zhao, H. Ether-and alcohol-functionalized task-specific ionic liquids: attractive properties and applications. Chemical Society Reviews 41, 4030-4066 (2012).

23 Higgins, D. A. et al. Natural variation in the multidrug efflux pump SGE1 underlies ionic liquid tolerance in yeast. Genetics 210, 219-234 (2018).

24 Eng, T. et al. Restoration of biofuel production levels and increased tolerance under ionic liquid stress is enabled by a mutation in the essential Escherichia coli gene cydC. Microbial cell factories 17, 159 (2018).

25 Foo, J. L. et al. Improving microbial biogasoline production in Escherichia coli using tolerance engineering. MBio 5, e01932, doi:10.1128/mBio.01932-14 (2014).

26 Gibson, D. G. et al. Enzymatic assembly of DNA molecules up to several hundred kilobases. Nat Methods 6, 343-345, doi:10.1038/nmeth.1318 (2009).

27 Sun, N. et al. Understanding pretreatment efficacy of four cholinium and imidazolium ionic liquids by chemistry and computation. Green Chemistry 16, 2546-2557, doi:10.1039/C3GC42401D (2014).

28 Ruan, Y., Zhu, L. & Li, Q. Improving the electro-transformation efficiency of Corynebacterium glutamicum by weakening its cell wall and increasing the cytoplasmic membrane fluidity. Biotechnology letters 37, 2445-2452 (2015).

29 Unthan, S. et al. Beyond growth rate 0.6: What drives Corynebacterium glutamicum to higher growth rates in defined medium. Biotechnology and Bioengineering 111, 359-371, doi:doi:10.1002/bit.25103 (2014).

30 Keilhauer, C., Eggeling, L. & Sahm, H. Isoleucine synthesis in Corynebacterium glutamicum: molecular analysis of the ilvB-ilvN-ilvC operon. Journal of bacteriology 175, 5595-5603 (1993).

31 Kang, A. et al. Isopentenyl diphosphate (IPP)-bypass mevalonate pathways for isopentenol production. Metab Eng 34, 25-35, doi:10.1016/j.ymben.2015.12.002 (2016).

32 Goh, E. B. et al. Substantial improvements in methyl ketone production in E. coli and insights on the pathway from in vitro studies. Metab Eng 26, 67-76, doi:10.1016/j.ymben.2014.09.003 (2014).

33 Batth, T. S. et al. A targeted proteomics toolkit for high-throughput absolute quantification of Escherichia coli proteins. Metab Eng 26, 48-56, doi:10.1016/j.ymben.2014.08.004 (2014).

34 Sharma, V. et al. Panorama: a targeted proteomics knowledge base. J Proteome Res 13, 4205-4210, doi:10.1021/pr5006636 (2014).

35 Ouellet, M. et al. Impact of ionic liquid pretreated plant biomass on Saccharomyces cerevisiae growth and biofuel production. Green Chemistry 13, 2743-2749, doi:10.1039/C1GC15327G (2011).

36 Zhao, H. et al. Regenerating cellulose from ionic liquids for an accelerated enzymatic hydrolysis. Journal of Biotechnology 139, 47-54, doi:10.1016/j.jbiotec.2008.08.009 (2009).

37 Smith, K. M., Cho, K. M. & Liao, J. C. Engineering Corynebacterium glutamicum for isobutanol production. Appl Microbiol Biotechnol 87, 1045-1055, doi:10.1007/s00253-010-2522-6 (2010).

38 Lowry, O. H., Carter, J., Ward, J. B. & Glaser, L. The effect of carbon and nitrogen sources on the level of metabolic intermediates in Escherichia coli. J Biol Chem 246, 6511-6521 (1971).

39 Gulcicek, E. E. et al. Proteomics and the analysis of proteomic data: an overview of current protein-profiling technologies. Curr Protoc Bioinformatics Chapter 13, Unit 13 11, doi:10.1002/0471250953.bi1301s10 (2005).

40 Lange, V., Picotti, P., Domon, B. & Aebersold, R. Selected reaction monitoring for quantitative proteomics: a tutorial. Molecular systems biology 4, 222 (2008).

41 Redding-Johanson, A. M. et al. Targeted proteomics for metabolic pathway optimization: application to terpene production. Metab Eng 13, 194-203, doi:10.1016/j.ymben.2010.12.005 (2011).

42 Heider, S. A., Peters-Wendisch, P., Beekwilder, J. & Wendisch, V. F. IdsA is the major geranylgeranyl pyrophosphate synthase involved in carotenogenesis in Corynebacterium glutamicum. The FEBS journal 281, 4906-4920 (2014).

43 Konda, N. M. et al. Understanding cost drivers and economic potential of two variants of ionic liquid pretreatment for cellulosic biofuel production. Biotechnol Biofuels 7, 86, doi:10.1186/1754-6834-7-86 (2014).

44 Lawrence, C., Chi, Y.-I., Rodwell, V. & Stauffacher, C. Crystallization of HMG-CoA reductase from Pseudomonas mevalonii. Acta Crystallographica Section D: Biological Crystallography 51, 386-389 (1995).

45 Ma, S. M. et al. Optimization of a heterologous mevalonate pathway through the use of variant HMG-CoA reductases. Metab Eng 13, 588-597, doi:10.1016/j.ymben.2011.07.001 (2011).

46 Meadows, A. L. et al. Rewriting yeast central carbon metabolism for industrial isoprenoid production. Nature 537, 694-697, doi:10.1038/nature19769 (2016).

47 Ajikumar, P. K. et al. Isoprenoid pathway optimization for Taxol precursor overproduction in Escherichia coli. Science 330, 70-74, doi:10.1126/science.1191652 (2010).

48 Zheng, Y. et al. Metabolic engineering of Escherichia coli for high-specificity production of isoprenol and prenol as next generation of biofuels. Biotechnology for Biofuels 6, 57, doi:10.1186/1754-6834-6-57 (2013).

49 Ginésy, M., Rusanova-Naydenova, D. & Rova, U. Tuning of the Carbon-to-Nitrogen Ratio for the Production of L-Arginine by Escherichia coli. Fermentation 3, 60 (2017).

50 Wang, G., Bai, T., Miao, Z., Ning, W. & Liang, W. Simultaneous production of single cell oil and fumaric acid by a newly isolated yeast Aureobasidium pullulans var. aubasidani DH177. Bioprocess and Biosystems Engineering 41, 1707-1716 (2018).

51 Hua, Q., Yang, C., Oshima, T., Mori, H. & Shimizu, K. Analysis of gene expression in Escherichia coli in response to changes of growth-limiting nutrient in chemostat cultures. Applied and environmental microbiology 70, 2354-2366 (2004).

52 He, N., Li, Y. & Chen, J. Production of a novel polygalacturonic acid bioflocculant REA-11 by Corynebacterium glutamicum. Bioresource Technology 94, 99-105, doi:https://doi.org/10.1016/j.biortech.2003.11.013 (2004).

53 Zha, J. et al. Metabolic engineering of Corynebacterium glutamicum for anthocyanin production. Microbial Cell Factories 17, 143, doi:10.1186/s12934-018-0990-z (2018).

54 Xu, P., Ranganathan, S., Fowler, Z. L., Maranas, C. D. & Koffas, M. A. Genome-scale metabolic network modeling results in minimal interventions that cooperatively force carbon flux towards malonyl-CoA. Metabolic engineering 13, 578-587 (2011).

55 Cui, X., Kavvada, O., Huntington, T. & Scown, C. D. Strategies for near-term scale-up of cellulosic biofuel production using sorghum and crop residues in the US. Environmental Research Letters 13, 124002 (2018).

56 Dibble, D. C. et al. A facile method for the recovery of ionic liquid and lignin from biomass pretreatment. Green Chemistry 13, 3255-3264, doi:10.1039/C1GC15111H (2011).

57 Shi, J. et al. One-pot ionic liquid pretreatment and saccharification of switchgrass. Green Chemistry 15, 2579-2589, doi:10.1039/C3GC40545A (2013).

58 Frederix, M. et al. Development of an E. coli strain for one-pot biofuel production from ionic liquid pretreated cellulose and switchgrass. Green Chemistry 18, 4189-4197, doi:10.1039/c6gc00642f (2016).

Chapter IV Production of Tetra-methylpyrazine Using Engineered *C. glutamicum* hydrolysates

Alkylpyrazines are naturally distributed, heterocyclic aromatic compounds with a nutty or roasted flavor profile[1]. Of the alkylpyrazine compounds, 2,3,5,6-tetra-methylpyrazine (also known as TMP or ligustrazine) is a biologically active alkaloid commonly found in the rhizobiome of *Ligusticum wallichii*[2]. It has been used as a flavoring agent[3], studied as a potentially pharmacologically active molecule[4-6], or applied onto surfaces as a coating[7,8]. While TMP has been examined for potential use in many fields, its extensive evaluation is hindered due to its limited commercial availability. Chemical synthesis routes to TMP are consisted of multiple synthesis steps and reported to be inefficient[9,10]. Commercially available TMP is often purified through an ethanol-ethyl ether extraction from plants such as *Ephedra sinica*[11]. More sustainable, biological routes towards TMP production have focused on optimizing cultivation conditions of *Bacillus subtilis*, which can naturally produce the TMP precursor, acetoin[12,13]. The conversion of acetoin into TMP requires heating of the cell lysate under ~65 ˚C for 2 hours, which results in the 26% yield[13]. Outside of *B. subtilis*, trace amounts of alkylpyrazines (e.g., TMP) have been detected in the headspace of *Corynebacterium glutamicum*[10]. Of note, a single *C. glutamicum* isolate (MB-1923) is the only strain that can produce higher titers of TMP, nonetheless, this strain is not publicly available and has no associated genomic metadata[14]. The biological synthetic route of TMP has been postulated and it could be produced from pyruvate via a four-step reaction (**Figure 1**): The two units of the proposed immediate precursor, acetoin[15], would spontaneously react with each other to form TMP under high nitrogen concentrations.

In this study, I examined engineered strains of *C. glutamicum* for TMP production. Specific gene substitutions in a heterologous gene pathway generated strains producing high (>5 g/L) titers of TMP, or co-producing TMP with an acetyl-CoA derived compound, isopentenol[16].

Other factors that enhance and trigger the production of TMP in these engineered *C. glutamicum* strains are also described.

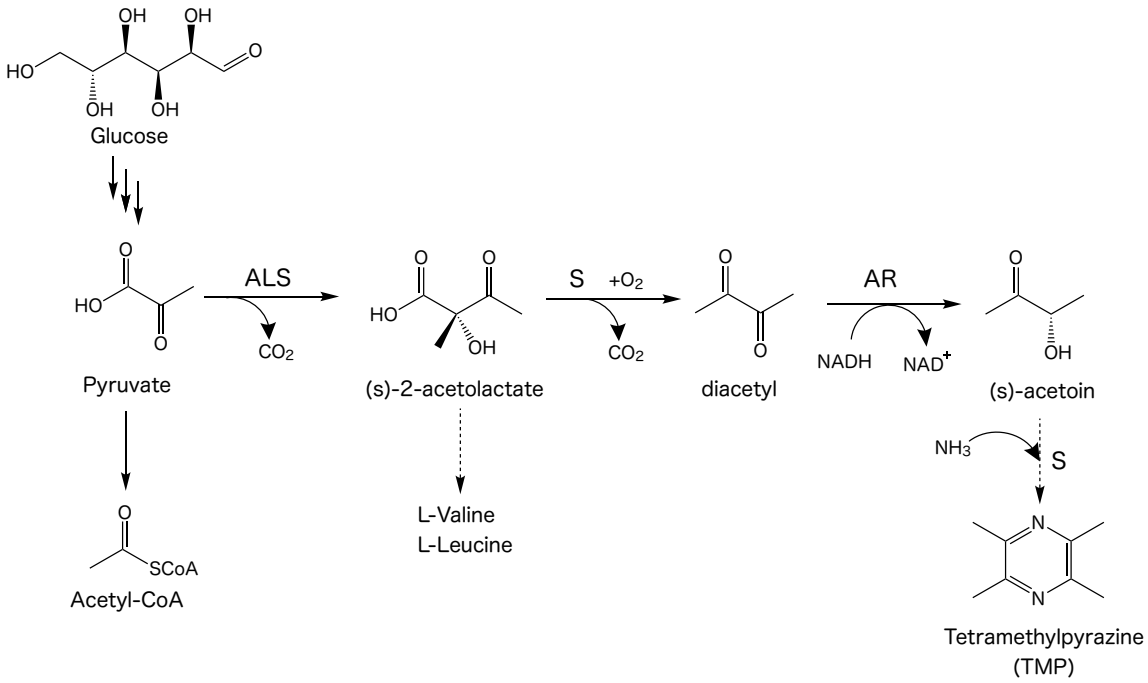

Figure 1. Diagram of Proposed Tetra-methylpyrazine (TMP) Production Pathway in *C. glutamicum*.
Model. Pyruvate is generated from glucose using the Embden-Meyerhof-Parnas (EMP) pathway and converted to TMP in four steps, as indicated. ALS, acetolactate synthase (*ilvB*, Cgl1271; *ilvN*, Cgl1272); AR, acetoin reductase (*butA*, Cgl2674). The upper-case letter S with arrows represents non-enzymatic spontaneous reactions (see Xiao *et al*, 2014[43]).

Materials and Methods

Chemicals and Reagents

All chemicals and reagents were purchased from Sigma-Aldrich (St. Louis, MO) or as otherwise indicated, and were of molecular biology grade or higher. When cells were cultivated in a microtiter dish format, plates were sealed with a gas-permeable film (Sigma-Aldrich, St. Louis, MO).

Strain and Plasmid Construction

All strains and plasmids used in this study are listed in Table 1. Oligo-nucleotide primers were synthesized by Integrated DNA Technologies, Inc. (San Diego, CA). Q5 High-Fidelity DNA Polymerase (New England Biolabs, Ipswich, MA) was used for a polymerase chain reaction. Isothermal DNA assembly[17] was utilized to assemble plasmids using 40 nucleotide overhangs (NEBuilder HiFi DNA Assembly Master Mix, New England Biolabs, Ipswich, MA). Plasmids were constructed using chemically competent *E. coli* DH10β (New England Biolabs). Where indicated, a heterologous isopentenol production pathway was modified to incorporate both *hmgr* and *mk* homologs from *S. aureus* or *C. kroppenstedtii*, to replace the existing gene from *S. cerevisiae*. For *S. aureus*, the *mk* homolog is encoded by *mvaK1* (NCBI: WP_000197034.1) and similarly, the *hmgr* homolog is encoded by *mvaS* (NCBI: WP_045179588.1). For *C. kroppenstedtii,* the *mk* homolog is encoded by *mvaK1* (NCBI: ACR16826.1) and likewise, the *hmgr* homolog is encoded by *mvaA* (NCBI: WP_012730718.1). All sequences were confirmed by colony PCR and Sanger sequencing.

Table 1. Strains and plasmids used in this study

Strain	Description	Selection	Reference
JBEI-7936	*Corynebacterium glutamicum* ATCC 13032 / NHRI 1.1.2, biotin auxotroph	Nx^R	Sasaki et al., 2019
JBEI-19571	JBEI-7936 harboring p/JBEI-19559	Kan^R	Sasaki et al., 2019
JBEI-19652	JBEI-7936 harboring p/JBEI-19628	Kan^R	This study
JBEI-19658	JBEI-7936 harboring p/JBEI-19634	Kan^R	This study
JBEI-19566	JBEI-7936 Δ*poxB* Δ*ldhA*	Suc^R, Kan^S	Sasaki et al., 2019
E. coli DH1	*F^- λ^- endA1 recA1 relA1 gyrA96 thi-1 glnV44 hsdR17($r_K^-m_K^-$)*		Meselson and Yuan, 1968
E. coli DH10β	F^- *endA1 deoR*$^+$ *recA1 galE15 galK16 nupG rpsL Δ(lac)X74* φ80*lacZΔM 15 araD139 Δ(ara,leu)7697 mcrA Δ(mrr-hsdRMS-mcrBC)* Str^R λ^-		Invitrogen

Plasmid	Description	Selection	Reference
JBEI-2600	pEC-XK99E, *E. coli-C. glutamicum* shuttle expression vectors based on the medium-copy number plasmid including *pGA1*, Kan^R, *ori*V, P_{trc}	Kan^R	Kirchner et al., 2003
JBEI-19559	pEC-XK99E-AK-IP-bypass	Kan^R	Sasaki et al., 2019
JBEI-19628	pTE221 pEC-XK99E-AK-IP-bypass-*S. aureus mvaK1, mvaS* (substitution)	Kan^R	This study
JBEI-19634	pTE222 pEC-XK99E-AK-IP-bypass-*C. kroppenstedtii mvaK1, mvaA* (substitution)	Kan^R	This study

Growth Media Composition

Production was analyzed in several different common growth media. Lysogeny-Broth (LB): 10 g/L tryptone, 5 g/L yeast extract, and 5 g/L NaCl. Tryptone and yeast extract were purchased from BD Biosciences (Franklin Lakes, NJ). NCM media[18]: 17.4 g/L K_2HPO_4, 11.6 g/L NaCl, 5 g/L D-glucose, 5 g/L tryptone, 1 g/L yeast extract, 0.3 g/L trisodium citrate, 0.05 g/L $MgSO_4 \cdot 7H_2O$, and 91.1 g/L sorbitol, pH 7.2. CGXII minimal medium was prepared as previously described[16,19]. D-glucose was used as a carbon source at the 4 % (w/v) concentration or as otherwise indicated.

Preparation of Electrocompetent C. glutamicum Cells

C. glutamicum was made electrocompetent, as previously described[16]. In brief, cells were grown in NCM medium supplemented with 3% (v/v) glycine and electroporated with a Micro Pulser Electroporator (Bio-Rad Laboratories, Inc., Hercules, CA) at 10 μF, 600 Ω, and 1800 V. After electroporation cells were immediately mixed with 400 μL of BHIS broth and heat-shocked for 6

minutes at 46 ˚C. After a two-hour outgrowth at 30 ˚C, cells were plated on the appropriate selective agar plate.

Cultivation of C. glutamicum for Isopentenol and TMP production

All cells taken from -80 ˚C glycerol stocks were plated on LB agar plates containing the appropriate antibiotic following standard laboratory procedures. Single colonies were inoculated and grown overnight in 5 mL LB media (with antibiotics as necessary) at 30 ˚C on a rotary shaker at 200 rpm. Kanamycin was added to the growth media at a final concentration of 50 μg/mL. Unless otherwise noted, all seed cultures were first inoculated for growth in culture tubes. If cells were grown in a 24-well deep well format, 2 mL of culture media was used per well. Deep well plates were incubated in an Infors Multitron Incubator with a 3 mm Orbital Shaking Platform shaken at 999 rpm (Bottmingen, Switzerland).

To measure TMP or isopentenol production, the adapted cultures of *C. glutamicum* were first back-diluted to OD_{600} of 0.1 into CGXII minimal medium including 4% (w/v) D-glucose at the concentrations described above. Cells from a seed culture were sub-cultured twice to adapt cells to grow in the media, as previously described[16]. The production pathway was then induced as before when cultures reached an OD_{600} of ~0.8. Exogenous ionic liquids were added to the adapted cultures at the same time of induction with IPTG.

Analytical Methods for Chemical Identification and Quantification

For metabolite quantification, 300 μL of cell culture media was combined with 300 μL of ethyl acetate containing n-butanol (10 mg/L) as an internal standard and processed as described previously[16,20,21]. Briefly, samples were shaken at maximum speed for 15 minutes using an MT-400 microtube mixer (TOMY Seiko, Tokyo, Japan) and then centrifuged at 14,000*g* for 3 mins to separate the organic phase from the aqueous phase. 60 μL of the organic layer was transferred into a GC vial and 1 μL was analyzed by Agilent GC/MS equipped with a DB-5 column (Agilent

Technologies, Santa Clara, CA, USA) or Thermo GC-FID equipped with a DB-WAX column (Agilent Technologies, Santa Clara, CA, USA) for quantification of TMP, acetoin, diacetyl, and isopentenol (3-methyl-3-buten-1-ol). Analytical grade standards were purchased from Sigma-Aldrich (St. Louis, MO) and used to calculate analyte concentrations and confirm the identification of peaks. To compare the extraction efficiency of TMP into dichloromethane, the same protocol as above was used where dichloromethane was used in place of ethyl acetate as the extraction solvent. Reported TMP titers were calculated using a linear curve of TMP peak areas normalized to n-butanol generated from authentic standards resuspended directly into ethyl acetate. Values were corrected for inefficient extraction from CGXII media into ethyl acetate by multiplying GC-FID values by 5.88 (**Figure 2A**).

To determine the spontaneous conversion rate of acetoin or diacetyl to tetra-methylpyrazine, pure 100 mM of pure analytical grade standards were added to CGXII media supplemented with 4% D-glucose. These cultures were then incubated at 30 ˚C as described in section 2.5 for 48 hours, after which samples were harvested for ethyl acetate extraction and quantification by GC-FID. Conversion of acetoin or diacetyl to TMP was quantified using authentic standards, and samples were tested in triplicate. A commonly used extraction solvent, ethyl acetate, showed a 17% extraction efficiency for TMP from CGXII culture media (**Figure 2A**). While toxic and more challenging to handle, dichloromethane showed a higher extraction efficiency for TMP at 50% from culture media (**Figure 2B**).

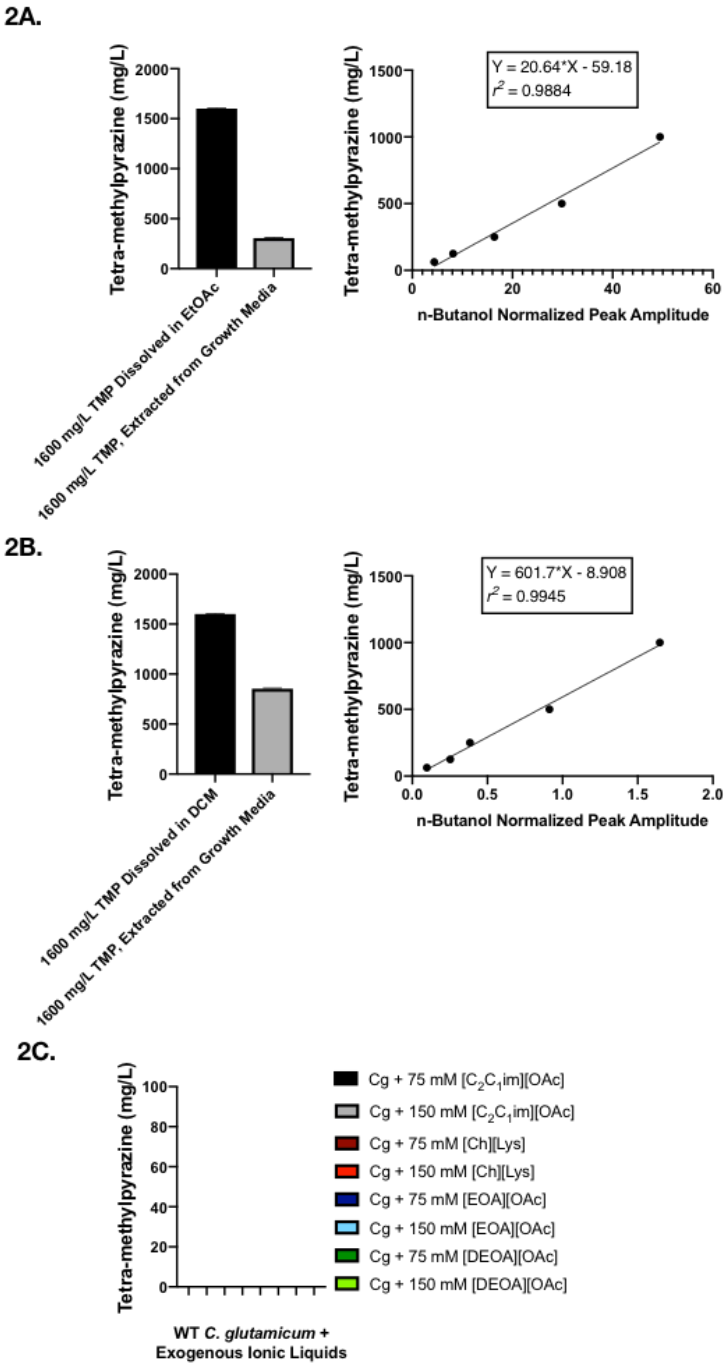

Figure 2. The extraction efficiency of TMP. **A.** Extraction efficiency of TMP using ethyl acetate as the extraction solvent. The linear range of TMP dissolved in ethyl acetate is plotted on the right. **B.** The extraction efficiency of TMP using dichloromethane. The linear range of TMP dissolved in dichloromethane is plotted on the right. **C.** Impact of exogenous ionic liquid on wild-type *C. glutamicum*. Without the presence of a heterologous gene pathway, no TMP was detected with any ionic liquid treatment.

Comparison of Pathway Protein Abundance in E. coli and C. glutamicum

E. coli (DH1) and *C. glutamicum* (ATCC 13032) strains harboring plasmid pTE220 were cultivated as described in section 2.5. They were grown in LB media supplemented with 56 mM glucose and 50 µg/mL Kanamycin + 500 µM IPTG to ensure an equitable comparison between these two hosts. Crude cell extracts were prepared exactly as described before[22] and analyzed with an Agilent 6550 iFunnel Q-TOF mass spectrometer (Agilent Technologies, Santa Clara, CA) coupled to an Agilent 1290 UHPLC system, with a method as described previously[23]. To measure global proteomic changes between pathway variants in *C. glutamicum*, I analyzed the set of proteins absent in wild-type *C. glutamicum* but were detected in the pathway variant samples by shotgun proteomics, filtering for proteins with at least two unique total peptides detected. Endogenous proteins were functionally annotated using eggNOG-mapper[24] to assign COG annotations[25]. Hierarchical clustering using a one minus Pearson correlation was calculated for both proteins and strains using the Morpheus software package (https://software.broadinstitute.org/morpheus).

Fed-batch Production of TMP in a 2 L Bioreactor Format

Fed-batch production was performed using a 2 L bioreactor equipped with a Sartorius BIOSTAT B plus control unit for regulating dissolved oxygen (DO), pH, and temperature. A seed train was used to generate the starting inoculum for the bioreactor, which was electronically controlled to a pH of 7.0 +/- 0.3 using 7.5 M ammonium hydroxide and 4 M sulfuric acid. The temperature of the bioreactor was kept constant at 30 ˚C throughout the production time course. Diluted 10% (v/v) PEG-PPG-PEG, Poly(ethylene glycol)-block-poly(propylene glycol)-block-poly(ethylene glycol) (Sigma-Aldrich) was added as needed to control foaming. During the initial growth phase, DO was controlled at 30% saturation by varying agitation speed from 400 to 1,200 rpm, and then the air-flow rate was subsequently varied from 0.5-1.5 volume of air per volume of medium per minute (vvm). Cultures were induced with 500 µM IPTG after 3 hours of the batch phase. After

depletion of the starting D-glucose (~10 g/L), feeding was initiated in low oxygen conditions by dropping DO levels down to 0-5% of saturation by varying agitation speed from 400 to 750 rpm and gassing with 0.25 vvm, and the feeding rate was controlled to keep the D-glucose concentration above 10 g/L. The feed solution contained 500 g/L D-glucose, 5 g/L $(NH_4)_2SO_4$, 1.5 g/L KH_2PO_4, 1.5 g/L K_2HPO_4, 5 g/L yeast extract, 0.5 mM IPTG, and kanamycin. At specific time points, 5 mL samples were collected from the bioreactor by syringe affixed to the sampling tube and used for growth, GC-FID, and HPLC analysis.

Results

Engineered Strains Harboring a Heterologous Gene Pathway Produce Tetra-methylpyrazine

I observed the formation of tetra-methylpyrazine (TMP) while analyzing heterologous gene pathway variants expressed in engineered *C. glutamicum* strains. In the previous study, I had engineered *C. glutamicum* for the production of isopentenol using a heterologous, mevalonate-based five gene pathway, referred to as the "original" pathway[16]. Pathway variants were constructed because two of the genes (*mk* and *hmgR* derived from *Saccharomyces cerevisiae*) were poorly expressed under standard laboratory growth conditions (refer to **Additional Table**[1]). These variants were constructed by substituting *mk* and *hmgR* gene homologs from either *Staphylococcus aureus* or *Corynebacterium kroppenstedtii* into the heterologous gene pathway and assayed for TMP production over a 48 hour time course.

I report that these strains with two successfully expressed *mk* homologs (from *S. aureus* and *C. kroppenstedtii*) and *hmgR* from *S. aureus* resulted in the production of TMP as detected by GC analysis (**Figure 3**). In the absence of a heterologous gene pathway, no new products were detected. The *C. glutamicum* strain harboring the original pathway produced 300 mg/L isopentenol and did not produce detectable TMP. In contrast to the original pathway, the *S. aureus Mk*, *HmgR* pathway variant produced 2.2 g/L of TMP and ~200 mg/L of isopentenol. Furthermore, the *C. kroppenstedtii Mk*, *HmgR* pathway variant produced 5 g/L of TMP and did not produce isopentenol. These results indicate that the choice of pathway variant expressed in *C. glutamicum* impacted the amount of TMP produced.

[1] The table is available at https://doi.org/10.1016/j.mec.2019.e00115

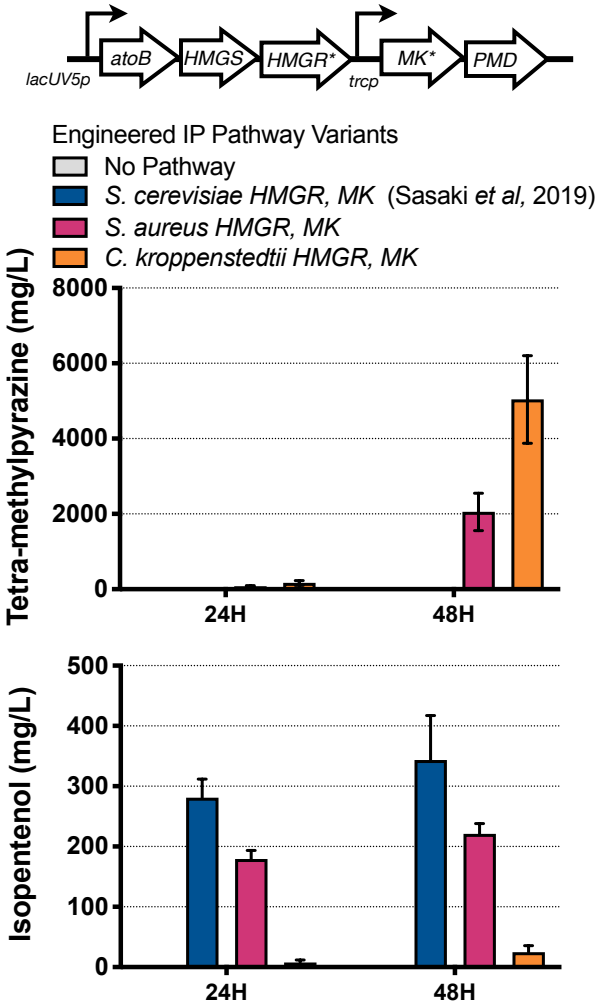

Figure 3. *mk* and *hmgR* Variants from Bacterial Species bias Production Towards Tetra-methylpyrazine.

Top panel. Schematic of the heterologous isopentenol production pathway. The two genes selected for optimization by substitution with homologs are indicated with an asterisk (*). The proposed metabolic pathway for the conversion of glucose to isopentenol has been previously described before[16].

Bottom panels. Analysis of the engineered isopentenol production pathway in *C. glutamicum* using *mk* and *hmgR* homologs from *S. aureus* and *C. kroppenstedtii* in a 24 well plate format. *C. glutamicum* Δ*poxB* Δ*ldhA* strain harboring the original isopentenol production pathway (JBEI-19559) was compared with variants where the *S. cerevisiae MK* and *HMGR* were replaced with *mk* and *hmgR* from *S. aureus* (JBEI-19652) or *C. kroppenstedtii* (JBEI-19658). Samples were cultivated in CGXII media 4% D-glucose in a 24 well plate format. TMP or isopentenol titers were analyzed at the time points indicated and are an average of three biological replicates. The error bars represent standard error.

Next, I examined if candidate TMP pathway proteins (**Figure 1**) had increased expression in these two new strains. However, no significant difference in protein abundance was detected for the three candidate pathway genes, IlvB, IlvN, or ButA among the strain variants **(Table 3)**. As there was no detectable change in protein abundance for the pathway genes, I searched for proteome-wide changes to cellular metabolism, which could favor spontaneous conversion to TMP.

Four proteins involved in the tryptophan synthesis pathways (TrpE/CgR_2916, TrpG/CgR_2917, TrpB/CgR_2920, TrpA/CgR_2921) were newly detected in strains expressing the isopentenol pathway variants from *S. aureus* or *C. kroppenstedtii* (**Figure 4A** and **Additional Table** [2]). Additionally, two proteins involved in nitrogen metabolism (ArgJ/CgR_1458, CgR_1470) were also identified as enriched in these strains. There were four native proteins that were upregulated only in the *C. kroppenstedtii* pathway variant strain: CgR_1697 (a putative cadherin-like superfamily protein); CgR_2760 (a putative polyketide synthase); CgR_0268 (a short-chain dehydrogenase); and CgR_2530 (uncharacterized protein, no predicted homologs). A systems-level analysis[25] of the 83 upregulated proteins indicated that 53% of these proteins were involved in cellular physiology (**Figure 4B**). In particular, ortholog groups of translation-related activities (category J) and amino acid metabolism and transport (category E) are enriched (**Figure 4C**). Complete data of all enriched proteins from these engineered strains are plotted in Additional Figures[2]. As the expression of specific heterologous gene pathways favored nitrogen-accumulating processes that could enhance TMP production[15], it was reasonable that the enrichment of new compounds could be favored in these variant strain backgrounds.

[2] The table and figure are available at https://doi.org/10.1016/j.mec.2019.e00115

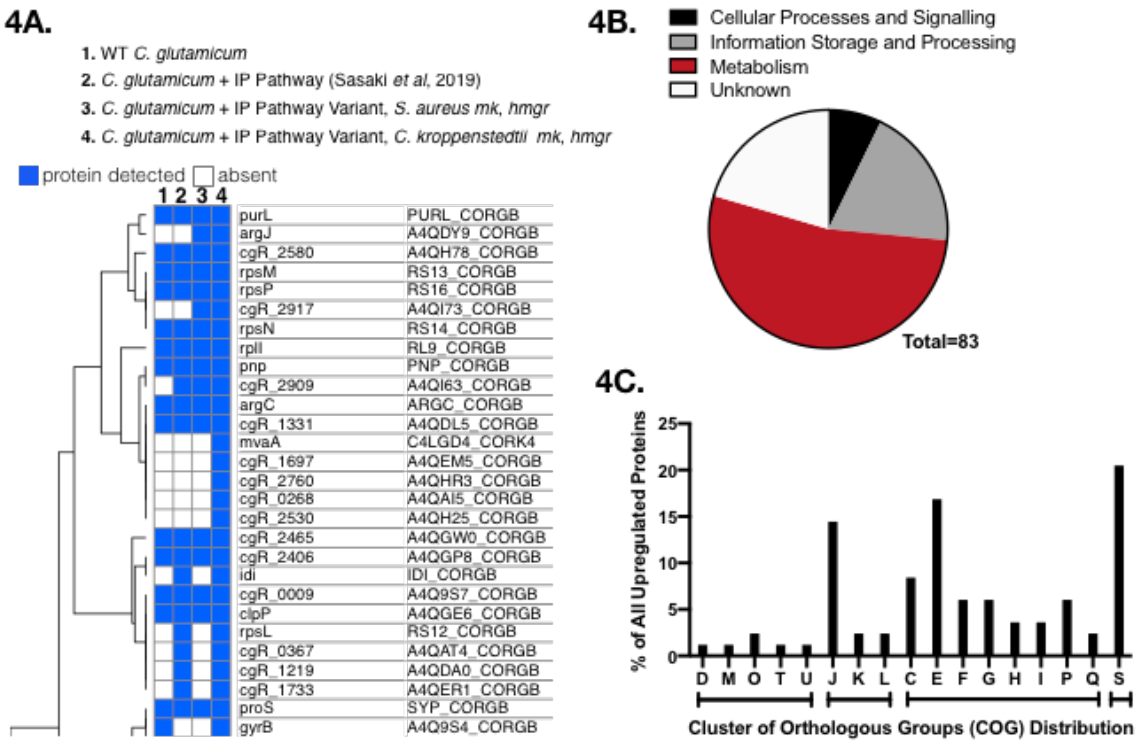

Figure 4. Proteomic Analysis of Engineered *C. glutamicum* Strains.
A. Hierarchical clustering of proteins enriched after the heterologous gene pathway expression in the engineered *C. glutamicum* strains. **B.** Gene functions of enriched proteins as modeled with eggNOG-mapper to assign genes into categories of orthologous groups (COGs). WT *C. glutamicum* (JBEI-7936) was compared against strains harboring the original isopentenol pathway (JBEI-19571) or the plasmid variants (JBEI-19652 and JBEI-19658). **C.** Distribution of enriched proteins into specific COGs. COGs falling into related categories from the top panel are grouped in brackets below. COG definitions: D, cell division and chromosome partitioning; M, cell wall structure and biogenesis and outer membrane; O, molecular chaperones and related functions; T, signal transduction; Intracellular trafficking, secretion; J, Translation, ribosomal structure and biogenesis; K, transcription; L, replication, recombination, repair; C, energy production and conversion; E, amino acid transport and metabolism; F, nucleotide transport and metabolism; G, carbohydrate transport and metabolism; H, coenzyme transport and metabolism; I, lipid transport and metabolism; P, inorganic ion transport and metabolism; Q secondary metabolite transport and metabolism; S, unknown function.

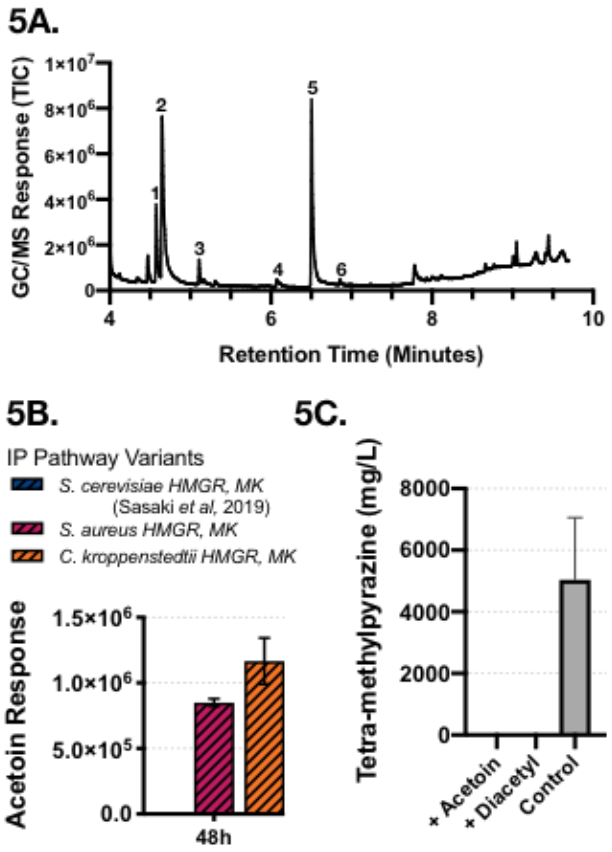

Figure 5. GC/MS Analysis of Tetra-methylpyrazine and S-acetoin. A. Identification of tetra-methylpyrazine and other peaks by GC/MS analysis. The genotypes of the strains used were the same as described in Figure 2. *Peak identification. 1.* Acetoin (3-hydroxy-2-butanone). *2.* Isopentenol (3-methyl-3-buten-1-ol). *3.* 4-penten-1-ylacetate. *4.* 2,3,5-tri-methyl-pyrazine. *5.* 2,3,5,6-tetra-methyl-pyrazine. *6.* 3,5-diethyl-2-methyl-pyrazine. **B.** Comparison of acetoin peak height across different engineered strains by GC/MS analysis **C.** Assessment of spontaneous conversion of acetoin or diacetyl to TMP in the absence of cells using 100 mM of either starting compound spiked into CGXII growth media. No TMP was detected.

Analysis of Tetra-methylpyrazine Biosynthesis and Its Downstream Extraction

To understand how TMP might be produced in these strains, I examined the GC/MS trace files from these samples to determine if other related pathway intermediates might also be detected. GC/MS analysis of the additional analytes indicated the additional main peak to be tetra-methylpyrazine, TMP (**Figure 5A** peak no. 5 and **Figure 6**). I also detected the accumulation of tri-methylpyrazine and 3,5-diethyl-2-methyl-pyrazine but did not investigate either of these products any further (**Figure 5A,** peak no. 4 and peak no. 6**)**.

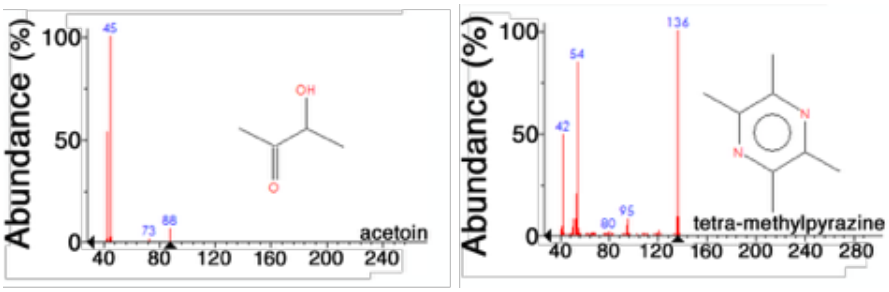

Figure 6. Mass fragmentation pattern of acetoin and TMP.

Consistent with the proposed pathway for pyrazine synthesis (**Figure 1**), I also detected S-Acetoin (3-Hydroxybutanone; **Figure 5A** peak no. 1 and **Figure 6**), the proposed precursor of tri/tetra-methylpyrazine[13,26]. S-Acetoin was specifically identified in samples with detectable TMP production levels and absent in samples that did not produce TMP (**Figure 5B**). The accumulation of acetoin in these strains strengthens the evidence in support of the proposed biological route to produce TMP. I next examined if TMP could form spontaneously from acetoin or diacetyl in the absence of a microbial host under biologically relevant cultivation conditions. Commercially purchased authentic standards for acetoin and diacetyl were spiked into CGXII media and tested for the formation of TMP after the same cultivation period of 48 hours. I did not detect the spontaneous conversion of either acetoin or diacetyl to TMP, suggesting that the reaction most efficiently produces TMP in the presence of a cell (**Figure 5C**).

Ionic Liquids, a Renewable Pretreatment Reagent, Enhances Production of Tetra-methylpyrazine

Most sustainable production requires the use of renewable carbon sources such as plant-derived biomass and pose trade-offs due to the incompatibilities between processes[16,22,27-29]. I evaluated the behavior of *C. glutamicum* strains when cultivated with reagents used in the pretreatment of sustainable carbon streams. Specifically, I asked if trace levels of ionic liquids, a promising reagent for plant biomass deconstruction[30,31], changed the amount of TMP produced in strains expressing the original IP pathway.

I characterized the effect of three different classes of ionic liquids on the behavior of engineered *C. glutamicum* strains for TMP production. The ionic liquids chosen were acetate salts with 1-ethyl-3-methyl imidazolium ($[C_2C_1im]^+$); cholinium ($[Ch]^+$); ethanolamine [ETA]; and diethanolamine [DEOA], [ETA] and [DEOA] cations. $[C_2C_1im]$ and [Ch] are two biogenic ILs, whereas [ETA] and [DEOA] are two representative protic ILs. I detected TMP at the 48 hour time point under these ILs-stressed conditions (**Figure 5**). In the presence of exogenous 150 mM $[C_2C_1im][OAc]$, I detected 63 mg/L TMP. Interestingly, in contrast to bioproduction in other microbial hosts[22,27], I did not observe inhibition of the production in the presence of ILs. Rather, when treated with 150 mM [Ch][OAc], I detected higher levels of TMP production, with titers reaching 1021 mg/L. Of the protic ILs, treatment with 150 mM [ETA][OAc] produced a similar titer to [Ch][OAc], with measured titers around 1050 mg/L. 150 mM [DEOA][OAc] treatment resulted in an accumulation of TMP to 585 mg/L. When expressed in *C. glutamicum*, the original IP pathway does not produce TMP under standard cultivation conditions, but treatment with specific ILs result in TMP production from undetectable to over 1 g/L.

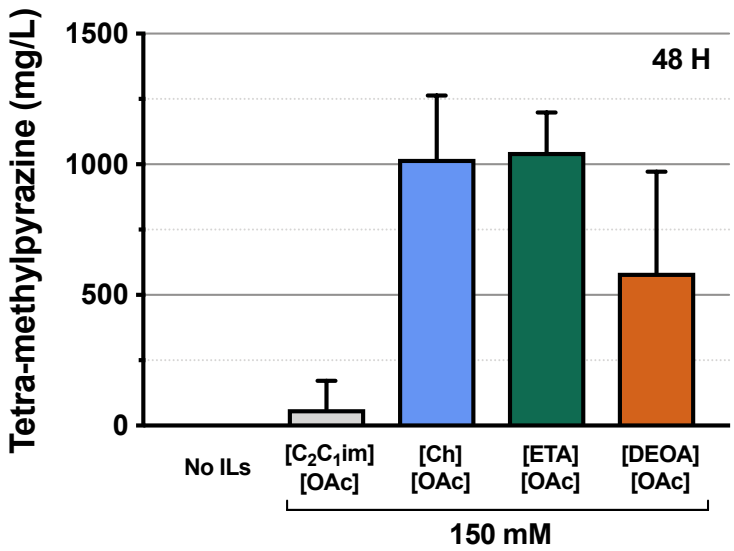

Figure 7. Specific Forms of Ionic Liquids Induce Tetra-methylpyrazine Production in *C. glutamicum*.
The production profiles of the *C. glutamicum* (JBEI-19571) against three types (imidazolium, cholinium, and protic form) of ionic liquids were examined in CGXII media with 4% D-glucose in a 24 well plate format. ($[C_2C_1im]^+$); cholinium ($[Ch]^+$); ethanolamine acetate [ETA][OAc]; and

diethanolamine acetate [DEOA][OAc] A. Produced titers of tetra-methylpyrazine are shown at 48 hours post induction under 75 mM (A) or 150 mM (B) [C_2C_1im][OAc], [Ch][OAc], [ETA][OAc], and [DEOA][OAc]. The control experiment was performed without IL supplementation (No ILs). Data shown are an average of biological triplicates, and the error bars represent standard error.

Ionic liquids alone were not sufficient to induce TMP production in wild-type *C. glutamicum* (**Figure 2C**). The amount of TMP produced in response to the IL was more variable when treating cells with 75 mM ILs, but TMP still accumulated in the same set of ILs. These strains also co-produced TMP and ~350 mg/L isopentenol using the unmodified isopentenol production pathway (**Figure 8**). These results provide a new perspective on using ILs as pretreatment reagents. Rather than framing ILs as pretreatment contaminants that must be removed, trace ionic liquids remaining from biomass pretreatment regimes could be beneficial as inducers allowing the coproduction of TMP and isopentenol.

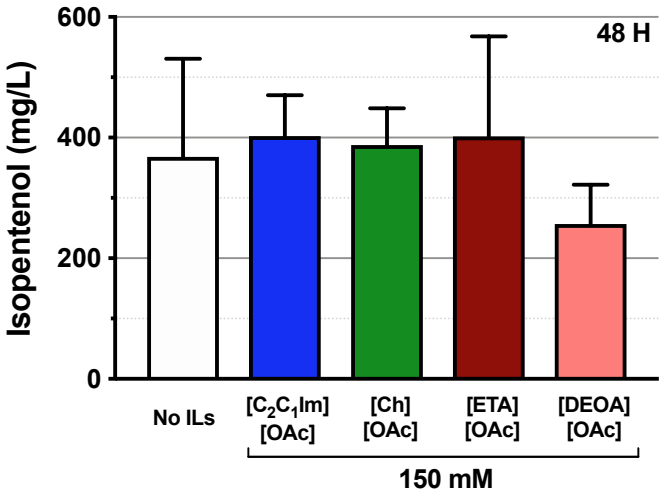

Figure 8. Related to Figure 7. Quantification of isopentenol production in production strains treated with exogenous ionic liquids. The data shown are an average of biological triplicates, and the error bars represent standard error.

Production of TMP in Fed-Batch Mode Cultures

Having observed the accumulation of TMP in our engineered strains, I wanted to determine next if TMP production could be produced under more industrially relevant cultivation conditions. I thus changed our cultivation format from a 24 well deep well microtiter dish to a 2L bioreactor format in fed batch mode. To retain flexibility in the choice of the final product, I added 50 mM of the IL [Ch][Lys] to stimulate TMP production in the engineered *C. glutamicum* strain using the original pathway. In fed-batch mode, the rate of TMP production was slower than what was observed in batch mode, as I only detected 700 mg/L of TMP after 48 hours of cultivation (**Figure 9**, compare to time course in **Figure 3**). It is possible that TMP is only produced after nutrient exhaustion in the stationary phase, as I only detected TMP production 6 hours after the final addition of the feed solution. The TMP titer after 65 hours cultivation reached 2 g/L (**Figure 9**), which was higher than the final titer in the smaller lab-scale format using IL-stimulated production (compare with **Figure 8**). Isopentenol production under these cultivation conditions was near the detection limit (5 mg/L) potentially due to the increased aeration from the impeller driven mixing inherent to cell growth conditions in the bioreactor (**Figure 9**). I attempted to phase separate isopentenol with a dodecane overlay[32], but dodecane inhibited the growth of *C. glutamicum* under these conditions. These results indicate the scalability of TMP production under industrially relevant formats, but further work would be required to co-produce isopentenol.

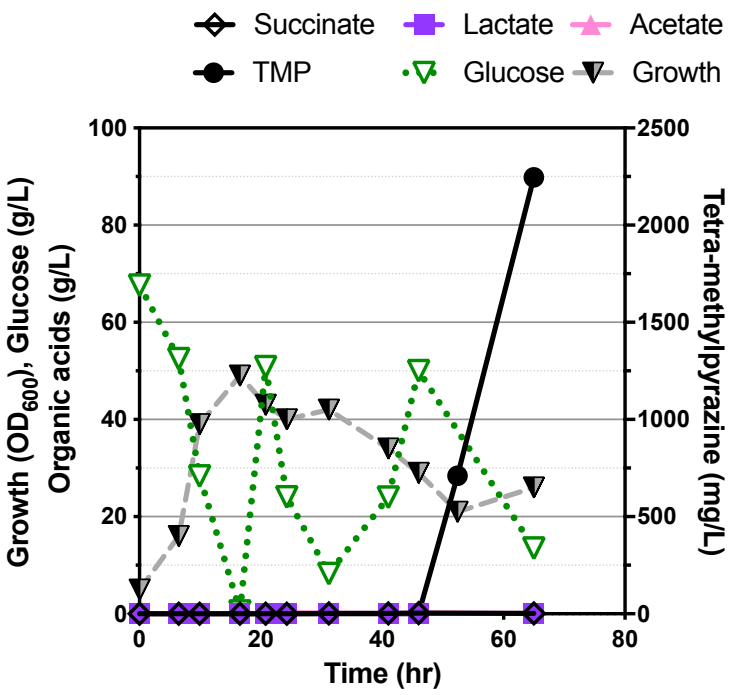

Figure 9. Fed-batch Mode Production of TMP in the Engineered *C. glutamicum*.
C. glutamicum (JBEI-19571) was initially cultivated in batch mode using CGXII minimal media including 8% starting D-glucose and 50 mM [Ch][Lys] in a 2L Sartorius Bioreactor. Subsequently, the fed-batch mode was initiated when the initial D-glucose concentration decreased below 1%. A pulse mode feeding strategy was utilized to raise the D-glucose concentration above 1%. Final products and organic acid concentrations were quantified and are indicated as labeled in the legend above.

Discussion

This report illustrates two parameters by which *C. glutamicum* can be modified to produce tetramethylpyrazine. Our highest final titers from batch and fed-batch production modes compare favorably with published titers from *Bacillus subtilis*[13,33] and do not require a post-cultivation denaturing step to produce TMP. Unlike *E. coli*, *C. glutamicum* responds to the burden of expressing a heterologous IP pathway by accumulating TMP. A previous report had indicated that redirecting central metabolism in *C. glutamicum* away from acetate led to the accumulation of high intracellular levels of acetoin[34], but did not report TMP in their strains. This result from Mao *et al.* is consistent with our hypothesis, in which the burden of a specific heterologous gene pathway can instead favor high-level TMP accumulation. Moreover, the kinetics of TMP formation is dependent on the specific pathway variant analyzed. There are likely interactions between the heterologous gene pathway and native metabolism at the metabolite level, or activation of a native cryptic regulatory system. Efficient and universal metabolite quenching for metabolic flux analysis could be utilized to examine these possibilities[35,36].

Certain ionic liquids are known to impact cellular morphology and physiology[37]. Their impact on engineered strains can also be pathway-specific; in *E. coli*, the addition of an isopentenol production pathway to an IL-tolerant strain can result in acetate accumulation rather than isopentenol[22]. In contrast, limonene can be produced from the same IL-tolerant strain without detectable acetate accumulation[22]. While additional studies are required to understand the beneficial impact of ionic liquids on the production of TMP in engineered *C. glutamicum* strains, this study provides alternative paradigm of ILs as a useful chemical for improving production instead of merely being an unwanted contaminant. The added burden of ionic liquids could be a new metric for assessing how a heterologous gene pathway can impinge upon native metabolism, especially when evaluating hosts originating from different environmental niches and primary carbon sources[38].

The production of TMP is correlated with the accumulation of acetoin, providing additional evidence to strengthen participation of the proposed biosynthetic pathway (**Figure 1**). As I do not detect the spontaneous accumulation of TMP from either acetoin or di-acetyl when added directly into culture media (**Figure 5C**), I favor the hypothesis that this reaction occurs in the cellular environment. These observations highlight the importance of considering both the specific heterologous gene pathway as well as potential feedback on the chosen microbial host. With high titers of TMP, these *C. glutamicum* strains will facilitate the rapid evaluation of TMP derivatives using candidate enzyme libraries to be expressed in a gram-positive microbial host[39-41]. Being able to produce >1 g/L quantities of many TMP derivatives will unlock the potential of this emerging molecule for a broader spectrum of applications.

While I report the exclusive production of TMP, examples of the co-production of two different final products from the same microbial host can also be of value[42]. As these two compounds have distinct applications, such an industrial process would likely require refinement of existing purification techniques for efficient separation. Isopentenol easily partitions into organic solvents such as ethyl acetate, and TMP can be precipitated from the aqueous phase after cooling to ~4 ˚C[43]. Nevertheless, this report is the first instance in which either TMP or isopentenol has been the final product for a co-production study. The use of TMP as a possible co-produced compound with isopentenol will allow more nuance and control in the technoeconomic analysis of scaling up either product[28,44].

Summary

This chapter describes the successful use of the gram-positive industrial microorganism, *C. glutamicum,* for the high titer (> 5 g/L) production of TMP. These strains can also be used to co-produce TMP as well as the biofuel candidate, isopentenol. Production of TMP was scaled-up to industrially relevant conditions in a 2L fed-batch bioreactor, where I observed 2 g/L TMP when cells were treated with exogenous ionic liquid.

References

1 Masuda, H. & Mihara, S. Olfactive properties of alkylpyrazines and 3-substituted 2-alkylpyrazines. Journal of agricultural and food chemistry 36, 584-587 (1988).

2 Ke-ji, C., Zhen-huai, Q., Wei-Liang, W. & Mu-Ying, Q. Tetramethylpyrazine in the treatment of cardiovascular and cerebrovascular diseases. Planta medica 47, 89-89 (1983).

3 Zhu, B.-F., Xu, Y. & Fan, W.-L. High-yield fermentative preparation of tetramethylpyrazine by Bacillus sp. using an endogenous precursor approach. Journal of industrial microbiology & biotechnology 37, 179-186 (2010).

4 Ferreira, S. B. & Kaiser, C. R. Pyrazine derivatives: a patent review (2008–present). Expert opinion on therapeutic patents 22, 1033-1051 (2012).

5 Kao, T.-K. et al. Tetramethylpyrazine reduces cellular inflammatory response following permanent focal cerebral ischemia in rats. Experimental neurology 247, 188-201 (2013).

6 Chen, H. et al. A Novel Tetramethylpyrazine Derivative Protects Against Glutamate-Induced Cytotoxicity Through PGC1α/Nrf2 and PI3K/Akt Signaling Pathways. Frontiers in Neuroscience 12, doi:10.3389/fnins.2018.00567 (2018).

7 Ng, H., Seto, Keitaro, Zhang, Wei. Flame retardant vinyl addition polycycloolefinic polymers. United States patent US9765168B2 (2017).

8 Lee, J. L. Halogen-free flame retardant material. United States patent US8871843B2 (2014).

9 邓泽庭陶德胜罗荣邓钦鹏. Method for preparing tetramethyl pyrazine. (2006).

10 Dickschat Jeroen, S. et al. Pyrazine Biosynthesis in Corynebacterium glutamicum. European Journal of Organic Chemistry 2010, 2687-2695, doi:10.1002/ejoc.201000155 (2010).

11 Li, H.-X., Ding, M.-Y., Lv, K. & Yu, J.-Y. Separation and determination of ephedrine alkaloids and tetramethylpyrazine in ephedra sinica Stapf by gas chromatography-mass spectrometry. Journal of chromatographic science 39, 370-374 (2001).

12 Kosuge, T. & Kamiya, H. Discovery of a pyrazine in a natural product: tetramethylpyrazine from cultures of a strain of Bacillus subtilis. Nature 193, 776 (1962).

13 Xiao, Z., Hou, X., Lyu, X., Xi, L. & Zhao, J.-y. Accelerated green process of tetramethylpyrazine production from glucose and diammonium phosphate. Biotechnology for biofuels 7, 106 (2014).

14 Demain, A., Jackson, M. & Trenner, N. Thiamine-dependent accumulation of tetramethylpyrazine accompanying a mutation in the isoleucine-valine pathway. Journal of bacteriology 94, 323-326 (1967).

15 Rizzi, G. P. Formation of pyrazines from acyloin precursors under mild conditions. Journal of agricultural and food chemistry 36, 349-352 (1988).

16 Sasaki, Y. et al. Engineering Corynebacterium glutamicum to produce the biogasoline isopentenol from plant biomass hydrolysates. Biotechnology for Biofuels 12, 41, doi:10.1186/s13068-019-1381-3 (2019).

17 Gibson, D. G. et al. Enzymatic assembly of DNA molecules up to several hundred kilobases. Nat Methods 6, 343-345, doi:10.1038/nmeth.1318 (2009).

18 Ruan, Y., Zhu, L. & Li, Q. Improving the electro-transformation efficiency of Corynebacterium glutamicum by weakening its cell wall and increasing the cytoplasmic membrane fluidity. Biotechnology letters 37, 2445-2452 (2015).

19 Keilhauer, C., Eggeling, L. & Sahm, H. Isoleucine synthesis in Corynebacterium glutamicum: molecular analysis of the ilvB-ilvN-ilvC operon. Journal of bacteriology 175, 5595-5603 (1993).

20 Kang, A. et al. Isopentenyl diphosphate (IPP)-bypass mevalonate pathways for isopentenol production. Metab Eng 34, 25-35, doi:10.1016/j.ymben.2015.12.002 (2016).

21 Goh, E. B., Baidoo, E. E., Keasling, J. D. & Beller, H. R. Engineering of bacterial methyl ketone synthesis for biofuels. Appl Environ Microbiol 78, 70-80, doi:10.1128/AEM.06785-11 (2012).

22 Eng, T. et al. Restoration of biofuel production levels and increased tolerance under ionic liquid stress is enabled by a mutation in the essential Escherichia coli gene cydC. Microbial cell factories 17, 159 (2018).

23 Gonzalez Fernandez-Nino, S. M. et al. Standard flow liquid chromatography for shotgun proteomics in bioenergy research. Front Bioeng Biotechnol 3, 44, doi:10.3389/fbioe.2015.00044 (2015).

24 Huerta-Cepas, J. et al. Fast Genome-Wide Functional Annotation through Orthology Assignment by eggNOG-Mapper. Molecular Biology and Evolution 34, 2115-2122, doi:10.1093/molbev/msx148 (2017).

25 Galperin, M. Y., Makarova, K. S., Wolf, Y. I. & Koonin, E. V. Expanded microbial genome coverage and improved protein family annotation in the COG database. Nucleic acids research 43, D261-D269 (2014).

26 Karp, P. D., Latendresse, M. & Caspi, R. The pathway tools pathway prediction algorithm. Stand Genomic Sci 5, 424-429, doi:10.4056/sigs.1794338 (2011).

27 Ouellet, M. et al. Impact of ionic liquid pretreated plant biomass on Saccharomyces cerevisiae growth and biofuel production. Green Chemistry 13, 2743-2749, doi:10.1039/C1GC15327G (2011).

28 Baral, N. R. et al. Approaches for More Efficient Biological Conversion of Lignocellulosic Feedstocks to Biofuels and Bioproducts. ACS Sustainable Chemistry & Engineering (2019).

29 Wang, S. et al. Tolerance Characterization and Isoprenol Production of Adapted Escherichia coli in the Presence of Ionic Liquids. ACS Sustainable Chemistry & Engineering 7, 1457-1463 (2018).

30 George, A. et al. Design of low-cost ionic liquids for lignocellulosic biomass pretreatment. Green Chemistry 17, 1728-1734 (2015).

31 Li, C. et al. Comparison of dilute acid and ionic liquid pretreatment of switchgrass: Biomass recalcitrance, delignification and enzymatic saccharification. Bioresour Technol 101, 4900-4906, doi:10.1016/j.biortech.2009.10.066 (2010).

32 Peralta-Yahya, P. P. et al. Identification and microbial production of a terpene-based advanced biofuel. Nat Commun 2, 483, doi:10.1038/ncomms1494 (2011).

33 Yin, D. et al. High tetramethylpyrazine production by the endophytic bacterial Bacillus subtilis isolated from the traditional medicinal plant Ligusticum chuanxiong Hort. AMB Express 8, 193 (2018).

34 Mao, Y. et al. Systematic metabolic engineering of Corynebacterium glutamicum for the industrial-level production of optically pure d-(−)-acetoin. Green Chemistry 19, 5691-5702, doi:10.1039/C7GC02753B (2017).

35 Zhang, Q. et al. Comprehensive optimization of the metabolomic methodology for metabolite profiling of Corynebacterium glutamicum. Applied Microbiology and Biotechnology 102, 7113-7121, doi:10.1007/s00253-018-9095-1 (2018).

36 Wellerdiek, M., Winterhoff, D., Reule, W., Brandner, J. & Oldiges, M. Metabolic quenching of Corynebacterium glutamicum: efficiency of methods and impact of cold shock. Bioprocess and biosystems engineering 32, 581-592 (2009).

37 Mehmood, N. et al. Impact of two ionic liquids, 1-ethyl-3-methylimidazolium acetate and 1-ethyl-3-methylimidazolium methylphosphonate, on Saccharomyces cerevisiae: metabolic, physiologic, and morphological investigations. Biotechnol Biofuels 8, 17, doi:10.1186/s13068-015-0206-2 (2015).

38 Wehrs, M. et al. Engineering Robust Production Microbes for Large-Scale Cultivation. Trends in microbiology (2019).

39 Stankevičiūtė, J. et al. Oxyfunctionalization of pyridine derivatives using whole cells of Burkholderia sp. MAK1. Scientific Reports 6, 39129, doi:10.1038/srep39129 https://www.nature.com/articles/srep39129#supplementary-information (2016).

40 Zhang, Z. et al. Tetramethylpyrazine nitrone, a multifunctional neuroprotective agent for ischemic stroke therapy. Scientific Reports 6, 37148, doi:10.1038/srep37148 https://www.nature.com/articles/srep37148#supplementary-information (2016).

41 Hu, S. et al. A Novel Tetramethylpyrazine Derivative Prophylactically Protects against Glutamate-Induced Excitotoxicity in Primary Neurons through the Blockage of N-Methyl-D-aspartate Receptor. Frontiers in Pharmacology 9, doi:10.3389/fphar.2018.00073 (2018).

42 Liang, Q. & Qi, Q. From a co-production design to an integrated single-cell biorefinery. Biotechnology advances 32, 1328-1335 (2014).

43 Xiao, Z., Xie, N., Liu, P., Hua, D. & Xu, P. Tetramethylpyrazine production from glucose by a newly isolated Bacillus mutant. Applied microbiology and biotechnology 73, 512-518 (2006).

44 Baral, N. R. et al. Techno-economic analysis and life-cycle greenhouse gas mitigation cost of five routes to bio-jet fuel blendstocks. Energy & Environmental Science 12, 807-824 (2019).

CONCLUSION

This study explored biosynthetic strategies for ethanol production from xylose, isopentenol and tetramethyl pyrazine from glucose from the perspective of metabolic engineering and synthetic biology.

In chapter II, I designed and developed xylan fermentation system via co-culturing of xylan-degrading yeast strain and xylose-isomerizing yeast strain. Using the yeast cell surface display technology, xylanases and xylose isomerase were displayed on the cell surface of *S. cerevisiae*. As a critical metal cation against xylose isomerase, Co^{2+} was identified and validated the increased enzyme catalytic activity and contribution to improved xylose fermentation.

In chapter III, I harnessed a heterogeneous mevalonate pathway into *C. glutamicum* for isopentenol production. To validate if *C. glutamicum* is suitable host microbe, its tolerances against the final product and three representative classes of ionic liquids were confirmed. Through extensive media optimization, I revealed that the specific media including absolute substrate concentration was the key parameter. Proteomics analysis of the pathway proteins revealed that NADH-dependent HMGR is the rate-limiting enzyme for isopentenol production. Replacing the bottleneck enzyme with NADPH-dependent HMGR successfully improved the production titer. Using lignocellulosic hydrolysate from switchgrass as a carbon source, the engineered strain enabled to produce 1.25 g/L isopentenol.

In chapter IV, I identified that harnessing a specific mevalonate pathway into *C. glutamicum* leaded to tetra-methyl pyrazine production. The production was also enhanced in the presence of ionic liquids. Through metabolome analysis, activation of endogenous proteins grouped as amino acid metabolism and transport was assumed to mainly involve in the production. Using fed-batch fermentation, 2 g/L tetra-methyl pyrazine production was demonstrated with the stimulation of ionic liquids.

ACKNOWLEDGMENT

I would like to sincerely thank all the committee members, Dr. Eiichi Yamaguchi, Dr. Koichiro Oshima, Dr. Mitsuyoshi Ueda, and Dr. Yosuke Yamashiki for their support and guidance. Continuous support of the office staffs and the friendship of students at the Graduate School of Advanced Integrated Studies in Human Survivability as well as the Laboratory of Biomacromolecular Chemistry at the Division of Applied Life Sciences at the Graduate School of Agriculture in Kyoto University are very important to get through the turbulent journey of my Ph.D. First, I would like to express my sincere gratitude to Dr. Eiichi Yamaguchi for his fruitful discussion, and warm encouragement throughout the domestic and international service learning, the overseas internship (knight-errantry), and the project-based research. I would like to sincere thanks to Dr. Koichiro Oshima who gave me a chance to enter this course, and he gave me insightful advice and warmly encourage my journey. I also really appreciate Dr. Mitsuyoshi Ueda and Dr. Koichi Kuroda for their educational training of molecular biology and providing me with opportunities to improve my research skills and knowledge. During the training at the Biomacromolecualr Chemistry Lab, I had many encouragements and discussion with Dr. Toshiyuki Takagi, and I am very thankful to him. In the period of the overseas internship, Dr. Aindrila Mukhopadhyay kindly hosted me as a visiting student at the Joint BioEnergy Institute (JBEI)/Lawrence Berkeley National Laboratory (LBNL) and gave me a chance to work with other talented scientists and learn skills and knowledge of synthetic biology and metabolic engineering. Also, I cannot help expressing sincere gratitude to Dr. Thomas Eng working at JBEI as a project scientist who educated me overall my research at JBEI by sharing their experience and thoughts with me. Further, I would like to thank Dr. Yasuo Yoshikuni at Joint Genome Institute (JGI)/LBNL to accept my research stay there and give me chances to interact with potential collaborators and learn new knowledge and skills. Also, I would like to thank all coworkers at JBEI and JGI for their discussion and daily conversation. I would like to sincere thank Mr.

Alexander Antony Kaymak who initially helped to improve my English level, but after a while who became my mental trainer to deal with a hardness of life. Last but not least, I would like to sincere thank my father, Hideyuki Sasaki, and my sister Miho Sasaki, for letting me explore the journey of study and keeping my way of thinking and belief.

Yusuke Sasaki

Graduate School of Advanced Integrated Human Survivability
Kyoto University

PUBLICATION

Chapter II

Yusuke Sasaki, Toshiyuki Takagi, Keisuke Motone, Kouichi Kuroda, Mitsuyoshi Ueda "Enhanced direct ethanol production by cofactor optimization of cell surface-displayed xylose isomerase in yeast", *Biotechnology progress*, 33(4):1068-1076 (2017).

Chapter III

Yusuke Sasaki*, Thomas Eng*, Robin A. Herbert, Jessica Trinh, Yan Chen, Alberto Rodriguez, John Gladden, Black A. Simmons, Christopher J. Petzold, Aindrila Mukhopadhyay "Engineering *Corynebacterium glutamicum* to produce the biogasoline isopentenol from plant biomass hydrolysates", *Biotechnology for Biofuels*, 12:41 (2019). *co-first author

Chapter IV

Thomas Eng*, Yusuke Sasaki*, Robin Herbert, Andrew Lau, Jessica Trinh, Yan Chen, Mona Mirsiaghi, Christopher J. Petzold, Aindrila Mukhopadhyay "Production of Tetra-methylpyrazine Using Engineered *C. glutamicum*", *Metabolic Engineering Communications* (2020), doi: https://doi.org/10.1016/j.mec.2019.e00115 *co-first author

Other Publications

Yusuke Sasaki, Toshiyuki Takagi, Keisuke Motone, Toshiyuki Shibata, Kouichi Kuroda, Mitsuyoshi Ueda"Direct bioethanol production from brown macroalgae by co-culture of two engineered *Saccharomyces cerevisiae* strains", *Bioscience, Biotechnology, & Biochemistry*, 82(8):1459-1462 (2018).

Shutaro Takeda, Go Okui, Nanao Fujimura, Hisae Abe, Yuka Ohashi, Yuki Oku, Kyoko Kiriyama, Naoki Saeki, Yusuke Sasaki, Yingying Zhu, Keitou Shu, Tomoharu Takahashi, Shuntaro Noda, Kazuki Hao, Kazumasa Hirao, Senichi Kimura "The Success of the Link Model Programme in Rural Bangladesh: An Empirical Analysis", *Journal of Development Policy and Practice*, 2455133318777163 (2018).

Toshiyuki Takagi, Yusuke Sasaki, Keisuke Motone, Toshiyuki Shibata, Reiji Tanaka, Hideo Miyake, Tetsushi Mori, Kouichi Kuroda, Mitsuyoshi Ueda "Construction of bioengineered yeast platform for direct bioethanol production from alginate and mannitol", *Applied Microbiology and Biotechnology*, 101(17):6627-6636 (2017).

Keisuke Motone, Toshiyuki Takagi, Yusuke Sasaki, Kouichi Kuroda, Mitsuyoshi Ueda "Direct ethanol fermentation of the algal storage polysaccharide laminarin with an optimized combination of engineered yeasts", *Journal of Biotechnology*, 231, 129-135 (2016).